Investigating long-term, high-resolution records of climate and extreme events in the Southeast Indian and Southwest Pacific Oceans using the δ^{18}O of stalagmites

JORDAHNA ELLAN-ANN HAIG
BSc(Hons) Qld

Submitted for the degree of

DOCTOR OF PHILOSOPHY

In the College of Science, Technology and Engineering
within the
Division of Tropical Environments and Societies

JAMES COOK UNIVERSITY

Supervisor: Professor Jonathan Nott
College of Science, Technology and Engineering

January 2015

Statement on the contribution of others

The table below provides a general statement on the contribution of others towards this thesis. Including contributions from my supervisor, colleagues, collaborators and any financial assistance I received during my candidature. A more specific statement on the contribution of others is provided at the end of chapters which have either been published or prepared for publication.

Nature of Assistance	Contribution	Name	Affiliation
Intellectual Support	Proposal Writing	Prof. Jonathan Nott	James Cook University
	Editorial Assistance	Prof. Jonathan Nott Mr. Costijn Zwart Prof. Michael Bird Dr. Gert-Jan Reichart	James Cook University James Cook University James Cook University Utrecht University
	Laboratory Access	Dr. Gert-Jan Reichart Prof. Jonathan Nott	Utrecht University James Cook University
	Data Analysis	Prof. Jonathan Nott Mr. Costijn Zwart	James Cook University James Cook University
	GIS	Dr. Damien O'Grady	James Cook University
Financial Support	Stipend	Australian Postgraduate Award	Australian Department of Education
	Write-Up Scholarship	Graduate Research School	James Cook University
	Research	Australian Research Council	Discovery Projects Scheme Reference No: DP0772691
	Top-Up Scholarship	Smart State	Queensland Government

Acknowledgements

I would firstly like to thank my supervisor Professor Jonathan Nott for his guidance, generosity and for allowing me the freedom and space to explore this research topic and taking the time to teach me. Thanks are also extended to Costijn Zwart for his endless help with my Matlab and LaTex scripts, discussion on statistics, meteorology and support in general. Thanks are given to those who edited various chapters in this thesis and made contributions to publications including Prof. Michael Bird, Dr. Damien O'Grady, Allison Hoskin-Kain, Renske Löffler and Prof. Gert-Jan Reichart. Thanks are also extended to the anonymous reviewers who greatly contributed to the final version of the publications presented in this thesis.

Funding for this project was provided by the Australian Research Council (ARC) Discovery Projects Scheme (reference number: DP0772691). An APA stipend and Smart State Top-Up scholarship was provided by the Australian Department of Education and the Queensland Government. Analytical procedures were conducted at James Cook University and the University of Utrecht, the Netherlands.

Abstract

There has been much debate in recent years over the impact of rising global temperatures on the climatology of tropical storms. Various disciplines employ a range of differing techniques to assess the likely impact of enhanced greenhouse conditions on the frequency and severity of natural hazards such as severe tropical storms and tropical cyclones. Often, highly sophisticated statistical and climate models and geological proxy records are used to obtain a picture of historical and prehistorical climatology. Geological proxy records are often of low temporal resolution (decades to centuries) while statistical and climate models are based on instrumental records of tropical cyclones (covering only the last 50 years) which are not of sufficient length to decipher natural variability from human induced change. This complicates the issue of identifying long-term trends in tropical cyclone activity and the associated causes and may explain to a certain extent the disparity between current trend estimates. This thesis investigates long-term tropical cyclone activity over the last 1500 years using the stable isotope composition of seasonal growth layers in stalagmites from Eastern and Western Australia (Chillagoe, Queensland and Cape Range Western Australia respectively). Specifically does tropical cyclone activity within the instrumental record reflect natural variability, are there any discernible trends in activity and do these have climatic control/s, and lastly, what impact have these changes had (if any) on the natural environment. The approach that this thesis takes to addressing this issue is three fold. The first step, and thus first aim of the thesis was to develop a new palaeo-tropical cyclone activity index thus extending the current tropical cyclone record 1500 years back in time (Chapter 4) in order to compare the present to the past, comparing the new record with long-term climatic indices (Chapter 5) and lastly, investigating the potential environmental impacts of a changing tropical cyclone regime on both regions (Chapter 6).

This thesis effectively bridges the gap between the high-temporal resolution instrumental tropical cyclone record and geological proxy record by generating one seamless, quantifiable record spanning the last 1.5 millennia at two locations in Eastern and Western Australia (Chapter 4). This involved the development of a new tropical cyclone index (CAI) by linking isotope dynamics within tropical cyclones with their meteorological characteristics, and applying these principles to long-standing, annually resolved records of rainfall δ^{18}O from terrestrial carbonate deposits (stalagmites). The components of CAI were tested against measured records of tropical cyclone rainfall δ^{18}O. The high-resolution, long-term isotope record was then calibrated against the instrumental tropical cyclone record after de-trending the influence of the monsoon from the carbonate δ^{18}O. The second aim of this thesis was to examine the tropical cyclone climatology in these two regions at annual, decadal and centennial scales in an attempt to decipher natural variability from anthropogenically induced change. The third aim was to take steps towards applying this new index, by comparing the long-term CAI against other climate indices in an attempt to identify potential drivers of change within the geological record and thus shortlist potential inputs for long-range tropical cyclone forecast models (Chapter 5). In Chapter 6 we assess the potential impacts (if any) on the surrounding environment by applying a duel isotope approach thus, investigating changes in δ^{13}C within the stalagmite carbonate in conjunction with the observed enrichment in δ^{18}O over the most recent 100 years (the period corresponding to the reduction in tropical cyclone activity noted in Chapter 4.)

The results of this thesis indicate that tropical cyclone activity has been highly variable over the past 1,500 yr and wavelet analysis indicates the presence of decadal, inter-decadal, centennial and inter-centennial scale oscillations at both sites. Trend analysis indicates that tropical cyclone activity in the Australian region has been significantly less in recent years when compared to the last 550-1,500 yr. In fact, tropical cyclone activity on the West coast of Australia is at an all time low. Analysis of the CAI using classical statistical techniques indicate that high-frequency oscillations in CAI may be driven by

other climate phenomena such as the Northern Oscillation Index, highlighting the influence of meridional atmospheric patterns in addition to zonal atmospheric patterns (e.g. Southern Oscillation Index), and cross basin teleconnections between CAI in Western Australia and the ENSO Precipitation Index, Northern Oscillation Index, Trade-wind Index and between CAI in Eastern Australia and Atlantic Meridional Mode which have not been previously identified (with the exception of Trade-wind Index). In addition, cross wavelet analysis reveals a link between tropical cyclone activity in Western and Eastern Australia and solar cycles at decadal, and centennial scales, within both the instrumental record (Sun Spot Number) and over geological time scales through the comparison with cosmogenic isotope data i.e. southern hemisphere tree ring δ^{14}C data and NGRIP Greenland ^{10}Be concentration data. The application of a dual isotope approach ($\delta : \delta$ defined later in Chapter 6) indicates that the reduction in tropical cyclone activity noted in both regions has an alternate effect, resulting in a reduction in vegetation cover in Western Australia (the C4 community) which we believe is owing largely to the dominance of grasses at the site and the large contribution of seasonal tropical cyclone activity to annual rainfall totals at the site and conversely, an increase in vegetation cover in the C3 community (the Eastern Australian site) due to a reduction in large scale disturbances within the dry tropical woodland.

Contents

List of Figures

List of Tables

Chapter 1
Introduction

The world community faces many risks from climate change. Subsistence communities, major agricultural producers as well as urban and industrial communities are in need of long-term understanding of how climate change may impact upon, economy and industry. It is important to understand the nature of these risks, where natural and human systems are likely to be most vulnerable, and what may be achieved by adaptive responses. The perceived increase in the frequency and severity of hazards in coastal areas coupled with population growth, poverty, urbanization and inappropriate development activities, compound the risk posed to coastal nations.

Changes in climate regimes have a multitude of potential impacts including but not limited to: World and regional food supply through impacts on industry e.g. fisheries (particularly the geographic ranges of species), and agriculture (i.e. the growing capacity of various geographical locations) and protected area management (i.e. changes in species distribution relative to the climatic limits of species). For example, insured losses from tropical cyclones in the Australian region averages AUD 210 million per year[42], the majority of which is incurred by industry. There is clearly a need for a greater understanding of how climate change may impact upon the economy given the cost of recovering from these events and the disruption caused by their impact. Gaining a greater understanding of past climate regimes will enable us to predict with greater accuracy the degree to which humans may influence climate, future climate change and its potential impact on both the natural and built environment.

Risk assessments are used to determine the level of risk posed to a community by such events and therefore the most appropriate method for mitigating against, planning for, re-

sponding to and recovering from an event. Risk is determined in part, by estimating the recurrence intervals of particular events of varying magnitudes. In Australia, these recurrence intervals are determined by extrapolating short instrumental records to estimate the natural variability of the hazard[96, 103]. However, with regards to tropical cyclones specifically, geological evidence over several millennia show that short instrumental records are a poor reflection long-term, tropical cyclone behavior[59, 108, 164, 191, 184]. Yet, neither the short-term, high-resolution instrumental record; nor long-term, low-resolution geological record alone are sufficient to estimate confidently the recurrence interval of tropical cyclone events of differing intensities. There is therefore a need for a high-resolution, long-term record of tropical cyclone activity.

Tropical cyclones as great carnot heat engines, may play a significant role in the planetary heat transport system serving to stabilize tropical temperatures and de-stabilize polar temperatures[81]. There has been much debate in recent years over the impact of rising global temperatures on the climatology of tropical storms. Various disciplines employ a range of differing techniques to assess the likely impact of an enhanced greenhouse on the frequency and severity of natural hazards such as severe tropical storms and tropical cyclones. Often, highly sophisticated statistical and climate models and geological proxy records are used to obtain a picture of historical and prehistorical climatology. However, due to the complicated nature of the thermodynamics of tropical cyclones, successfully modelling tropical cyclone activity under enhanced greenhouse conditions has proven difficult. Results vary depending on the climate model used[65] and the choice of convective parameterization used in the tropical cyclone simulations[133, 172]. Concerns have also been voiced which relate to inaccurate estimates of tropical cyclone intensities in the instrumental record due to the subjective nature of certain techniques and inconsistent procedures between and/or within agencies[142]. This complicates the issue of statistically identifying trends in tropical cyclone intensity from the instrumental record and may explain to a certain extent the disparity between current trend estimates[64, 119, 133, 223].

Instrumental tropical cyclone records comprise detailed measurements of a range of meteorological parameters gathered via reconnaissance aircraft, satellite data, radar, rawindsonde, and conventional surface observations. Some of these datasets span the last half-century, therefore providing a well-documented record of tropical cyclone frequency, intensity and track data for the latter part of the industrial era. Whist being of high resolution, these records alone are not sufficient in length to provide an accurate picture of human influence on the climatology of tropical cyclones. Nor are they sufficient to convey long-term trends in behaviour and therefore accurately predict potential future frequencies and intensities. Palaeotempestology employs geological techniques to recover longer-term, lower-resolution records of tropical cyclone climatology from environmental archives such as; overwash deposits, sediments, shingle/coral ridges and just recently, cave dripstones. Whilst not generating a detailed record of the thermodynamics of these systems overtime, a long-term geological record allows for the comparison of tropical cyclone frequency and intensity between the two periods of interest i.e. the Holocene (to 1500 yrs BP); and the latter part of the anthropocene (to 209 yrs BP, at the onset of the industrial revolution). Thus, neither instrumental records nor geological records alone are sufficient to be able to accurately predict future change due to the questionable nature of the data, which may be either temporally or spatially limited or of insufficient resolution. In addition, estimating the number or intensity of tropical cyclones within the Australian region is notoriously difficult to predict. Recent works have highlighted the need for a greater understanding of the climate parameters which may influence seasonal tropical cyclone activity for inputs into forecast models given the shortfall in recent decades of the Southern Oscillation Index and regional sea-surface temperatures (the traditional inputs) in predicting tropical cyclone occurrences within the Australian region[139].

Speleothems (cave carbonate deposits) have been previously used to document palaeoclimate regimes as they are formed via the meteoric water cycle and their growth is sensitive to external climatically driven processes such as rainfall (amount and composition) and biological processes within the soil zone[10,15,71,72,136,146,180,237]. Thus the composition of

this calcite can therefore give an indication of the climatic conditions at the time of deposition. Previous works have concentrated on using δ^{13}C, δ^{18}O, trace elements barium (BA), sodium (Na) magnesium (Mg), strontium (Sr), phosphorous (P), and uranium (U)[212]; and layer thickness to determine palaeoclimate parameters such as the intensity and duration of rainfall events, temperature, ENSO[34] and changes in dominant vegetation types at the site[11,47,54].

Given that the oxygen isotope ratio of tropical cyclone precipitation has been found to be markedly lighter than normal summer precipitation[87,90,88,153,154,147]. Malmquist[167] hypothesised that oxygen isotopes in cave carbonate deposits may provide high-resolution proxy records of tropical cyclone activity. At the time, analysis techniques were not advanced enough to allow such high resolution sampling of the carbonate. Subsequent analysis by Frappier[84,82,83,78] found that brief negative excursions in stable oxygen isotope ratios of recent speleothem calcite from Actun Tunichil Muknal in central Belize corresponded to eight recent tropical cyclone events passing within 25-400 km of the cave. Nott et al[188] subsequently published a high-resolution seasonal δ^{18}O record from tropical cyclone prone North Eastern Queensland, Australia spanning the last 800yr and attributed the negative excursions in δ^{18}O to tropical cyclone activity in the region.

Before this new palaeocyclone proxy can be implemented into risk assessment methodologies by risk assessors and hazard/disaster management practitioners a number of questions must be answered. Primarily, what is the relationship between the intensity of the tropical cyclone and the δ^{18}O signal within the stalagmite calcite and over what distance is the stalagmite sensitive to tropical cyclone precipitation? Furthermore, how does the frequency and severity of theses events change under differing climate regimes? Can the long-term high resolution palaeocyclone and palaeoclimate record be used to predict future changes in tropical cyclone climatology based on this relationship? Is it possible to decouple anthropogenic influences on the natural variability of tropical cyclone frequency and intensity?

Following on from the earlier works mentioned above, the aim of this thesis was to not only develop further palaeocyclone records from stalagmites in tropical cyclone prone regions but to develop this into a new, quantifiable tropical Cyclone Activity Index (CAI). An index which would allow for a direct comparison between the modern instrumental record and long-term palaeotempest (prehistoric tropical cyclone) records derived from the $^{18}O/^{16}O$ ratio of these seasonally accreting stalagmites. This new technique, calibrates high-resolution, long-term palaeorecords of tropical cyclone activity against the instrumental tropical cyclone record, allows for a direct comparison between the past and present, and enables an examination of tropical cyclone climatology at higher temporal resolution and on annual, decadal or millennial scales simultaneously, without the need to interpolate or extrapolate to account for missing data. We have in turn used this new index to examine the natural variability within the geological past (over the last 1500 years) against the most recent period. In addition, we have made steps towards applying the palaeorecord, by comparing the long term CAI against other climate indices in an attempt to deduce the drivers of change within the geological record and thus shortlist potential inputs for long-rage tropical cyclone forecast models.

This thesis is organised into seven chapters comprising journal articles that have been published, submitted for publication or prepared for publication. Chapter 2 provides a synthesis of methods previously used to investigate tropical cyclones and climate change (not submitted for publication). Chapter 3 is an introduction to the three study sites, and a description of the general methods used. Chapter 4 describes the development of the CAI which assesses the long-term trends in tropical cyclone activity in the region. Chapter 5 builds on this by examining the potential longer-term drivers in tropical cyclone activity at the two sites. An examination of the potential impacts of the reduction in tropical cyclone activity at both sites is given in Chapter 6. This is examined through an analysis of the modern (last 100 years) of calcite deposition and its relationship to climate namely the Land Ocean Temperature Index (LOTI) and Atmospheric CO_2. A combined discussion

of the limitations of this work has been presented within the concluding chapter of this thesis (chapter 7. Chapter 7 summarises the results, highlights the potential applications of these findings and examines the future directions for this work.

Chapter 2

State of the Science: an integrated synthesis of attempts to resolve the tropical cyclones and climate change question - a methodological review.

Due to the high demand for energy globally, the equivalent of a million years of accumulated hydrocarbons are released each year; this equates to a 6.5 billion ton transfer of carbon from the earth to the atmosphere[235]. The earth reacts to environmental stresses in a non-linear fashion; as Zalasiewicz et al.[235] states, essentially flipping from one quasi-stable state to another. Thus, the Earth's response to change and the various feedback mechanisms associated with this response complicate the issue of accurately predicting future climate change. As the Earth's global carbon cycle is a significant driver of global climate, the question is not whether humans have influenced global warming, but what feedbacks could be expected.

Tropical cyclones as great heat engines occur as one such feedback responding to changes in sea surface temperature and increased instability in the atmosphere due to high evaporation rates; all of which are feedbacks to higher atmospheric temperature, a result of greater CO_2 gas emissions. There has been much debate in recent years over the impact of rising global temperatures on the climatology of tropical storms. Much of this debate arises from the complicated nature of the thermodynamics of tropical cyclones. In order to accurately predict future tropical cyclone frequencies and intensities we must first be able to decouple anthropogenic influences from natural variability. The purpose of this review is therefore to investigate methods of achieving this separation.

2.1 Research Problem

Instrumental tropical cyclone records comprise detailed measurements of a range of meteorological parameters gathered via reconnaissance aircraft, satellite data, radar, rawindsonde, and conventional surface observations. Some of these datasets span the last half-century, therefore providing a well-documented record of tropical cyclone frequency, intensity and track data for the latter part of the industrial era. Whist being of high resolution, these records alone are not sufficient in length to provide an accurate picture of human influence on the climatology of tropical cyclones nor is it sufficient to identify long-term trends in behaviour and therefore accurately predict potential future frequencies and intensities. Palaeotempestology is a relatively new discipline which employs geological techniques to recover longer-term, lower-resolution records of tropical cyclone climatology from environmental archives such as; overwash deposits, sediments, shingle/coral ridges and just recently, cave dripstones. Whilst not generating a detailed record of the thermodynamics of these systems overtime, a long-term geological record allows for the comparison of tropical cyclone frequency and intensity between the two periods of interest i.e. the Holocene; and the period in which humans may have had an impact on global climate, the latter part of the Anthropocene. However, whilst providing a longer scale picture of natural variability, the current geological record alone is perhaps too coarse to predict future tropical cyclone behaviour.

2.2 Tropical cyclones under enhanced greenhouse conditions - the debate

Many now agree that as the instrumental record is limited in its temporal extent, the analysis of the long-term natural variability of tropical cyclone behavior is limited[65, 109, 142, 162, 188]. This limitation has impelled the use of an array of modeling techniques to investigate the issue of warming induced changes in tropical cyclone activity. These highly sophisticated mathematical models generate predictions based on observed responses to changes in environmental parameters within the historical record and in some cases include theoretical

considerations of the thermodynamics of the system. The particulars of these models will not be discussed here; instead a general overview of the arguments resulting from these results will be presented.

Lighthill et al.[160] defines the three methodologies for investigating whether global warming will lead to more frequent or more intense tropical cyclones, these are: interpreting computational Global Climate Model (GCM) results in the context of theoretical considerations of tropical cyclone formation and intensification based on observational records; statistical analysis of the historical record and correlations with environmental parameters; and applying climate models to infer direct predictions of tropical cyclone statistics (the latter is considered less robust). Results vary depending on the climate model used[65] and the choice of convective parameterization used in the tropical cyclone simulations[133,172]. Concerns relating to inaccurate estimates of tropical cyclone intensities in the instrumental record due to the subjective nature of certain techniques and inconsistent procedures between and/or within agencies have also been voiced[142]. This complicates the issue of statistically identifying trends in tropical cyclone intensity from the instrumental record and may explain to a certain extent, the disparity between current trend estimates[64,119,133,223]. While efforts are being made to reassess existing tropical cyclone databases in light of current advances in forecasting and analysis[141,142] caution should be exercised when making statements based on these records.

2.3 Results of Statistical Approaches

In recent years, trend estimates have been generated using an array of statistical approaches based upon the instrumental tropical cyclone record. These methodologies attempt to infer regional decadal variability in tropical cyclone frequency and/or intensity. Many climate analysts have opted for a Bayesian approach to probability given the degree of uncertainty surrounding future tropical cyclone climatology[32,40,41,60,123,239]. This technique has also been recently incorporated into operational models for seasonal forecasts[60]. Bayesian probability is a form of reasoning which uses prior knowledge to predict future

events, particularly when uncertainty is an issue. Modelled results vary, as is the nature of Bayesian reasoning; however some general conclusions have been made, some of which are in agreement. Briggs[32], concluded that the rate at which storms have evolved into tropical cyclones has decreased while intensification to category 4 status and above has increased in the North Atlantic. Mean individual storm intensity has not increased yet the variability in intensity has. In short, the observed increase in severe tropical cyclones is most likely due to an increase in the number of tropical cyclones occurring and not in the intensity of these individual storms. While in the Central North Pacific, Chu and Zhao[40] predict this increase in tropical cyclone numbers to continue into the next decade. When modelling the maximum possible wind speed near the United States, Jagger and Elsner[123] concluded that higher return levels for extreme hurricane winds are associated with higher temperatures. While Zhao and Chu[239] infer less frequent, intense tropical cyclones will occur in the next decade by applying a data, parameter and hypothesis approach to the time series of major hurricane frequencies for the eastern North Pacific.

2.4 Global Climate Model (GCM) inferences based on theory and observational records

In order to deduce anthropogenic changes in tropical cyclone climatology, analysts have employed the use of Global Climate Models and predict changes based on both theory and observational records of tropical cyclones. Whilst a very useful technique, this gives rise to a large degree of uncertainty as the resolution of these models continues to be too poor to accurately model the complicated structure of these systems - particularly intensity[33,65,109,220,219,218,221]. However as Broccoli and Manabe[33] state, this technique does enable the quantitative simulation of tropical cyclone climatology and thus frequency of their genesis and can therefore give some insight into what we could expect under enhanced greenhouse conditions. Some experiments suggest that under conditions of doubled CO_2 there is a significant reduction in the number of storm days[33]. In this instance, Emanuel et al.[65] predict significant changes in the geographical zone of activity, inten-

sity and frequency under conditions of doubled CO_2. However as is logical, these results differ greatly between and within basins. Knutson and Tuleya[133] predict a 14% increase in storm intensity (central pressure fall) compared to Emanuel's 8%[66–68] and Holland's 16%[117]. Yet their conclusions remain the same, under an enhanced greenhouse state, frequency may remain the same however with a greater likelihood of more intense tropical cyclones. Knutson's et al.[132] most recent paper applies a regional atmospheric modelling framework specifically designed for dynamically downscaling Atlantic Hurricane activity. Their modelled results suggest that frequency will actually be reduced under enhanced greenhouse conditions. Potential changes in intensity of future tropical cyclones also remains a contentious issue. Some, such as Walsh et al[219,218] elude to a predicted increase in tropical cyclone intensity. However they are reluctant to make definitive predictions due to the noted deficiencies in current GCM's and the lack of knowledge of the effect of climate change on ENSO, just one of the many additional factors which have been found to strongly influence the regional genesis of tropical cyclones.

2.5 The emerging Field of Palaeotempestology

Palaeotempestology is the study of prehistoric 'tempests' or storms, both extra tropical and tropical cyclones. Paleotempestology is a relatively young field which employs the use of geological proxies to investigate the activity of tropical cyclones in the geological past. Its purpose is to extend our knowledge of their behaviour beyond the instrumental tropical cyclone record in order to investigate the longer-term periodicities in tropical cyclone activity (over several millennia) therefore remedying the restrictions imposed by the short-term instrumental record. One advantage of this method of investigation when considering the greenhouse question, is the ability to examine tropical cyclone behaviour under different climatic regimes. Thus, by selecting periods in the geological past which mimic present and/or warmer climatic conditions, we may infer changes in the behaviour of tropical cyclones using empirical data rather than relying solely on theoretical or simulated data. However, of these studies only few well dated and validated proxy records from the United States and Japan have been published[162] and even fewer from the Aus-

tralasian region[191,189].

Traditionally, the prehistoric record has been derived from sedimentary or erosional evidence deposited during tropical cyclone events. These palaeotempest proxies include: overwash deposits and ocean microfossils such as foraminifera, pollen, diatoms, dinoflagellates and phytoliths from coastal sediment cores; wave or flood deposits (tempestites) in marine or lagoonal sediment cores; parallel coral shingle, shell and/or sand beach ridges and; oxygen isotope signatures of tropical cyclone precipitation in shallow-water corals, terrestrial carbonates (speleothems), and tree rings.

2.5.1 Beach Ridges

Storm ridge accretion occurs when tropical cyclone generated surge and wave action transport coarse sediment shoreward, depositing the sediment above the tidal zone[108]. The deposition of beach ridges as a result of storm generated surge had been noted as early as the beginning of the 20th century[35]. The first of such studies surveying these storm ridge sequences conducted by Baines and McLean[7] examined parallel ridges of coral rubble at Funafuti atoll in the South Pacific. However it was not until the early 1980s at (Princess Charlotte bay) that storm ridge sequences had been both surveyed and dated and the first prehistoric tropical cyclone frequency record generated[38]. In the last few decades, additional methods have been developed to assess not only the frequency of these events but also intensity (quantifying central pressure) using numerical models that simulate both surge levels and wave characteristics based on standard principles of fluid dynamics[191,189].

Wasson[222] inferred that coral rubble ridges deposited on Vernon Island, Darwin are most likely deposited by storm surge from tropical cyclones as most ridges occur higher than the highest astronomical tides, and waves produced under normal conditions are small and have a limited run-up component. This ridge sequence was dated using two methods: historical aerial photographs and radiocarbon dates from the shell debris. Hayne

and Chappell[108] sampled coral material from two traverses of a series of storm ridges on Curacoa Island in the Palm Isalnd Group via stratigraphic pits and trenches. These samples were then dated using radiocarbon methods to determine a chronology of the events which accreted the ridges. Hayne and Chappell[108] go further to state that the volume and crest height of a ridge should reflect the local intensity of combined cyclonic surge and wave effects. Nott and Hayne[189] were able to estimate intensity (central pressure with uncertainty margins) from ridge height, thus determine both frequency and magnitude of tropical cyclones over millennia.

Nott[186] found that sand beach ridges composed of multiple depositional units record separate storm inundation events. In this instance frequency of events can be determined by dating the sedimentary units and intensity of these event determined via storm surge and wave models[190]. Recurrence intervals for tropical cyclones on the Eastern cost of Australia have been estimated using the Generalised Extreme Value distribution and Bayesian analysis presented by Nott and Jagger[192]. With respect to coral shingle storm ridges, prior development of the coral source is required for a ridge of this composition to accrete during a tropical cyclone event[108]. Therefore some time may be needed for the source to build up between events. In addition, the intensity and direction of the cyclonic waves depends on the configuration of the site and the sites position relative to the cyclone track[108]. Therefore it is not safe to assume that all tropical cyclones passing within the vicinity will necessarily accrete or erode existing storm ridges of the site. However, the application of this method has highlighted the degree to which the instrumental record underscores the frequency of more intense tropical cyclones. Nott and Hayne's[189] work along the Great Barrier Reef has estimated intense tropical cyclones occurring at a frequency one order of magnitude higher than that supposed from probability estimates generated from instrumental data.

2.5.2 Sediment Cores - Overwash Deposits

In the past few decades many studies have focussed on the information contained within overwash deposits from coastal sites particularly in the United States. Overwash is a process of swash overtopping the frontal dunes of a barrier island during storms (see 2.1). Successive overwash events will create multiple layers of sand alternating with the finer organic sediments usually present within coastal lakes and marshes[162]. These deposits are investigated though the use of techniques such as coring, trenching, ground-penetrating radar imaging, aerial photography (to assess historical beach migration), and pre- and post-storm beach-profile surveys. These deposits can be dated using radiometric methods (^{14}C, ^{210}Pb and ^{137}Cs) to generate a frequency curve. The intensity of these events have been interpreted in a number of ways using sand layer thickness, sediment grain size and via comparison of recent events of known intensity[49, 51, 164, 52, 163, 236, 231, 143].

Donnelly et al.[49] inferred that the distance this material is transported landward may be an indication of the intensity of the storm. Their 2004 survey of the New Jersey Coast found that at least two of the prehistoric overwash fans (7th and 14th century) were likely deposited by storms of much greater intensity than those within the historical record. Liu and Fearn[163] assumed the same when Hurricane Frederic (category 3) failed to leave a discernible sand layer in cores taken from the centre of Lake Shelby, Gulf of Mexico (A,B and E in Figure 2.2) yet was evident in cores taken nearer the beach (L and S in Figure 2.2). They therefore conclude that sand layers present in cores A, B and E were deposited as a result of tropical cyclones of greater intensity than Hurricane Frederic, assuming that the geomorphic setting has remained the same throughout time. This record represents the localised nature of this methodology as category 5 hurricane Camille in 1965 who made landfall 160 km West of Lake Shelby had limited impact on this section of coastline and did not leave a geological evidence of its occurrence within these sediment cores. However, from the evidence present at this site Liu[163] infers a recurrence interval of 600yr for intense tropical cyclones (category 4 and 5) in this locality. Donnelly et al.[50] inferred an annual landfall probability of 0.3% for intense tropical cyclones (winds of $>$50 m/s) at Whale Beach in New Jersey. Their inference of intensity is based on a comparison of

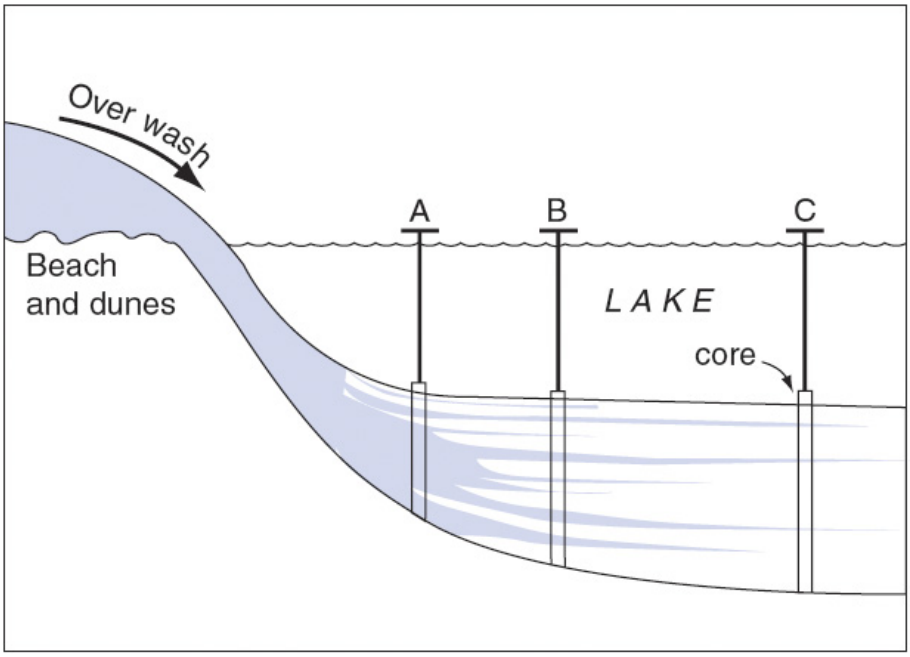

Figure 2.1: Graphic representation of overwash deposition from[162]. Storm surge overtops the back barrier, eroding sand from the beach and dunes and depositing a fan of course to fine-grained sediment in the coastal lake/marsh on the lee side of the dunes.

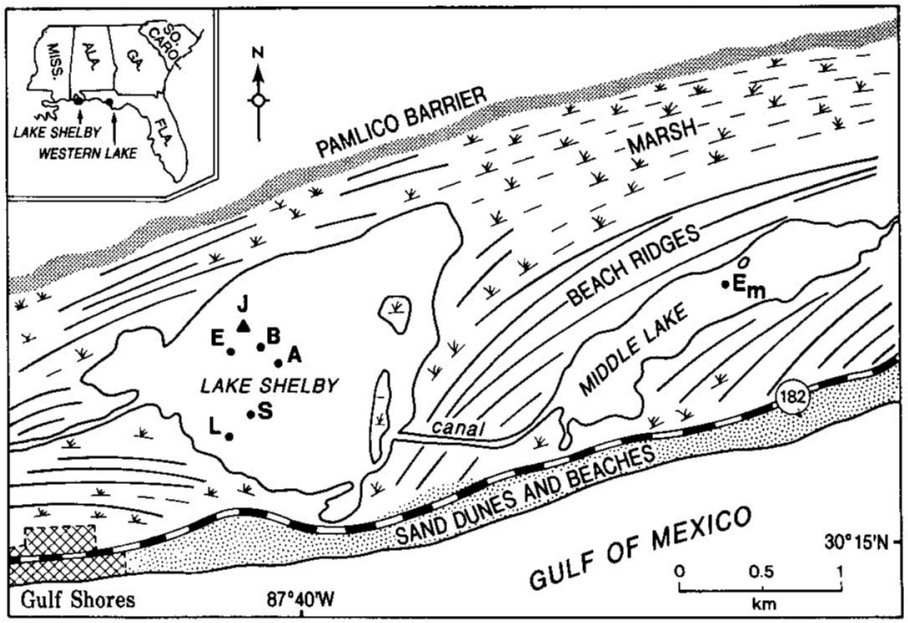

Figure 2.2: Location of sediment cores taken from Lake Shelby, New Jersey[163].

the thickness of prehistoric and historic sand layers which were calibrated to instrumental records of intensity and dated using ^{14}C methods. By correlating 14 sediment cores from Succotash salt marsh in Rhode Island with the historical record, Donnelly et al.[51] were able to identify 4 additional overwash fans deposited by intense storms in the early 13th and 15th centuries. Radiocarbon dates in addition to pollen and lead stratigraphic markers were used across multiple cores to verify the chronology of events based on atmospheric fluctuations of ^{14}C and ^{137}Cs (as a result of nuclear weapons testing), changes in land use (increasing agricultural production) and the onset of the industrial era marked by a rise in atmospheric Pb levels. More recently in 2007, Donnelly and Woodruff[52] generated a 5000 year record of intense tropical cyclone landfall in the Caribbean deducing intensity from the sediment grain size within the overwash deposits. In this paper they explored the issue further by comparing this record with regional palaeoclimate records. In this they noted that variations in El Niño and the West African Monsoon played a greater role in influencing tropical cyclone activity in this region. While sea surface temperature (comparable to current temperatures) had less influence on this activity.

An element of caution should be exercised when interpreting frequency and intensity of prehistoric cyclones from lake and marsh sediment cores. Donnelly et al.[51] highlights that the dynamic nature of these environments complicates the issue of interpreting the sedimentary record. A thorough understanding and assessment of the local geomorphology, landscape and any evidence of change throughout time in addition to an accurate record of historical tropical cyclone events are essential when using this evidence as a proxy. In addition, inferring intensity from the scope of these overwash fans is complicated somewhat by factors which may influence storm surge height such as; coastal bathymetry, the angle of approach of the hurricane, wind direction and the timing and duration of landfall with respect to the tidal regime[164]. The breadth of the overwash fan may also be affected by factors other than the intensity of the storm such as; lake morphometry, sand supply which may also be influenced by the time in-between tropical cyclone strikes and thus accumulation rates. In order to infer the intensity of prehistoric storms it must be

assumed that the geomorphic setting has remained unchanged throughout the period of investigation. In addition, only those storms intense enough to generate a surge capable of overtopping the barrier threshold and those which pass within reasonable proximity to the study area will create these overwash fans as sediment from the beach and nearshore environment is transported landward across back-barrier marshes, lakes and lagoons. As tsunamis have also been known to deposit similar sand layers within coastal lakes and marshes[4,5,163,176,46,230] it is important to be able to make a distinction between these two types of events within the sedimentary record of a site. Given that the source of sediment in both scenarios is the same and in the absence of heavy weighted source material, which could provide a distinction through hydrodynamic principles, caution should be exercised.

2.5.3 Sediment Cores - Tempestites and Microfossils

Tempestites provide the oldest geological evidence of storm deposits as they have often formed consolidated rock. These are composed of a succession of bedding planes, which correspond to changes in flow during the deposition of sediment entrained in the flow. Stratigraphically, these beds are often oscillatory in nature and exhibit periodic patterning suggesting the occurrence of periodic high-energy events resulting in the rapid deposition of some layers followed by longer periods of low-energy deposition. Brandt and Elias[31] suggested during the late 1980s that tempestite thickness being a reflection of storm intensity could reflect past atmospheric CO_2 levels thus indicating CO_2 enriched (greenhouse phases) and CO_2 depleted (icehouse phases) over geological time. Emanuel[63] notes in reference to this article that it is possible that proxies could be developed which would permit the investigation of tropical cyclone activity during glacial periods which would provide a test for the current climate Model inferences.

Duke[58] notes that only severe tropical cyclones and mid-latitude winter wave cyclones are intense enough to be able to modify shallow-marine depositional environments and thus infers that the presence of hummocky cross-stratification within tempstites (typically occurring within shallow-marine deposits) provides a distinction between these two storm

types and other storm deposits. Duke[58] argues further, that these severe storm types can be distinguished from one another due to the differing nature of their bottom flows (tropical cyclones generating oscillatory or multidirectional dominant flow and severe winter storms generating significantly unidirectional dominant flow). Through the distribution of Mesozoic and Palaeogene tempestities, Duke[58] inferred that tropical cyclones occurred more frequently at higher-latitudes during these warmer periods than they do at present, suggesting a future change in the geographical distribution of tropical cyclones.

Through field observations and model predictions, the hummocky cross-stratification wavelength has been found to be proportional to the orbital diameters of storm induced oscillatory flow[122,159,204,227]. Given this relationship, Ito et al.[122] proposes that hummocky cross-stratification wavelength could serve as a proxy for the orbital diameters of ancient storm waves thus possibly indicating the intensity of palaeotempests. When examining the hummocky cross-stratification wavelength structure of Mesozoic and Cenozoic tempestites from Japanese Islands, Ito et al.[122] found variations in the wavelength corresponded well with known greenhouse and icehouse cycles during this period (see Figure 2.3) and based on this evidence, they suggest that storm intensity may increase under enhanced greenhouse conditions in future. The palaeoclimatic and palaeotempest opportunities for tempestites are endless as they can be dated to produce a chronology of events, their stratification and/or thickness can give an indication of intensity (although only relative) and in the presence of microfossils such as foraminifera, diatoms, dinoflagellates and phytoliths and the assemblages and geochemical analysis of such, could give an indication of palaeoclimatology at the time of deposition. However, similar to storm ridges this methodology is again limited to larger more intense events and produces a lower-resolution record of frequency over time.

2.5.4 Isotope Signatures in Tree rings and Terrestrial Carbonates

The stable isotopes of carbon (^{12}C and ^{13}C) and Oxygen (^{16}O and ^{18}O) have been used extensively in the past to reconstruct past climates as they occur in a variety of forms (i.e.

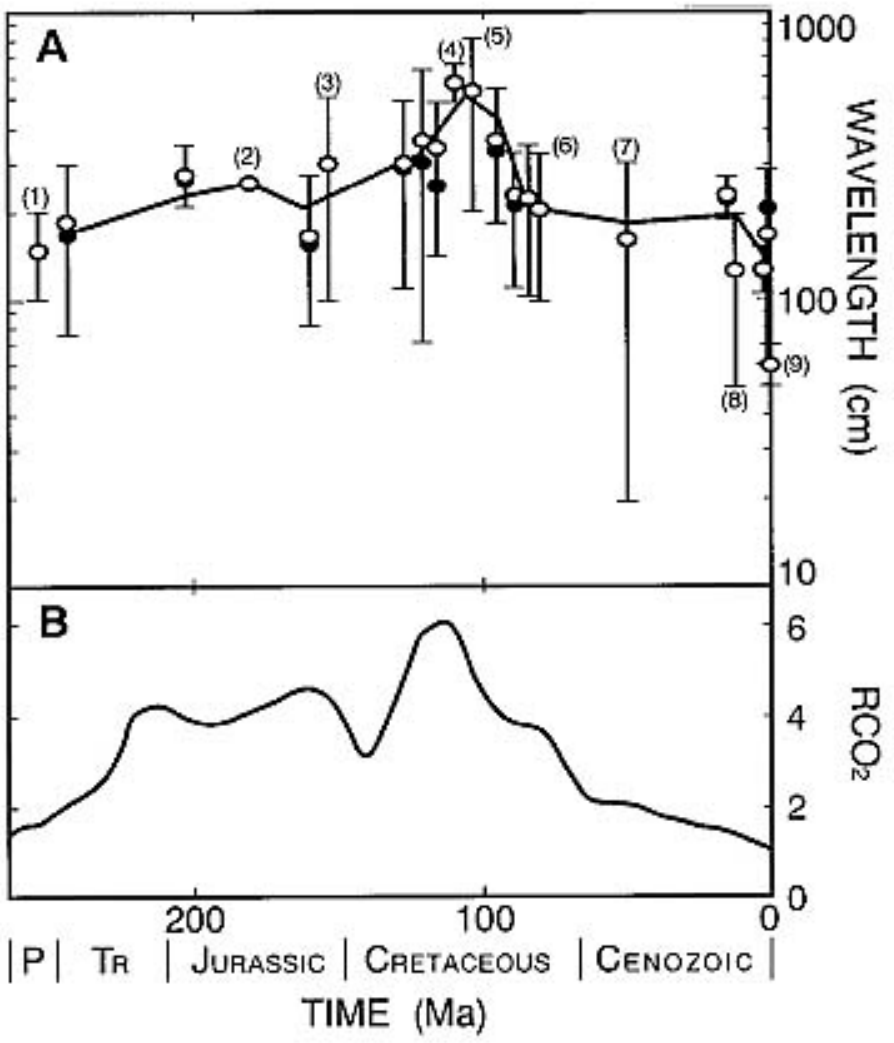

Figure 2.3: Wavelength variation throughout the Mesozoic and Cenozoic from Japanese island tempestites corresponding to modelled atmospheric CO_2 from Berner[21] cited in 346.

gaseous, liquid and solid states) and are an integral part of nearly all the geochemical processes on Earth[73]. Oxygen isotope ratios within ice cores, corals, tree rings, stalagmites (cave deposits) and other materials have been used in recent years as palaeo-temperature proxies due to the effect of temperature on isotope fractionation[154]. Signatures of tropical cyclone events may also be recorded in some of these materials as studies have shown there is a clear distinction between the oxygen isotope ratio of tropical cyclone precipitation and summer rain in tropical areas[153].

The notion that tropical cyclone precipitation may be recorded in the calcite of cave drip stones was first eluded to by Lawrence and Gedzelman[152]. However attempts made by Malmquist[167] to decipher a tropical cyclone signal from the normal monsoonal signal were unsuccessful. This was largely due to the limitations of microsampling and the large volume of material needed for high-resolution stable isotope analysis at the time. Since then, only four previous works have successfully identified tropical cyclone signatures through the isotopic composition of the calcite layers of stalagmites from Actun Tunichil Muknal in central Belize[81–83], Niue, South Pacific[199], southern Israel[135] and Chillagoe in North Queensland, Australia[188]. Samples collected from central Belize by Frappier[83] were analysed at high resolution (20μm: weekly to monthly intervals) across 27 of the most recent layers of calcite to identify individual tropical cyclone events through brief negative excursions in the δ^{18}O of the calcite. In this analysis, 8 of 9 tropical cyclones which passed within 25-400km of the cave produced distinctly negative excursions in δ^{18}O. Nott et al.[188] provided a lower resolution record (yearly intervals) of δ^{18}O over 777 annual layers. When comparing the instrumental tropical cyclone record for the region to the δ^{18}O results, Nott et al.[188] found each distinctly negative excursion in δ^{18}O corresponded to tropical cyclones passing within 400km of the cave. Other influences on the δ^{18}O of calcite such as the cave temperature effect, amount effect and kinetic isotope fractionation effects were found not to have influenced these results.

Stable isotope abundances are generally expressed in terms of the parts per thousand (i.e.

‰) difference from a laboratory standard. The stable isotope mass spectrometer compares the isotope ratio of the gas (usually CO_2) produced from the sample to that produced by the standard. As only two of the three oxygen atoms react with CO_2 the conversion is subject to a temperature dependent isotope fractionation and therefore can be controlled experimentally[137]. With respect to carbonates (Standard NBS-20 Limestone), the primary reference materials or standards for oxygen isotope ratios are δ^{18}O (SMOW) (26.64‰) and δ^{18}O (VPDB) (-4.14) (see Eqs. 2.1 and 2.2 for conversion). The Pee Dee Formation (PDB) standard was developed at the University of Chicago in the 1950s during the inception of the palaeo-temperature scale and is used primarily for low-temperature studies of carbonates. The second standard VSMOW or Standard Mean Ocean Water gives the predetermined δ^{18}O value of 26.64‰ for Ocean water and is used primarily in studies of high temperature carbonates and liquid samples[115, 145].

$$\delta^{18}O_{\,VSMOW} = 1.03091\delta^{18}O_{\,VPDB} + 30.91 \tag{2.1}$$

$$\delta^{18}O_{\,VPDB} = 0.97002\delta^{18}O_{\,VSMOW} + 29.98 \tag{2.2}$$

2.6 δ^{18}O of tropical cyclone Precipitation

The range of δ^{18}O values of almost all precipitation on earth falls in the range +10‰ VSMOW in the subtropics to -50‰ VSMOW at Vostok, Antarctica[45] cited in[153]. In most cases, δ^{18}O values in the humid tropics fall at the high end of the spectrum between 0‰ VSMOW and -5‰ VSMOW[45, 156, 153]. Studies conducted over the last few decades in the United States have found that the δ^{18}O value of tropical cyclone precipitation is typically $<$-6‰ VSMOW and therefore forms a population which is distinct from the summer rain signal. These studies have also shown that within tropical cyclones, the δ^{18}O value of water vapour and precipitation consistently decrease radially inward from the outer edge of the rain shield, generating the lowest values near the eye wall[147]. In addition, tropical cyclones which are either short lived or smaller in size produce more positive δ^{18}O VSMOW values than those which are more intense, larger and/or longer lived. A number of examples showing this distinction are provided below from the work of Gedzelman,

Lawrence and others.

Lawrence[147] compared the oxygen isotopic composition of normal summer rain from 166 events and tropical cyclone precipitation from 5 events in southeast Texas between 1985 and 1992; 4 tropical cyclones during the 1995 Atlantic hurricane season; and 95 samples of summer rainfall over a 7 year period in Mohonk Lake New York[148]. These analyses found that the δ^{18}O means differed by 1.96‰ VSMOW in that the mean δ^{18}O value of the normal monsoonal rain was -2.9‰ VSMOW and -9.4‰ VSMOW for the tropical cyclone rain (see Figure 2.4). Figure 2.5 shows the strongly negative signals from ground waters left by tropical cyclones Chantal and Allison in 1989 invariably below -7‰ VSMOW and as low as -14‰ VSMOW. Comparisons elsewhere in Mohonk Lake and City College, New York found δD values (deuterium:hydrogen ratios) as low as -89‰ δD VSMOW from Tropical Storm Dean (short lived with peak winds of 40 knots), -47‰ δD VSMOW from Tropical Storm David, -8.8‰ δ^{18}O VSMOW from Hurricane Luis in 1995 (a relatively intense, long lived cyclone), -11.1‰ δ^{18}O VSMOW from Hurricane Opal (very intense, long lived cyclone) and as low as -9.3‰ δ^{18}O VSMOW from Hurricane Bob in 1991[153] (see Figure 2.5 for a more detailed view of Hurricanes Opal, Luis and Tropical Storm Dean). In another example, Lawrence et al.[155] conducted flights into Hurricane Olivia which formed in the eastern Pacific Ocean near Puerto Vallarta in September of 1994. Sampling of the hydrogen and oxygen isotope ratios within precipitation and water vapour at an elevation of 3 km revealed a range of δ^{18}O values between -13.9‰ VSMOW and -28.8‰ VSMOW during the cyclones peak in intensity (i.e. 923 hpa). Lawrence et al.[154] also compared the δ^{18}O of water vapour at daily intervals during July 1998 in Puerto Escondido, Mexico and found δ^{18}O values of water vapour began to decrease rapidly during the genesis of tropical cyclones Celia, Darby and Estelle from positive values between 0‰ VSMOW and 12‰ VSMOW to strongly negative values between -10‰ VSMOW and -24‰ VSMOW.

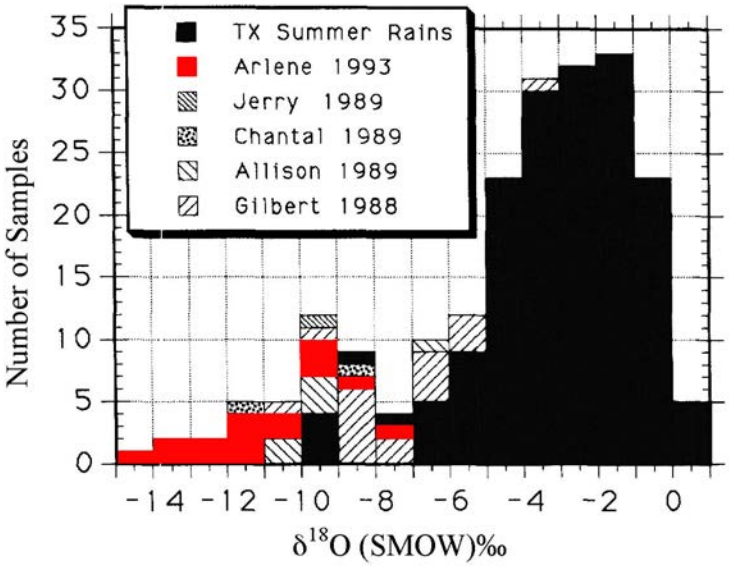

Figure 2.4: Comparison of the oxygen isotope data obtained from five tropical cyclones which made landfall in southeast Texas between 1985 and 1992, against summer rainfall for the entire period[147].

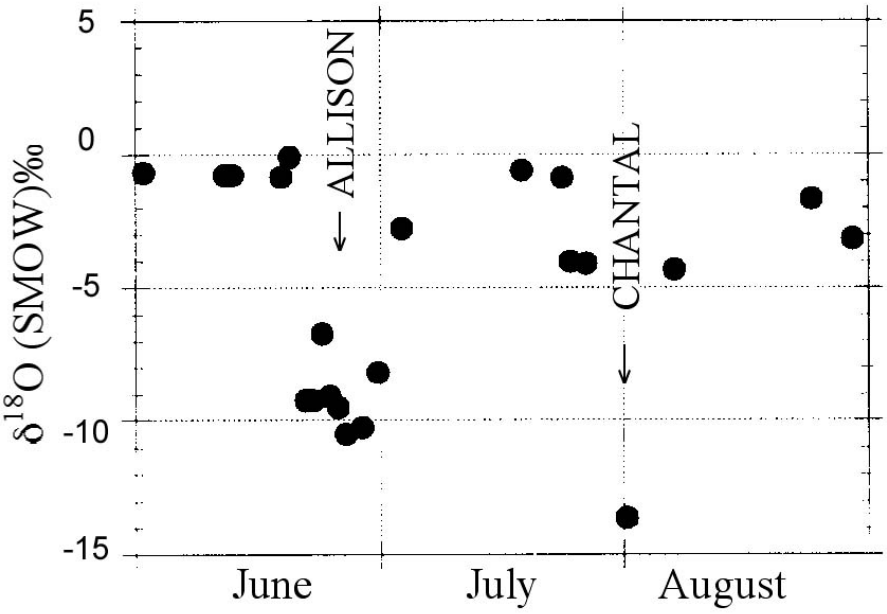

Figure 2.5: Oxygen isotope data obtained from tropical cyclone Allison (1989) and Chantal (1989) which made landfall near Texas. Note the distinctly negative δ^{18}O values compared to the more positive normal monthly rainfall values[147].

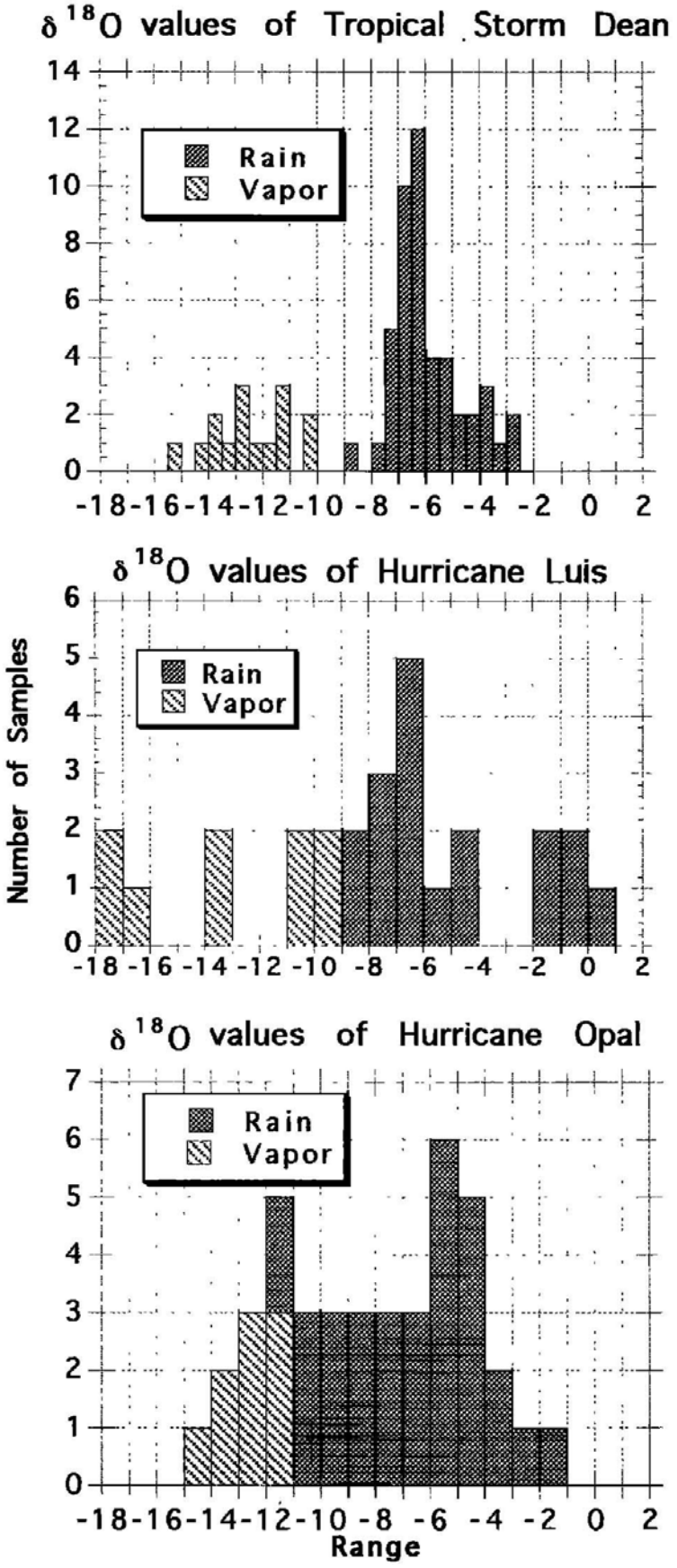

Figure 2.6: Hurricanes Opal, Luis and Tropical Storm Dean 1995. The above graphs show a comparison of the δ^{18}O values of both water vapour and precipitation collected from three of the Atlantic land-falling Hurricanes mentioned above. Note values as low as -9‰ in tropical storm Dean and a relatively weak hurricane Luis, and as low as -12‰ for severe hurricane Opal note that the δ^{18}O of water vapour is markedly less than that of precipitation[156]

2.6.1 Process of isotope Fractionation in Convective Systems

In order to understand why tropical cyclones produce such a distinct oxygen isotope signal, it is important to examine the process of isotope fractionation within a convective system i.e. the rainwater composition effect. The resulting oxygen isotopic composition of rainwater is a result of a series of reactions in which one isotope is preferentially enriched over another - this process is referred to as isotope fractionation. The two main factors which lead to isotope fractionation are isotope exchange reactions and kinetic processes. In isotope exchange reactions (or equilibrium isotope distribution) there is no net reaction. Whilst the concentrations of the isotopes (e.g.^{16}O and ^{18}O) may alter between different chemical substances (e.g. H_2O and $CaCO_3$), between phases or between molecules, δ^{18}O remains unaltered. Kinetic fractionation however, is the result of a unidirectional process where an isotope is enriched preferentially over another. This is often due to differences in the rate of a chemical reaction. Kinetic fractionation occurs during processes such as evaporation, condensation and diffusion. The following section will explain how kinetic fractionation determines the isotopic composition of precipitation; and how the degree of fractionation differs between tropical cyclones and tropical storms and across latitudes.

The degree of fractionation is a result of differences in vapour pressures and/or mass between the lighter and heavier isotopes of oxygen (i.e.^{16}O and ^{18}O) relative to temperature. Isotope fractionation occurs during evaporation of seawater (Stage 1), condensation and precipitation within the cloud (Stage 2), and due to diffusive isotope exchange between the precipitation and surrounding water vapour at the cloud base (Stage 3). Within tropical cyclones these processes are believe to be exacerbated by the high condensation efficiency (i.e. the height and thickness of cloud and overall size), their longevity as intense convective systems, the recycling of water within the storm and the large size of the system[91,87,90,92,89,88,151,153,154,147,149,148,152].

Fractionation during evaporation and condensation results from differences in the saturation vapour pressures of the isotopic compounds. The lighter isotope is generally more

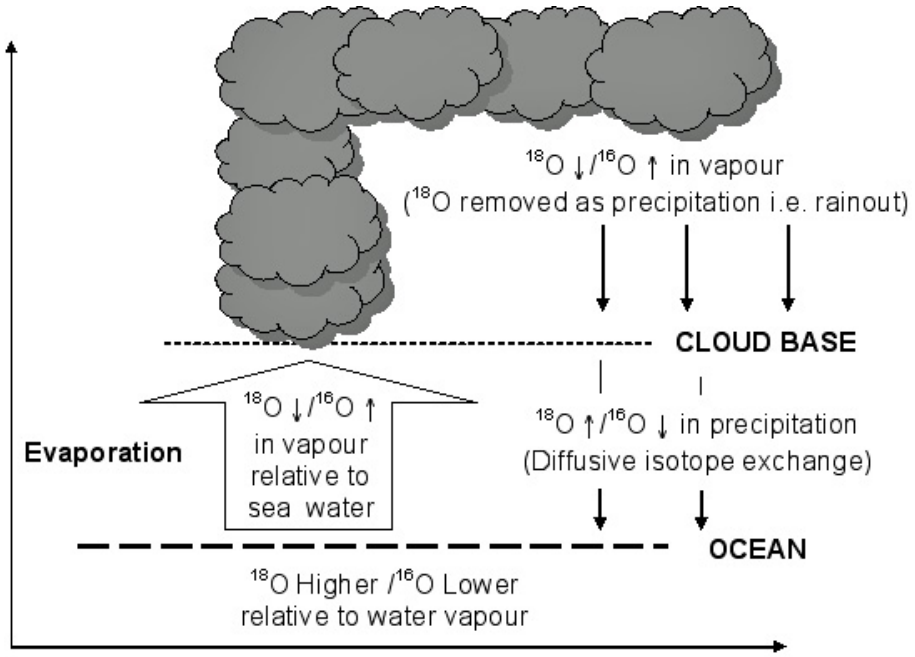

Figure 2.7: Oxygen isotope fractionation in a convective system: the effect of fractionation on the oxygen isotope ratio of water in vapour and liquid form during the three stages of evaporation, convection/precipitation and diffusion. Stage 1: The lighter isotope (^{16}O) is evaporated from seawater much faster than the heavier isotope (^{18}O). Stage 2: These heavier isotopes fractionate during condensation and are preferentially removed as rainfall. Stage 3: As these water droplets fall through the rain cloud they preferentially take up more of the heavier isotope from the surrounding isotopically heavier water vapour through diffusive isotope exchange with the ambient vapour thus further depleting the surrounding water vapour of the heaver isotope.

mobile and is therefore more readily separated from the heavier isotope. During evaporation the surrounding water vapour is preferentially enriched in the lighter isotope, the extent of which is temperature dependent (Stage 1 Figure 2.7). This is due to the lower saturation vapour pressure of the heavier isotope and the lighter atomic mass (and therefore greater vibrational frequency) of the lighter isotope[115]. This process can be explained in the following example showing the evaporation of water.

$$\frac{H_2^{18}O}{H_2^{16}O} = \frac{2.01565 + 17.999160}{2.01656 + 15.994916} = \frac{20.01481}{18.010565} = 0.55565 \tag{2.3}$$

In this example, the velocity of $H_2^{16}O$ is 0.55565 times greater than that of $H_2^{18}O$ and is therefore more readily converted from liquid to vapour[88]. The reverse is true when the isotopes fractionate as the water vapour condenses to form water droplets and ice crystals (Stage 2 in Figure 2.7), and are subsequently removed as precipitation. In this case the heavier isotope is more readily removed from the water vapour[115]. At 20°C, the ratio of the lighter to the heavier isotope in condensate is 9‰ greater than that in the vapour within the cloud.

As these water droplets fall through the rain cloud, they preferentially take up more of the heavier isotope from the surrounding isotopically heavier water vapour while the lighter isotope is drawn out of the droplet through diffusive isotope exchange (Stage 3 in Figure 2.7)[88]. During diffusion a molecule may favour one isotope over another; this favouring is largely dependent on the strength of the covalent bond between the isotope and the element. The strength of the bond arises from the reduction of the energy of the molecule as the two atoms approach each other. The heavier isotope forms a stronger bond with the molecule than the lighter isotope and is taken out of the surrounding water vapour more readily[22,73]. When the heavy isotope of an element replaces the light isotope, the energy of the molecule decreases because the increase in the mass of the molecule decreases its vibrational frequency. The lighter isotope is therefore more mobile due to its greater vibrational frequency. In addition, the species with the greater mass will migrate towards the cold end of the temperature gradient (i.e. from the vapour toward the water droplets). This process further depletes the surrounding converging water vapour of the

heaver isotope, thus enriching the precipitation at ground level with the heavier isotope. Consequently, the rainfall from storms is initially isotopically heavy yet quickly depletes overtime[88]. Therefore, the δ^{18}O of precipitation will become more negative (i.e. isotopically lighter) with time, increasing cloud height and increasing rainfall.

2.6.2 Latitude and amount effects on the oxygen isotope ratio of precipitation

The isotopic composition of rainwater is also largely dependent on the latitude and other geographic and climatic factors of the collecting site such as the amount of precipitation (amount effect). The latitude effect results in δ^{18}O values becoming increasingly negative with increasing geographic latitude. This is believed to be caused by the following factors: 1) progressive isotope fractionation associated with condensation of water vapour and removal of droplets from the air mass; 2) an increase in the degree of isotope fractionation caused by a decrease in temperature; 3) the re-evaporation of meteoric water from the surface of the earth; and 4) evapotranspiration of water by plants[73] although, these last two effects tend to cancel each other out[85,147]. At lower latitudes temperature fluctuations are less extreme, and oxygen isotopic changes due to temperature changes are minimal.

The amount effect was first observed by Dansgaard[45,92]. This effect is defined as a strong negative correlation between precipitation amount and their deuterium to hydrogen (D/H) ratios and δ^{18}O VSMOW values. This phenomenon was also identified in preceeding studies with tree rings[149], fossil teeth[111] and other ground water studies[45,92,149,232]. When environmental temperatures rise the amount effect threshold (i.e. 20°C), high humidity and high precipitation amounts and ^{18}O abundance in meteoric water decrease[16,59]. Therefore, at low latitudes, the annual wet season is marked by more negative δ^{18}O values than the dry season[156,150].

2.7 Tropical cyclone Stable Isotope Signatures Cave Deposits

In order to understand how stalagmites reveal high-resolution, long-term records of tropical cyclones, palaeoenvironmental and climatic changes, it is important to first review what they are, how they are formed and why they are sensitive to external environmental/climate change. The following section describes the formation and structure of stalagmite layers, including their coloration, optical properties and petrography; and how these have been used in the past to reconstruct environmental change.

A stalagmite is a form of speleothem (or cave deposit), which grows on the floor of a cave and is composed of growth layers of calcite, aragonite, gypsum or halite[101]. As the composition and amount of the drip water feeding the stalagmite is a reflection of conditions above the cave, variations in the annual couplets of a stalagmite can give an indication of environmental changes on the surface through time. For the purpose of this thesis, only the geochemistry, form and deposition of calcite stalagmites will be discussed in depth. For stalagmites to be of use in palaeo-environmental studies they must possess a definable time series. Suitable stalagmites are therefore composed of layers to which a chronology can be attached. Stalagmites (see Figure 2.8) form on the bottom of caves as cave drip water supersaturated with respect to calcium carbonate ($CaCO_3$) falls to the floor and precipitates on top of the growing stalagmite. Successive drips form in chronological layers or strata perpendicular to the growth axis. Stalagmites differ from stalactites which form as the $CaCO_3$ precipitates before falling to the ground; hence these structures form downward from the ceilings of caves typically along joints or bedding planes[125]. Stalactites are often unsuitable for palaeo-environmental studies as the calcite is often not deposited sequentially which therefore obscures the chronology of the layers[226]. In this instance the calcite is deposited in concentric rings around the stalactite forming a hollow centre through which cave drip waters flow. Over time this passage blocks and drip water tends to flow over the outside of the stalactite. Flowstone is another cave formation which has often been used for palaeo-climate reconstruction. These form as drip water flows over the floors and walls of caves precipitating calcite in chronological parallel layers or

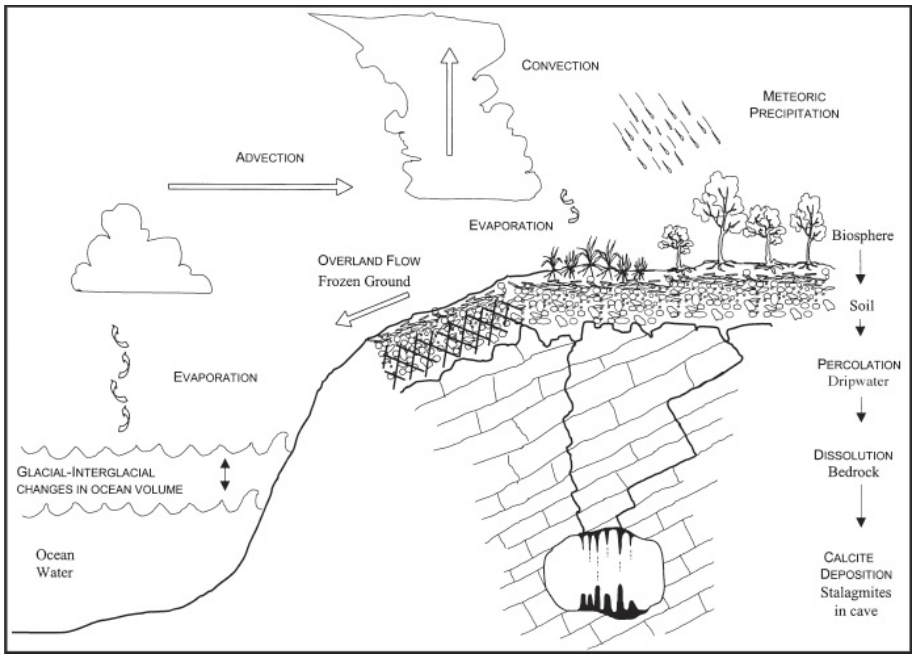

Figure 2.8: Stalagmite Formation adapted from[146].

strata[124,225]. Although stalagmites precipitate calcite in a similar manner to flowstone, they contain the most traceable time lines and have a higher resolution stratigraphy than stalactites or flowstone[226]. Figure 2.8 and eqs. 2.4, 2.5 and 2.6 show the process by which the stalagmite forms. As rainwater falls to the ground above the cave it takes up CO_2, detritus and other minerals from the atmosphere and soil layers. At this point the solution contains a signature of both the isotopic composition of the rainwater and the mineral composition of the soil.

$$H_2O + CO_2 \iff H_2CO_3 \tag{2.4}$$

$$H_2CO_3 + CaCO_3 \iff Ca^{2+} + 2HCO_3^- \tag{2.5}$$

$$Ca^{2+} + 2HCO_3^- \iff CaCO_3 + H_2O + CO_2 \tag{2.6}$$

The addition of dissolved CO_2 from the atmosphere and soil layers forms carbonic acid (2.4). This acidic drip water percolates through fissures in the limestone, eroding the bedrock until the solution becomes saturated with respect to calcium carbonate ($CaCO_3$). This occurs through the dissassocation of the $CaCO_3$ bedrock into its calcium and bicarbonate ions (2.5). Once the solution has reached the cave gallery, the secondary calcium carbonate mineral (in this case calcite) is precipitated on the growing stalagmite. The precipitation of calcite via degassing occurs as the dissolved CO_2 is removed from the solution in an attempt to reach equilibrium with the surrounding cave atmosphere (typically depleted in CO_2 relative to the drip water), resulting in the subsequent mineral precipitation of calcite (2.6)[24,43,94]. In highly evaporative conditions (usually within open cave systems in tropical areas), water is removed from the solution via evaporation rather than degassing. The process by which calcite is deposited becomes more important when analysing the isotope ratio of the calcite layers. The resulting thickness of the calcite layer can therefore give an indication of the amount of precipitation at the site; while the composition of the calcite layer can give an indication of the oxygen isotope ratio of the rainwater at the time of deposition, and the bio-productivity of the soil layer through its

trace element and humic acid content, and carbon isotope ratio.

2.7.1 Colouration, Petrography and Luminescence

Variations in the colour, crystalline structure and optical properties of stalagmite layers have been found to reflect changes in precipitation amount and intensity at the land surface[12,13,11,14,104,146,202,215,226]. For example, as the drip rate increases so to does the growth of the couplet, therefore reflecting changes in the cave reservoir and indirectly, precipitation external to the cave[104,146,226].

Gascoyne[86,226] was the first to conclude that stalagmite luminescence and colouration are caused by humic substances derived from the overlying soil. As the drip waters percolate down through the soil zone they pick up humic substances, trace elements and detrital material which are incorporated into the calcite lattice[104,146,215,226]. Spectroscopic and chemical extraction of humic substances from various speleothems worldwide has shown this to be the case[144,226]. Coloration in speleothems varies from white to pale tan, various shades of orange, red and dark brown which have been found to correspond to the type and quantity of impurities contained in the calcium carbonate solution (see Table 2.1 below).

Table 2.1: Examples of the coloration of layers and the responsible impurities adapted from[24].

Compound	Coloration
Pure Water	White
Iron Hydrate	Bright ochre to brown
Manganese Hydrate	Black
Organic Substances	Yellow, reddish, dark brown and black
Copper	Blue to green

Petrography, within the context of speleothem research, is the study of their crystalline structure. This can be used to define the flow conditions under which calcite layers were deposited[6,95]. Typically, slower drip rates produce laminae containing larger crystals and fewer crystallites with lower concentrations of detritus and oxides due to less soil entrain-

ment in the drip water. Conversely, higher drip rates result in smaller, randomly orientated equant to anhedral crystals with a larger concentration of detritus and oxides[6,95]. Consequently, a couplet of light and dark calcite indicates one years growth. A darker layer is deposited during the onset of the wet season during which large amounts of humic substances are flushed into the system; gradually fading through out the dry season to produce a lighter layer of calcite as the supply is exhausted[215].

The phosphorescent properties of speleothems have been known to speleologists for decades[226] yet it was not until the discovery of annual luminescent banding in stalagmites by Shopov et al.[202] that this property gained increased attention. Speleothem laminae exhibit two optical properties: varying degrees of colour, hue and intensity under visible light; and fluorescence under ultraviolet light. As the amplitude of this luminescence varies parallel to the growth layers, luminescent banding has been used to document climate, in particular rainfall[202]. Baker et al.[12] examined two stalagmites from Poole's Cavern in Buxton England and found that 12% of the stalagmites laminae exhibited double band structure which was attributed to years of high intensity (>60 mm) and high volume (>250 mm per month) rainfall. Yet when compared to the instrumental rainfall record for that region, Baker et al.[12] found that not all high intensity events generated this feature possibly due to soil moisture deficit in summer and/or concurrent months of prolonged rainfall which resulted in an exhaustion of the organic acid supply.

In combination, petrography, luminescence and coloration can give valuable insights into changes in precipitation amounts and temperature over long periods of geological history. As changes in drip rates are a result of changes in the amount of precipitation on the land surface, it is then logical to expect that variations in speleothem laminae crystal morphology may coincide with variations in other climate proxies. In support of this, Ayalon et al.[6] found that the colour, layer thickness, morphology of the crystals and amount of detrital material within the layers of 20 stalagmites collected from Soreq Cave in Israel, closely reflected climate changes as observed through the oxygen isotope ratios (δ^{18}O)

obtained from the samples. The oxygen isotope ratio within drip water reflects changes in the amount and duration of rainfall events and average annual temperature in addition to the initial composition of the source. Given this relationship it is possible to conclude that major changes in crystal morphology and coloration can give an indication of major changes in drip water flow rates and therefore precipitation amounts at the surface.

2.7.2 Carbon and Oxygen Isotopes

The oxygen isotopic composition of a carbonate precipitate is determined by a number of factors. Firstly, the cave temperature effect, which is the thermodynamic fractionation between water and calcite during precipitation (in most cases this is negligible due to meteoric dependent isotopic shifts); the ocean temperature effect, which is the temperature dependent fractionation between the liquid and vapour phase at the source of the atmospheric moisture (ocean source); the amount effect, which is the consistent depletion in δ^{18}O with precipitation amount; lastly, the rainwater composition effect which refers to the interactions between the isotopes during evaporation, condensation and precipitation. In all cases, these effects are a result of isotope fractionation (the enrichment of one isotope relative to another between two substances or within a substance in a chemical or physical process)[73,115]. An understanding of the process of fractionation between ^{16}O and ^{18}O and what influences the degree of fractionation is critical to the interpretation of palaeoclimate signals from δ^{18}O values.

Similarly to oxygen, the stable isotopes of carbon are affected by either isotope equilibrium exchange reactions within the organic carbon system or kinetic isotope effects during photosynthesis[115]. Lauritzen and Lundberg[145,146] highlight the five processes which will affect the δ^{13}C of calcite in speleothems: 1) photosynthetic pathways (i.e. C3/C4 vegetation), 2) biological activity in the soil layer, 3) rainfall, 4) drip rate and 5) water rock interactions. The δ^{13}C of dissolved organic carbon in the cave drip water is derived from processes occurring in the epikarst between biogenic and atmospheric CO_2, water and the limestone following equation 2.6[104].

Biogenic activity of the soil and vegetation above the cave can influence the resulting δ^{13}C of the carbonate and can vary with the amount and type of vegetation above the cave. As the level of soil biogenic activity increases, the δ^{13}C value of CO_2, HCO_3 and CO_3 decrease because of the depletion of ^{13}C in organic matter (Quade et al 1989, Cerling et al 1991, Deines et al 1974, Miotke 1974 cited in[104]). δ^{13}C fluctuations can therefore give an indication of vegetation change over time (see Table 2.2) which is also linked to climatic variations (i.e. cooler or drier climates will lead to higher δ^{13}C and lower δ^{13}C values in wetter warmer periods). However, interpretation of the results can be ambiguous as other factors such as evaporation of recharge water within the soil zone, CO_2 loss during degassing or evaporation within the cave and changes to the routing of recharge water within the epikarst may influence δ^{13}C values; therefore producing questionable results[11, 121, 134, 104, 23, 189].

Table 2.2: Linkages between plant type and their corresponding range of δ^{13}C values[104] * Tieszen and Boutton 1989 cited in[226].

Vegetation Type	Region	Photosynthetic Process	Vegetation δ^{13}C (vPDB)
C4 preferential to ^{13}C	Hot, arid/sub arid	Hatch-Slack	-14 to -12 ‰ — -9 to -18 ‰ *
C3 preferential to ^{12}C	Less arid	Calvin Cycle	-27 to -24 ‰ — -32 to -22 ‰ *

2.7.3 Fractionation between cave drip water and calcium carbonate

The two main fractionation mechanisms which occur between water and the calcium carbonate are isotope exchange reactions (equilibrium isotope distribution), and kinetic processes (differences in reaction rates of isotopic molecules). If the isotopes are exchanged due to equilibrium isotope distribution the isotopes within the calcite are deposited in thermodynamic equilibrium with the cave drip water. The extent of the equilibrium isotope distribution between water and $CaCO_3$ is defined by the equilibrium constant K or more commonly the fractionation factor α defined by the following equation:

$$\alpha_{CaCO_3-H_2O} = \frac{^{18}O/^{16}O_{CaCO_3}}{^{18}O/^{16}O_{H_2O}} \tag{2.7}$$

In this instance the partitioning of the lighter and heavier isotopes of oxygen between or within a compound is related to its vibrational energy which is solely dependent on temperature. As cave temperatures remain relatively constant, the temperatures derived from the δ^{18}O (δ^{18}O of the calcite) often represent the ocean temperature effect and therefore regional temperature changes over time by the equation below:

$$10^3 In\ \alpha_{CaCO_3-H_2O} = 2.78[10^6(T(K)^{-2})] - 2.89 \tag{2.8}$$

In this relationship, αCaCO$_3$ - H$_2$O decreases linearly with increasing temperature such that a drop of 0.28‰ δ^{18}O equates to an increase in 1°C. Thermodynamic equilibrium is achieved in closed systems where there is minimal evaporation and slow degassing rates. Therefore, the oxygen isotopes are deposited in equilibrium with the cave drip water (which is representative of the rainwater external to the cave). However, should the cave be subject to highly evaporative conditions (i.e. if the cave is relatively open) the fractionation of the oxygen isotopes occurs via differences in the reaction rates of the isotopes (kinetic fractionation)[43,56,57,94,104,125,146,225,226]. In this instance, ^{16}O is preferentially removed and the isotopes are deposited out of equilibrium with the cave drip water. In this case the δ^{18}O values cannot give a clear indication of the isotopic composition of the precipitation and/or temperature changes overtime.

One method for testing if calcite has been deposited in equilibrium uses the Hendy Criteria[23] which analyses a series of samples along the same layer. If the calcite has been deposited in thermodynamic equilibrium, minimal variation in δ^{18}O is expected (i.e. less than 0.8‰) while δ^{13}C will change progressively from the apex toward the edge of the layer due to the limited amount of bicarbonate within the solution[104,146,226]. Kinetic fractionation will reveal an enrichment of δ^{18}O which is >0.8‰ and the progressive enrichment of δ^{13}C which is almost twice that of δ^{18}O[75,104,226]. Variability in δ^{18}O indicates kinetic fractionation as during evaporation, ^{16}O will be removed from the solution quicker towards the sides of the stalagmite as this is where the layer is at its thinnest and slower in the centre where it is thickest. Fischer, et al[75] and Williams[228] argue that a progres-

sive enrichment of δ^{13}C and δ^{18}O should be expected from low latitude carbonates as the amount effect, the composition of the precipitation and circulation patterns have a greater effect on δ^{18}O in low latitude terrestrial carbonates than temperature (which dominates in temperate regions). In addition, Fisher[74] points out that samples taken from caves whose relative humidity is close to 100% may still be deposited in equilibrium as kinetic fractionation is limited. The amount of detritus in solution and thus δ^{13}C is a reflection of plant productivity which increases proportionally to soil moisture. As plants preferentially use the lighter isotope (^{12}C) during photosynthesis, increased plant productivity results in an enrichment of the heavier isotope (^{13}C)[157] and thus more negative values of δ^{13}C in the soil which is in turn reflected in the cave drip waters. Therefore, if the calcite of a low latitude carbonate has been deposited in equilibrium, a Hendy test should reveal minimal variation in δ^{18}O (i.e. $>0.8‰$) along the growth horizon and covariance between δ^{18}O and δ^{13}C.

2.8 Conclusion

Concerns over climate change and the possible economic and social impacts of a warming climate have prompted scientists to investigate what effect this could have on the frequency and severity of severe weather events such as tropical cyclones. In order to accurately predict future tropical cyclone frequencies and intensities we must first be able to decouple anthropogenic influences from natural variability. The purpose of this review was therefore to investigate methods of achieving this separation.

A number of approaches have been explored including the use of statistical techniques to extrapolate historical trends either alone or in combination with GCM outputs and geological datasets which examine prehistoric trends. Whist each approach has its advantages, neither dataset alone is sufficient to predict future tropical cyclone climatology under changed climate conditions. Limitations in the length of the detailed instrumental record and issues with its accuracy gives rise to a large degree of uncertainty when modelling future change using statistical methods. The low resolution of current GCMs and a

limited knowledge of how phenomena such as ENSO may behave in future further complicates the issue. Palaeo records such as those obtained from sedimentary or erosional evidence may provide a greater understanding of the natural variability of these systems. Stalagmites are ideal in that they may record annual variation in tropical cyclone activity irrespective of the storms magnitude as their strata are deposited annually. These are not reworked by other events and are somewhat protected from external weathering and erosive processes. While sedimentary records of marine inundation may have the potential to be confused with other inundation events such as riverine flooding and tsunami, neither is possible in the stalagmite record.

This new avenue of investigation has the potential to solve at least some of the current issues in the other methods discussed above. These records cannot provide a detailed account of the structure of individual storms as the intensity of these events is not yet quantifiable. Each record is limited somewhat in its spatial extent as only those tropical cyclones which pass within the vicinity of the cave are recorded. In this sense, the stalagmite record may be considered of lower resolution than the instrumental record. However, stalagmites do provide an annual record of occurrence which may span thousands of years depending upon the length of the sample. This high temporal resolution gives a greater picture of tropical cyclone frequency overtime and allows for a more detailed examination of the natural variability of these storms. The greatest advantage of these records is that they can provide information on the activity of these storms over time, the corresponding climatic conditions external to the cave and they span both the historical and prehistorical periods of interest.

Chapter 3
General Methods

3.1 Study site, sample selection and preparation

The stalagmites used in this analysis were selected based on the four stage screening process proposed by Frappier[79]. In this, we collected two stalagmites from regions which were vulnerable to tropical cyclones (i.e. those within 5-20°N or S of the equator) in areas where there was no interference from frosts or snow; from regions which exhibit distinct summer and winter rainfall patterns so as to ensure visible seasonal banding; stalagmites with relatively rapid growth $>$80μm annually; caves which were sufficiently deep to promote a stable environment where relative humidity is high, and ventilation is minimized; samples from areas which were not subject to flooding so as to preserve the stalagmite; and caves which are seldom frequented by humans so as to minimize any anthropogenic disturbance.

Two unique sites were chosen which pass each of the criterion listed above yet significantly differ both environmentally and geographically. The first was selected from the East of the continent (Chillagoe, Queensland: stalagmite CH-2) 120km inland from the Queensland coast; and a second from the West coast of the continent (Cape Range National Park, Western Australia: stalagmite CR-1) (Fig. 3.1).

3.2 Geological and Environmental Setting

The Chillagoe limestone terrain is located at 17.2°S and 144.6°E in northeast Queensland, Australia. Chillagoe falls within the summer dominant rainfall zone of Australia and on average receives approximately 858mm of rain each year, 84% of which falls between the months of December - March (fig. 3.2a). The dry season persists from April - October

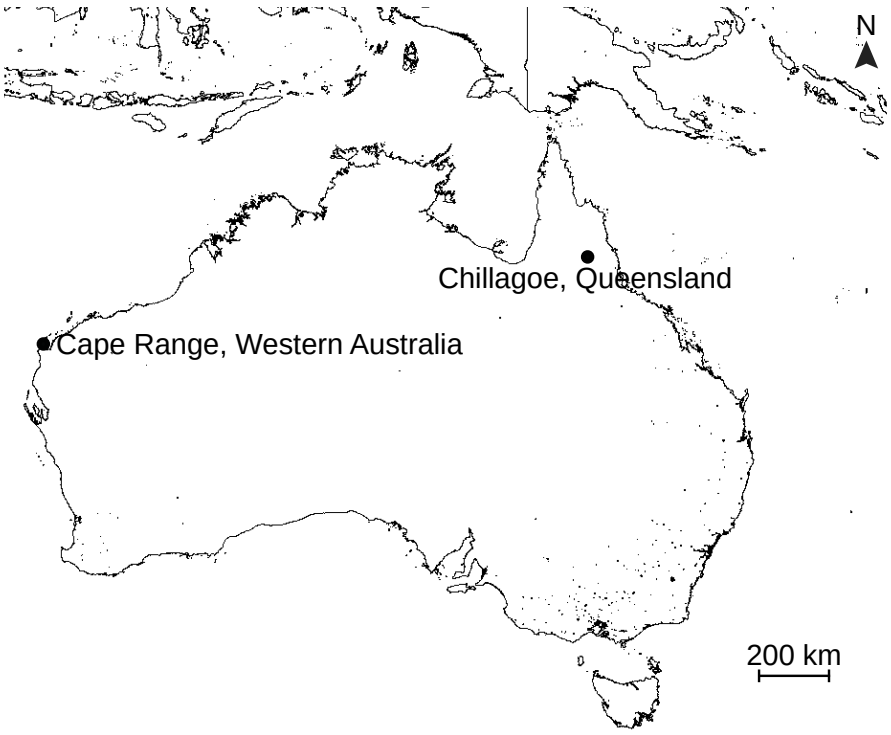

Figure 3.1: Map of the study area. Cave locations across tropical Australia.

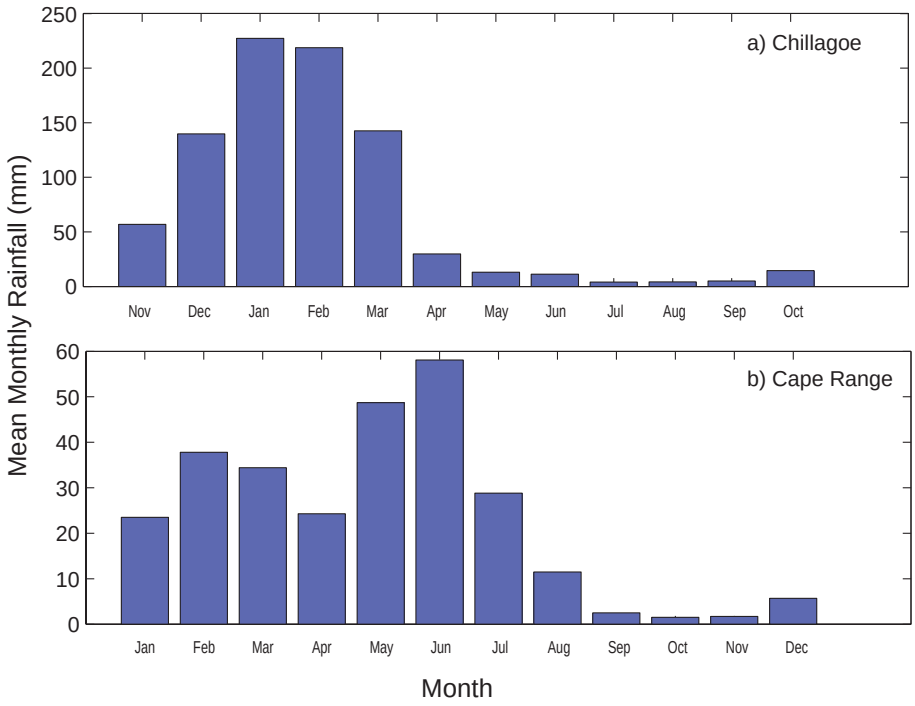

Figure 3.2: Instrumental Rainfall Data for Chillagoe (a) and Cape Range (b).

during which the region receives on average ∼20mm of rain per month. Monthly maximum and minimum temperatures are also indicative of the region's marginal status with maximum daily temperatures reaching 38°C during the summer months and a maximum of 25°C during the winter[25]. The landscape is characterised by dry tropical woodland and patches of deciduous vine thicket. Cape Range (22.10°S, 114.00°E), is situated on the western side of the North West Cape, 20km West of Exmouth on the Western Australian Coast. This coastal region receives on average 260mm of rainfall annually, 84% of which falls within the wet season (January-June) (fig. 3.2b). With an average annual temperature of 32°C[26]. Tertiary limestone ranges dominate the landscape with Acacia shrubs, sparse Eucalypt and hummock grasslands. Whist the western coastal plain is dominated by Melaleuca, Hibbertia and spinifex[129].

3.3 Analytical procedures

CH-2 and CR-1 are regular, symmetrical candle stalagmites exhibiting a very slow (spanning thousands of years) reduction in width over time. The stalagmites exhibit annual couplets of alternating light and dark calcite layers of lenticular shape. The diameters of the stalagmites are large i.e. 5-11cm (CH-2) and 6-8cm (CR-1). The stalagmites were each sectioned along their growth axes using a water-cooled diamond saw and a 1-2cm thick section prepared from one half. The remaining half was then archived. The centred face of the working sections were polished using fine sandpaper and steel wool in order to accurately resolve individual growth layers (fig. 3.3). The samples were then cleaned with UHQ water in an ultrasonic bath. These prepared sections were then sealed and stored when not in use.

In order to maximise the length of the series, only the dark layers of calcite representing wet season deposition were analysed as tropical cyclones occur during the monsoon season. The most recent 1500 dark calcite layers from each stalagmite were sub-sampled using a video-controlled micromill, comprising 3000 subsamples in total. The stalagmite sections were viewed in real time via a high-resolution digital camera, controlled by a

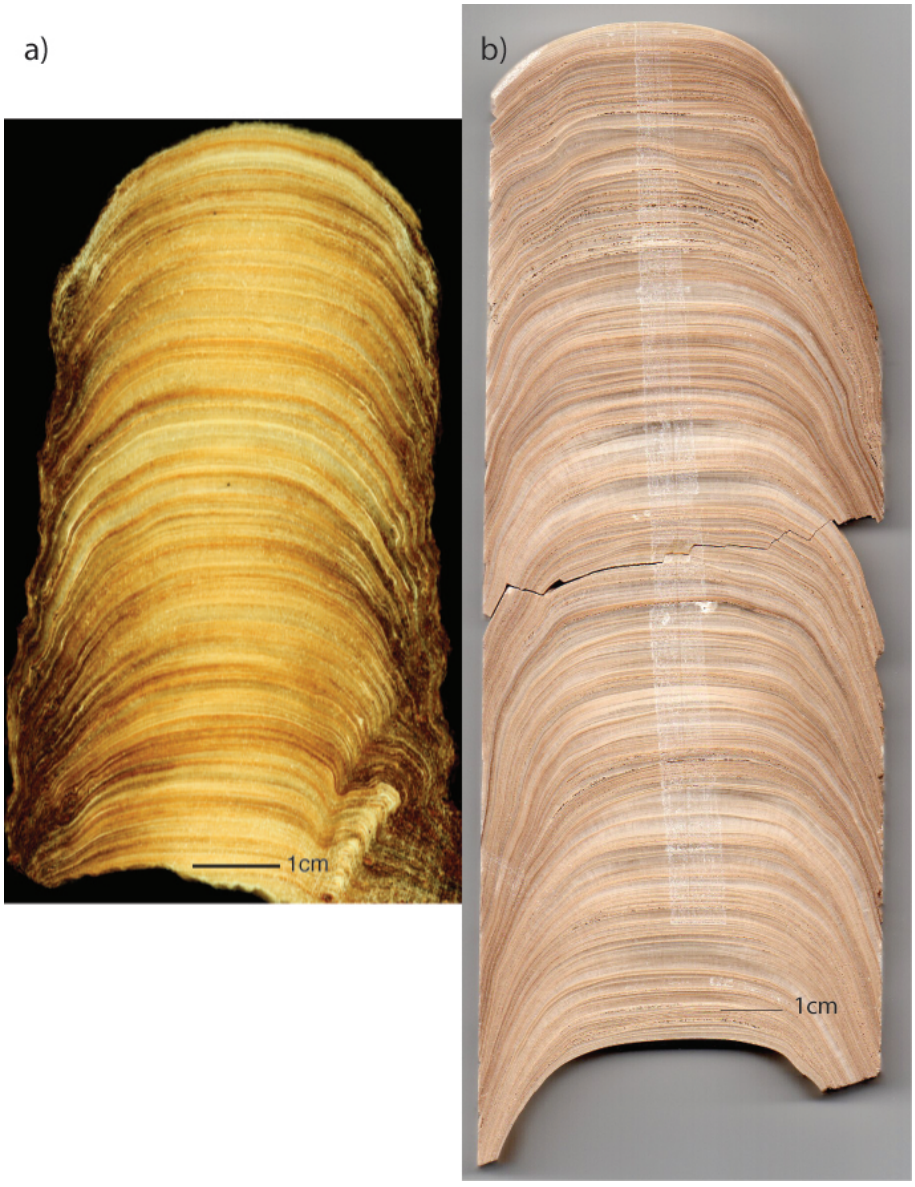

Figure 3.3: Profiles of CH-1(a) and CR-1(b) after they had been sectioned along their growth axis and polished so that their annual increments (couplets) could be resolved.

fourth linear actuator and motion controller for motorized focusing. Sample paths were digitized onto the image of the specimen in real-time, using an array of x-y-z coordinates. Trenches (10mm long, 60µm wide) were milled from the centre of the stalagmite in most cases extending 5mm each side of the growth axis. These trenches were kept well within half the radius of the sample in order to avoid collecting material towards the flanks. A modified dental drill was then used to mill a minimum of 10µg of carbonate according to the coordinates of the sampling paths. The powdered sample was collected from the specimen manually using a narrow scalpel and fine paintbrush. The dental drill and sample were thoroughly cleaned after each pass using compressed Ar or N and Ethanol. Oxygen and carbon isotope analyses were performed at the University of Utrecht using a Kiel III carbonate device coupled to a Finnigan MAT 253 IRMS. The calcite samples were reacted with 3 drops of H_3PO_4 at 70°C. Replicate analysis of the standard NBS-19 resulted in a standard deviation of 0.04‰ for δ^{13}C and 0.06‰ for δ^{18}O. All measurements are reported relative to Vienna PeeDee Belemnite (vPDB).

3.4 Hendy Test for Equilibrium Isotope Deposition and Cave Temperature Effect

To ensure that the isotopes within the calcite had been deposited in equilibrium with the cave drip water a Hendy Test for equilibrium deposition was conducted at 4.09cm and 16.2cm from the apex on CH-1 and CR-1 respectively. 3-5 subsamples were milled for each test at 1-8mm intervals along the growth horizon from the centre of the layer to the flanks. The Hendy test reveals a variation of 0.27‰ and 0.61‰ in δ^{18}O and 0.29‰ and 0.77‰ in δ^{13}C respectively. Both stalagmites pass Hendy's[110] first test for equilibrium as the variation in δ^{18}O is below 0.8‰ and neither exhibits significant progressive enrichment in either δ^{18}O or δ^{13}C towards the flanks. Whist the variation in δ^{13}C is greater than that of δ^{18}O, neither sample exhibits a range $>$0.8‰ (fig. 3.4).

3.5 Testing for Temperature Dependence

The δ^{18}O of temperate stalagmites is often used as a palaeotemperature proxy due to the relationship between temperature and oxygen isotope fractionation. In this, fractionation between carbonate and water is reported as between -0.24 to -0.28 per °C[158,194]. The measured δ^{18}O for the last 100 years of deposition are given in fig. 3.5. δ^{18}O varies considerably between years. Observed differences between maxima and minima over the time period are 4.38‰ (CH-1) and 5.81‰ (CR-1). Calcite in CR-1 is on average 2‰ lighter than CH-1 and exhibits annual perturbations of greater magnitude. In both locations δ^{18}O is highly variable between wet seasons, yearly differences range from -1.6‰ to 2.08‰ in CH-1 and -2.5‰ to 2.2‰ in CR-1. This implies a shift in annual temperatures of 6°C - 8°C. Should these δ^{18}O results be simply a function of temperature changes, this data would imply a difference in average annual temperatures over the last 100 years of 16°C in Chillagoe and 21°C in Cape Range which is neither probable nor present within the temperature records for the regions (see fig. 3.6).

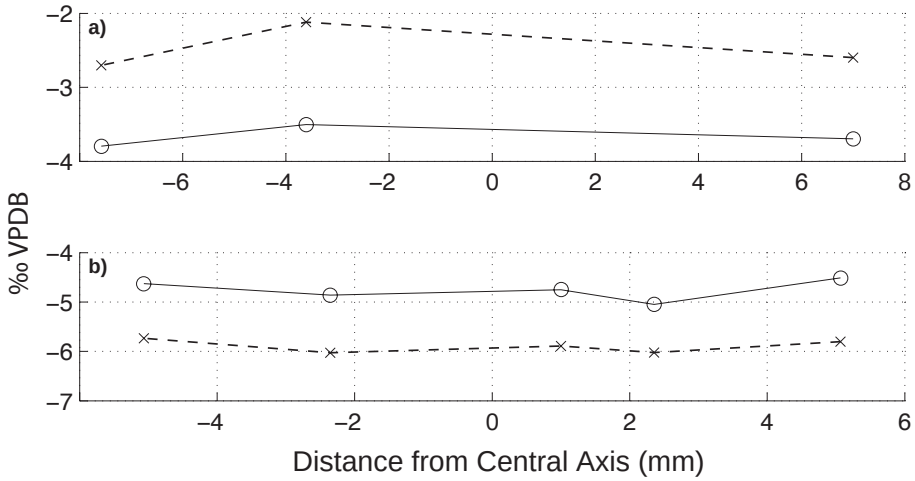

Figure 3.4: Hendy test for equilibrium isotope deposition in CH-1 (a) and CR-1 (b).

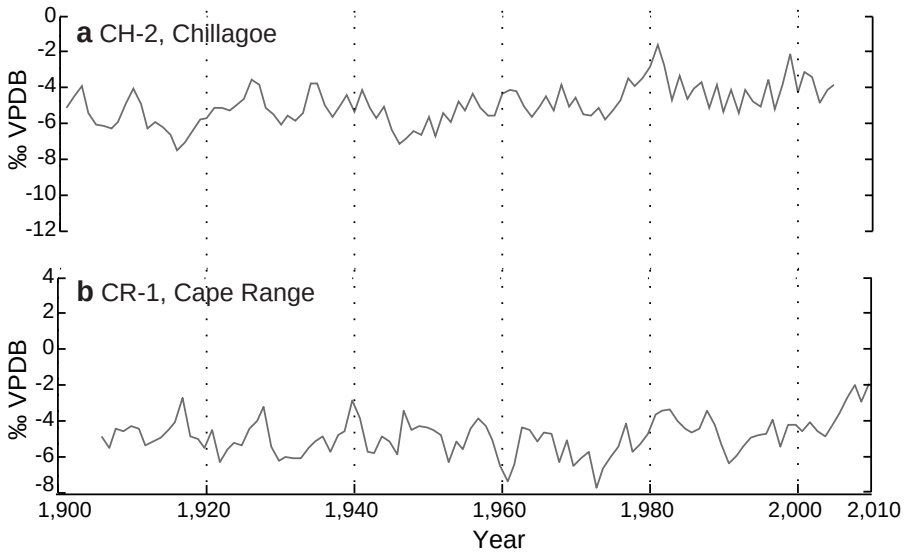

Figure 3.5: Wet season calcite δ^{18}O from samples CH-1 (a) and CR-1 (b), between 1906-2010

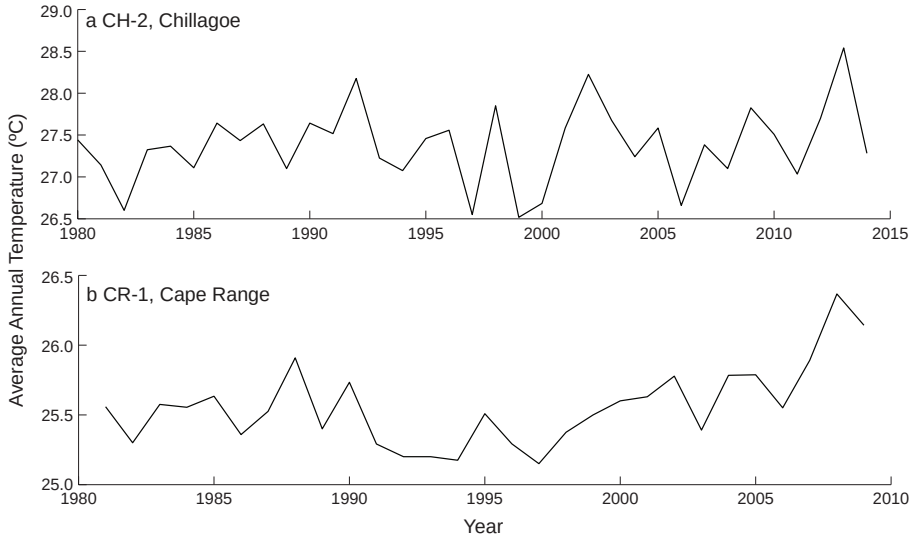

Figure 3.6: Instrumental temperature records for sites CH-1 (a) and CR-1 (b), between 1906-2010

Chapter 4

Australian tropical cyclone activity lower than at any time over the past 550 - 1,500 years

Jordahna Haig [1] Jonathan Nott [1] Gert-Jan Reichart [2,3]

[1] *Centre for Tropical Environmental and Sustainability Science, School of Earth and Environmental Science, James Cook University, Cairns, 4870 QLD, Australia.*

[2] *Department of Geochemistry, Utrecht University, Utrecht 3508 TA, The Netherlands.*

[3] *Geology Department, Royal Netherlands Institute for Sea Research, Den Hoorn (Texel) 1797 SZ, The Netherlands*

Published in: *Haig et al 2014. Nature 505(7485): 667-671.*

Assessing changes in tropical cyclone activity within the context of anthropogenically influenced climate change has been limited by the short temporal resolution of the instrumental tropical cyclone record[131,189] (less than 50 years). Furthermore, controversy exists regarding the robustness of the observational record, especially before 1990[105,126,142]. Here we show, on the basis of a new tropical cyclone activity index (CAI), that present low levels of storm activity on the mid west coast and northeast coast of Australia are unprecedented over the past 500 to 1,500 years. The CAI allows for a direct comparison between the modern instrumental record and long-term palaeotempest (prehistoric tropical cyclone) records derived from the $^{18}O/^{16}O$ ratio of seasonally accreting carbonate layers of actively growing stalagmites. Our results reveal a repeated multicentennial cycle of tropical cyclone activity, the most recent of which commenced around AD 1700. The present cycle includes a sharp decrease in activity after 1960 in Western Australia. This is in contrast to the increasing frequency and destructiveness of Northern Hemisphere tropical cyclones since 1970 in the Atlantic Ocean[62,64,65] and the western North Pacific Ocean[64,65]. Other studies project a decrease in the frequency of tropical cyclones towards the end of the twenty-first century in the southwest Pacific[65,195], southern Indian[195,238] and Australian[1] regions. Our results, although based on a limited record, suggest that this may be occurring much earlier than expected.

4.1 Introduction

Trend analysis of the instrumental tropical cyclone record has proven difficult owing to errors associated with changes in observational techniques (leading to inaccurate intensity estimates and storm counts in the recent past), detection issues, data homogeneity issues[64, 142, 179] and inconsistent procedures between and within agencies[105, 126, 131, 142]. As a result, differentiating natural variability from anthropogenically induced change is complicated; this may also explain to a certain extent the disparity between current trend estimates[64, 138].

In an effort to remedy this we have developed a new technique, which calibrates high-resolution, long-term palaeorecords of tropical cyclone activity against the instrumental tropical cyclone record. This scale allows for a direct comparison between the past and present, and enables an examination of tropical cyclone climatology at higher temporal resolution and on annual, decadal or millennial scales simultaneously, without the need to interpolate or extrapolate to account for missing data. Our tropical cyclone activity index (CAI), is based on tropical cyclone activity indices developed by the National Oceanic and Atmospheric Administration and others, which describe the severity of a season in terms of the number of storms, their intensity (V_{max}), their size (R_{max}) and their longevity. These indices include the accumulated cyclone energy index[19], the revised accumulated cyclone energy index[233], the power dissipation index[64] and the hurricane intensity index[127] (see Section 4.2). CAI is the average accumulated energy expended over the tropical cyclone season within range of the site, accounting for the number of days since genesis and the intensity and size of the storm relative to its distance from the site at each point along its track (fig. 4.1):

$$CAI = \frac{1}{N}\sum_{n=1}^{N} K_n \tag{4.1}$$

where $K_{n,t} = (K_t + K_{t-1})_n$, $K_t = R_{max}(t)/d(t)$, N is the number of storms within the season, n is each individual storm, t denotes the point along the storms track in time, recorded at 6 hourly intervals, d(t) is the distance from the site in kilometres at time t, $V_{max}(t)$ is the

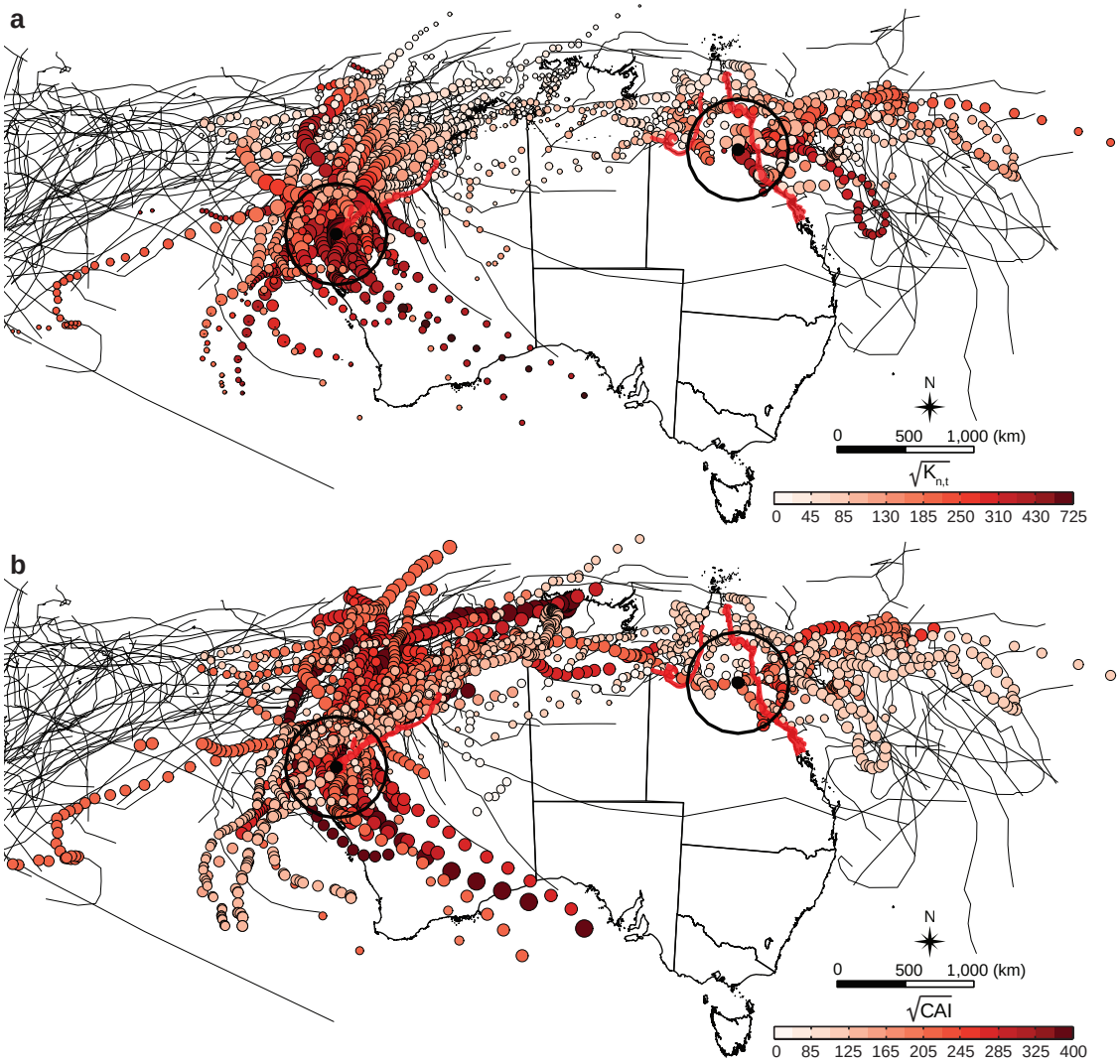

Figure 4.1: Site map showing the four-stage calculation of CAI. Chillagoe and Cape Range (black points) are shown with the 400-km radius around each study site. Tropical cyclones that did not track within the study area during the training period in Queensland and Western Australia are shown in black. Red shading indicates the coastlines most prone to tropical cyclones in both states. a, Tropical cyclones from the 1990-2010 training period and their corresponding K_t value (point size), showing the influence of V_{max}, R_{max} and distance; cumulative $K_{n,t}$ values are shown in colour. b, Point size indicates K_n (individual storm averages) calculated from a and subsequent seasonal CAI values (gradated colour).

maximum 10-minute mean wind speed in metres per second at time t, and R_{max}(t) is the radius of maximum winds in kilometres at time t.

Tropical cyclones produce precipitation that is depleted in the heavier oxygen isotope (^{18}O) by $>$6‰ relative to average monsoonal precipitation, owing to the recycling of water within the system, high condensation efficiency and large size and longevity of such cyclones as intense convective systems[88]. The resulting δ^{18}O content (expressed as δ^{18}O = [(^{18}O/^{16}O)sample/(^{18}O/^{16}O)standard- 1)]x 1000‰) of tropical cyclone precipitation at a site is influenced by a number of factors, including the number of days since genesis (that is, rainout) and the intensity of the storm, its source region[156] and the distance of its centre from the sampling path. Because tropical stalagmites are archives of monsoonal δ^{18}O, signatures of past tropical cyclones are also recorded within the δ^{18}O of their carbonate layers, typically within 400 km of the storm centre[82,188].

4.2 Methods

Two cylindrical stalagmites were collected from regions in Queensland and Western Australia prone to tropical cyclones (Chillagoe in Queensland, stalagmite CH-1; Cape Range in Western Australia, stalagmite CR-1). Both show a continuous, uninterrupted record of distinct seasonal growth banding composed of alternating layers of dark and light calcite corresponding to wet- and dry-season deposition. The first 1,500 wet-season (dark-calcite) layers were analysed for their carbonate δ^{18}O. Observed differences between maxima and minima in δ^{18}O over the time period are 4.38‰ (CH-1) and 5.81‰ (CR-1). In both locations, δ^{18}O is highly variable between wet seasons: yearly differences range from -1.6‰ to 2.08‰ in CH-1 and from -2.5‰ to 2.2‰ in CR-1, which are too large to be explained by a cave temperature effect because this would imply a shift in annual temperatures of 6-8°C (ref.[175]). Neither CR-1 nor CH-1 exhibits a significant relationship between δ^{18}O and the seasonal rainfall total, the annual rainfall total or the number of rain days at the sites (Spearman's Rho (ρ)$<$0.07, P $>$0.5 and $\rho<$-0.08, P $>$0.2 respectively). In the absence of cave temperature or rainfall 'amount effects' we conclude that

rainfall composition rather than cave temperature and rainfall amount or frequency, or both, influences the resulting δ^{18}O. However, periods of non-tropical cyclone rainfall and changes in the strength of the Australian-Indonesian monsoon are expected to dilute the cave reservoir. Stalagmite monsoon records from latitudes below 8°S (which are therefore less influenced by tropical cyclone activity) show variations of up to 0.7‰ to 1.2‰ (ref.[97]) over a 1,500-yr period. These values are considerably less than the 4‰ to 6‰ variation between the maxima and minima and the 1.6‰ to 2.5‰ seasonal variation within the stalagmite δ^{18}O presented here. Nevertheless, we account for the monsoonal contribution to δ^{18}O using empirical methods for determining the average value of precipitation δ^{18}O VSMOW (that is, δ^{18}O where the standard is Vienna standard mean ocean water) at both sites, and we account for centennial scale changes in monsoonal activity using published Australian-Indonesian monsoon records[97].

4.2.1 Analytical Procedures

The most recent 1,500 dark-calcite layers representing wet-season deposition were sub-sampled using a video-controlled micromill. Oxygen and carbon isotope analyses were performed using a Kiel III carbonate device coupled to a Finnigan MAT 253 IRMS. Each calcite sample was reacted with three drops of H_3PO_4 at 70 °C. Replicate analysis of the standard NBS-19 resulted in a standard deviation of 0.04‰ for δ^{13}C and 0.06‰ for δ^{18}O. All measurements are reported relative to Vienna PeeDee Belemnite (VPDB). To ensure that the isotopes within the calcite had been deposited in equilibrium with the cave drip water, we conducted a Hendy Test for equilibrium deposition at 4.09 and 16.2 cm from the apex on CH-1 and CR-1 respectively. 4-5 subsamples were milled for each test at 2-5mm intervals along the growth horizon from the centre of the layer toward the flanks. Both stalagmites pass Hendy's first test for equilibrium[110] because the maximum variation in δ^{18}O across the layer is less than 0.8‰ (specifically 0.27‰ for CH-1 and 0.61‰ for CR-1) and neither stalagmite exhibits progressive enrichment in either δ^{18}O or δ^{13}C towards the flanks.

4.2.2 CAI formulation

We calculate $K_{n,t}$ for each tropical cyclone that passes within 400 km of either of the two sites, at each observation point along its path since genesis. $K_{n,t}$ is cumulative, and so reflects not only the condition of the system at time t but also its history up until that point:

$$K_{n,t} = (K_t + K_{t-1})_n \tag{4.2}$$

$$K_t = \frac{V_{max}^3(t) R_{max}(t)}{d(t)} \tag{4.3}$$

Here n enumerates individual storms, t denotes the point along the storms track in time, these are recorded at 6 hourly intervals, d denotes the distance from the site in kilometres at time t, V_{max} is the maximum 10-minute mean wind speed in metres per second at time t and R_{max} is the radius of maximum winds in kilometres at time t. The resulting δ^{18}O of the stalagmite carbonate is an average of the collective precipitation events over a season, and we therefore average rather than sum the resulting $K_{n,t}$ values. Thus, CAI is the average accumulated energy expended over the tropical cyclone season within range of the site, accounting for the number of days since genesis of the storm and the intensity and size of the storm relative to its distance from the site at each point in time:

$$CAI = \frac{1}{N} \sum_{n=1}^{N} K_n \tag{4.4}$$

Here N is the number of storms within the season.

CAI differs from the accumulated cyclone energy index, the revised accumulated cyclone energy index, the power dissipation index and the hurricane intensity index in that it is tailored to reflect the effects of tropical cyclone activity on the resulting δ^{18}O of the carbonate layers. CAI is location specific (that is, it accounts for the distance between the site and the centre of the storm track) and gives an average of these tropical cyclone events rather than the sum of the total energy expelled within a season. Because tropical cyclone δ^{18}O precipitation values are radially asymmetrical within a storm (4.2), the inclusion of

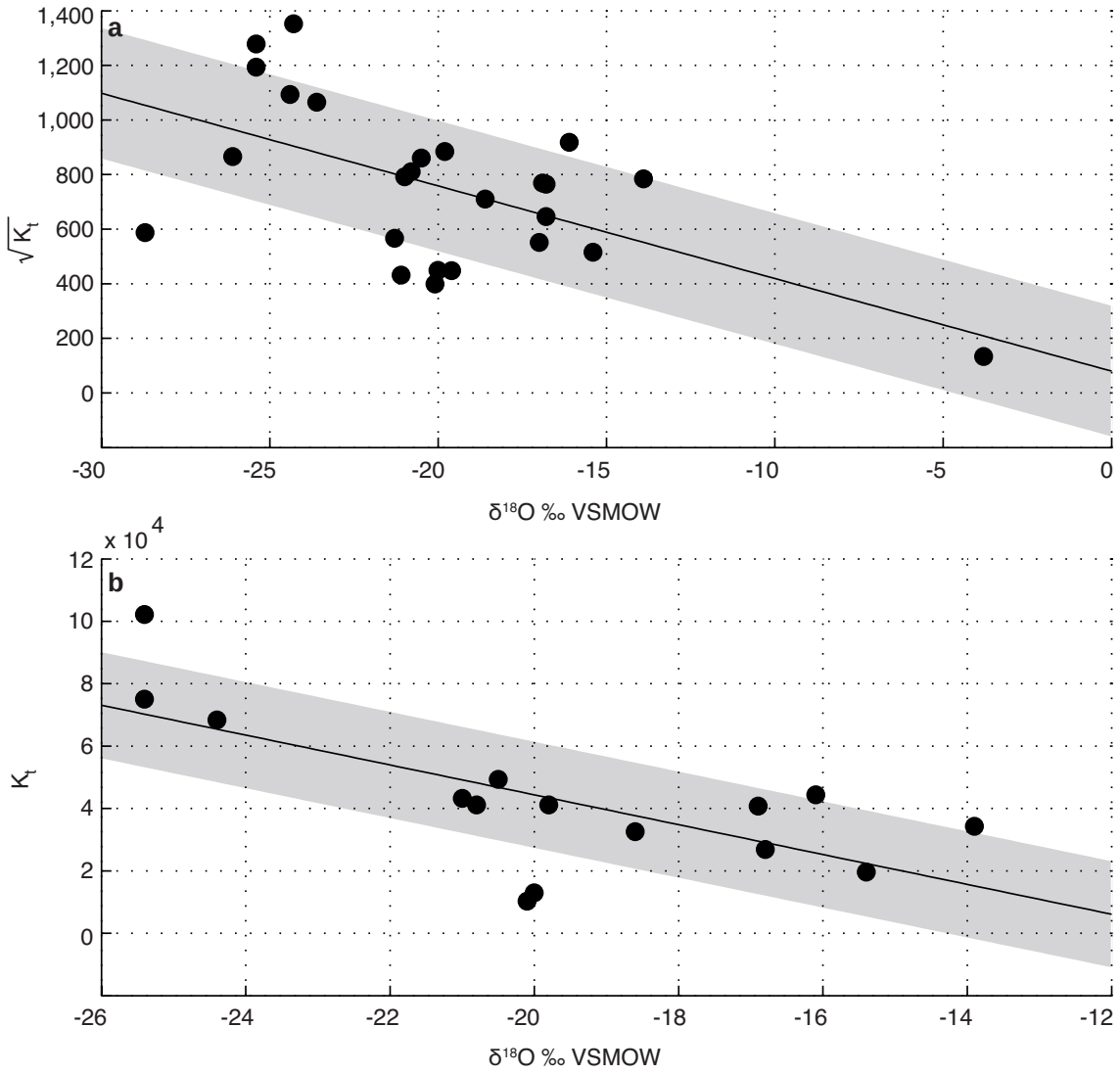

Figure 4.2: δ^{18}O VSMOW measured from Hurricane Olivia (1995) versus the calculated K_t values for the corresponding measurement interval. a, δ^{18}O versus K_t for all rain types in Hurricane Olivia, r = -0.58, P = 0.02, n = 25. b, δ^{18}O versus K_t within the eye wall. Shaded area indicates the r.m.s.e, r = -0.70, P = 0.02, n = 15.

distance in the calculation of K_t has a dampening effect on the resulting K_n value of that storm with increasing distance. As such, a tropical cyclone located 400 km from the study site at K_t = 1, is weighted less than when located 200 km from the site at K_t = 2, given the same V_{max} and R_{max}. $K_{n,t}$ does not, however, take into account the angle of approach (for example, the parameter d does not take into account the orientation of the system relative to the study site and does not distinguish between approach or retreat of the system).

4.2.3 K_t versus δ^{18}O VSMOW

In the absence of tropical cyclone rainfall measurements in Australia, to test how well K_t is reflected in the δ^{18}O of tropical cyclone precipitation we calculated the corresponding K_t values for Hurricane Olivia (a 1994 eastern North Pacific hurricane) using the NHC's updated HURDAT Best Track Database[183]. These were compared against δ^{18}O VSMOW measurements[155] made at 30-min intervals between 24 and 26 September 1994. The results are plotted in Fig. 4.2. We find that δ^{18}O depletion increases with increasing K_t (ρ = -0.5, P = 0.02, n = 25), supporting our derivation of K_t and, thus, CAI. Within the eyewall (the ring or belt of thunderstorms surrounding the central eye within the radius of maximum wind), R_{max} is statistically not significant, K_t in 4.2b is therefore calculated as a function of V_{max} and distance alone.

4.2.4 De-trending monsoon

Because tropical cyclone rainfall accounts for 20.05% and, respectively, 17% of the total rainfall at Chillagoe and Cape Range, it is necessary to exclude the average monsoonal component of the stalagmite carbonate ($\delta^{18}O_M$). We estimated $\delta^{18}O_M$ at Chillagoe and Cape Range using:

$$\delta^{18}O(‰) = -0.005Longitude(^\circ) - 0.034Latitude(^\circ) - 0.003Altitude(m) - 4.753 \quad (adjusted\ R^2 = 0.79) \tag{4.5}$$

$$\delta^{18}O = (6.67 \times 10^{-6})P^2 - 0.009P + 0.015Eva + 0.007Rad - 9.670 \quad (adjusted\ R^2 = 0.645) \tag{4.6}$$

which are empirical equations for geographical (eq. 4.5) and local (eq. 4.6) meteorological controls on δ^{18}O derived from an analysis of Global Network of Isotopes in Precipitation (GNIP) and instrumental meteorological data[161]. Here P is total monthly precipitation, Eva is average monthly evaporation and Rad is average monthly radiation. Rainfall events 3 days on either side of a tropical cyclone event within 400 km of our sites were excluded from our calculations. It is important to note that Liu's geographical model does not take into account factors such as the source region, transport and condensation history of the air masses. Precipitation at Chillagoe is derived from sources in the Coral Sea and the Gulf of Carpentaria. These may have originally been part of a larger air mass, which has travelled north from cooler waters or south from warmer waters. In contrast, precipitation at Cape Range is largely derived from oceanic air masses from the Indian Ocean. However, at this stage there are no other longitudinal, in-depth analyses of δ^{18}O in precipitation from the east or west coast of Australia excepting the model used here from ref.[161]. Using this relationship and local historical climate data from the two sites, we calculated the average seasonal $\delta^{18}O_M$ VSMOW from 1990 to 2010. $\delta^{18}O_M$ was then normalized and used to de-trend the modern δ^{18}O to remove the modern monsoonal trend. $\delta^{18}O_M$ beyond the instrumental record was de-trended from the δ^{18}O data using a spline-interpolated, normalized data set generated from an established Australian-Indonesian monsoonal proxy record[97]. This record has a resolution of 10 yr and extends from 7 yr BP to 12,000 yr BP, the region experiences a relatively low tropical cyclone frequency (on average, 0.24 tropical cyclones per year pass within 400 km of the site[27]), and the record is comparable with other established monsoonal records from the region[97].

4.2.5 CAI calculation from the Australian tropical cyclone database

From the period 1990-2010, CAI values for Chillagoe and Cape Range were calculated within 400 km of each site using the data available within the Australian Bureau of Me-

teorology's tropical cyclone database[27]. Of the tropical cyclones recorded within the database, 32 and 35 passed within 400 km of Chillagoe and Cape Range, respectively. Of the 2,114 observation points within the combined data sets, 225 do not contain wind speed measurements. Given the limited number of environmental pressure measurements available, V_{max} was estimated using the Atkinson/Holliday wind-pressure relationship[3]:

$$V_{max} = 0.514[6.7(1010 - P_c^{0.644}] \tag{4.7}$$

Here P_c is the central pressure in millibars and V_{max} is the maximum 10-minute mean wind speed in metres per second. There was an average discrepancy of 3 m s^{-1} between the value of V_{max} estimated using eq. 4.7 and the recorded V_{max} (Dvorak technique[217]) within the remaining 1,889 observations. Missing R_{max} estimates from 1,702 observations were calculated using[229].

$$R_{max} = 46.4exp(-0.0155V_{max} + 0.0169\varphi) \tag{4.8}$$

An average discrepancy of 17.5 km was found between the measured and estimated values.

4.3 Results

Figure 4.4 shows the relationship between CAI, calculated from 'best tracks' in the recently updated tropical cyclone database for the region[27], and the de-trended δ^{18}O (that is, $\delta^{18}O_A$) for the corresponding period 1990-2010. The model predicts CAI well in 67% of cases (P <0.001) within the $\delta^{18}O_A$ range of -6.37‰ to -1.03‰. As such, larger negative excursions in δ^{18}O correlate with higher CAI values. Although this range is representative of the data obtained from the whole series (2,276 measurements in total), $\delta^{18}O_A$ values that fall outside the model range may not be calculated effectively. However, $\delta^{18}O_A$ values exceeded or fell below the range in only 28 or 88 cases, respectively. Of these, only four were more than 1 s.d. outside the range. Each series was standardized before statistical analysis. No patterns are discernable within the residuals and an even spread of error

is indicated. The relationship is expressed as follows:

$$CAI = (-40.27\delta^{18}O_A = 43.12)^2 \tag{4.9}$$

Because our CAI-$\delta^{18}O_A$ relationship was developed using best-track records for 1990-2010, our model is not likely to be subject to the degree of intensity bias generated by changes in observational techniques. Nonetheless, when the period of investigation is extended to include 1970-2010, the relationship between CAI and $\delta^{18}O_A$ still holds (Pearson's correlation coefficient (r) = -0.5, P = 0.0001, n = 60) and the average difference in model estimates of CAI is 103 that is, less than half the r.m.s.e. of the model. In addition, CAI after 1990 is modelled from $\delta^{18}O$ and is therefore not subject to the same errors noted previously in the pre-1990 instrumental and historical data sets.

Figure 4.4a and c give the calculated CAI values over the past 1,500 and 700 yr in Cape Range and Chillagoe, respectively. Although it is clear from the analysis of instrumental records that the west coast of Australia is more prone to tropical cyclones than the east coast[106,165], our data indicates that this is not a recent phenomenon. Tropical cyclone activity on the mid west coast of Australia is on average three times higher than on the northeast coast, with CAI values ranging from 1 x 10^4 to 1.3 x 10^5 at Cape Range compared with CAI values of 0.25 x 10^4 to 1.2 x 10^5 in Chillagoe. Analysis of CAI indicates that tropical cyclone activity has been highly variable over the past 1,500 yr and that tropical cyclone activity in the past was higher than it is today. There has been significantly less tropical cyclone activity at Chillagoe in the past century than in the previous 550 yr (z-test statistic (Z) = 24.73, P $<$ 0.001). At Cape Range, tropical cyclone activity since 1970 has been significantly lower than it was during the 1,460 years prior (Z = 22.42, P $<$ 0.001). Wavelet analysis of the time series (Fig. 4.4b, c) indicates a reduction in the variance of CAI between the mid 1800s and today at Cape Range within the 16-128-yr band. It also highlights an increase in variability within the 4-8-yr band before 1960 (although at relatively low power). Significance testing indicates that the majority of the oscillations occur within the 4-32-yr frequency band, although the emergence of a 128-yr oscillation

is indicated between AD ∼1100 and ∼1200 and again between ∼1400 and ∼1600 (however, there is less than 95% confidence in the evidence for the latter). Figure 4.4c indicates that, relative to the rest of the time series, the variability at Chillagoe was limited during the period before 1400 and after 1900. Significant variations in power are evident between 1700 and 1800 within the 16-64-yr band, during which time CAI in Chillagoe was highest (Fig. 4.4d). We assessed the rate of the decline in activity over the past few centuries at both sites by conducting a Mann-Kendall test in conjunction with a Theil-Sen estimator. Serial correlation was accounted for by removing the lag-1 autoregressive process after computing the lag-1 serial correlation coefficients for both data sets. Chillagoe shows a significant decline in activity towards the present day since AD 1743 (Kendall's tau (τ) = -0.4, $P < 0.001$, n = 262); similarly, an overall decline in activity is seen in Cape Range since 1650 (τ = -0.4, $P < 0.001$, n = 360). A more abrupt decline at Cape Range since 1960 is evident in Fig. 4.4. We assessed this period in relation to the rest of the Cape Range record using a sliding window of 50 yr with a 1-yr step. The significant downward trend since 1960 is unprecedented in the Cape Range record (τ = -0.5, $P < 0.001$, n = 50). These factors in conjunction suggest that the modern instrumental era (1970-2010) provides a poor reflection of the true natural variability of tropical cyclone activity in both regions.

Trend analysis of instrumental data globally has shown a reduction in frequency in all basins[223] (excluding the Atlantic[64,169]) but in many cases an increase in the number and proportion of severe tropical cyclones[223]. Within the Australian region, the downward trend in tropical cyclone activity over the past 30 yr on the east[37] and west coasts[106] is in contrast to reports of no trend[105]. It has been suggested that the downward trend noted in the former studies is probably due to an improvement in the ability to differentiate tropical cyclones from severe tropical lows and to the greater number of El Niño events since 1970[30]. We performed a Mann-Kendall trend test within both the Chillagoe and the Cape Range data sets on the timescales used in the studies referred to above. Our results agree with those of Harper et al[105] in that no significant trends in tropical cyclone activity in

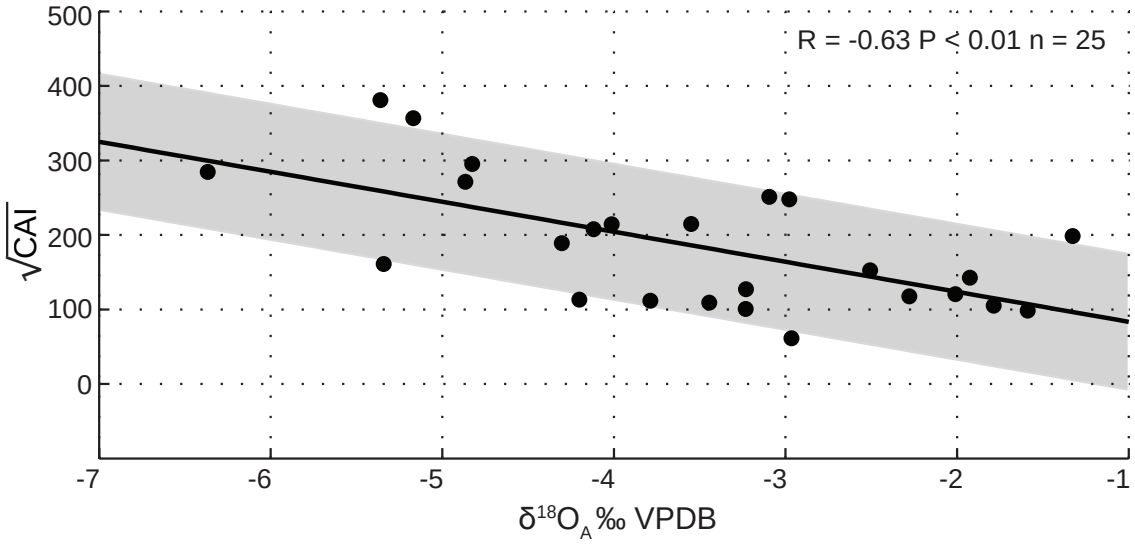

Figure 4.3: Calculated CAI versus the de-trended carbonate values from CR-1 and CH-1 ($\delta^{18}O_A$). Grey region indicates the root mean squared error (r.m.s.e.) of the model (difference between actual and modelled CAI values for 1970-2010). Pearsons correlation coefficient (r) = 0.63, P = $<$0.01, n = 25.

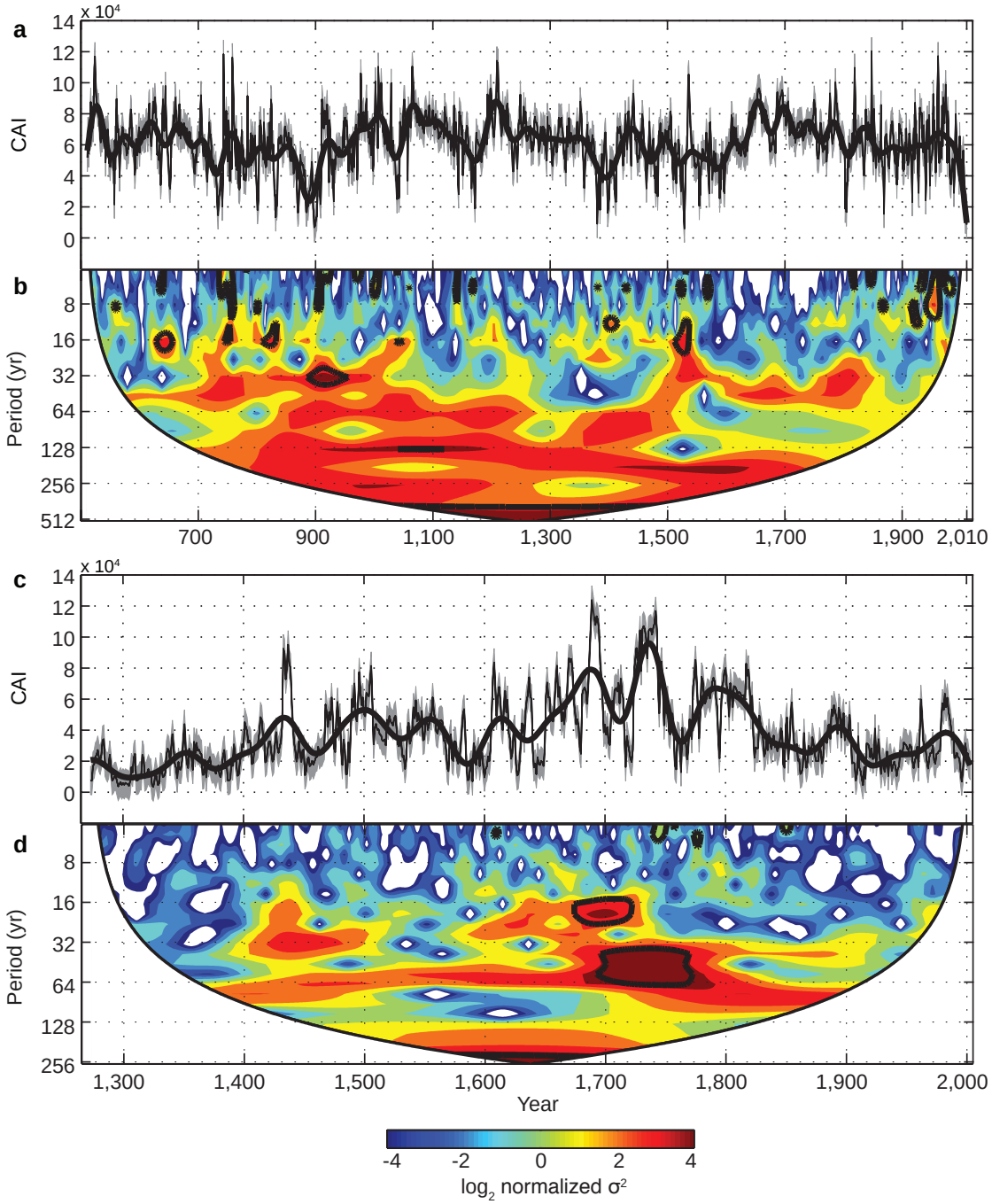

Figure 4.4: CAI over the last 1,500 and 700 yr. Cape Range (a) and Chillagoe (c); black line indicates smoothing of the series using ref.[168] (smoothed data were not used in the statistical analysis). Grey shading indicates the r.m.s.e. of the model. Four values, which were more than 1 s.d. outside the $\delta^{18}O_A$ range specified in Fig. , were removed from the series. b, d, Wavelet power spectra (Morlet wavelet) of Cape Range (b) and Chillagoe (d) from blue to red (red contours indicating greater power), black contours indicate regions above the 95% confidence level, with lag-1 autocorrelation coefficients of 0.75 (CR-1) and 0.78 (CH-1) and a region subject to edge effects (white shading). Software provided by C. Torrence and G. Compo (http://atoc.colorado.edu/research/wavelets/).

central Western Australia are indicated within the period 1980-2007 (τ = -0.2, P = 0.103); however, a significant decrease in activity is evident when the period of investigation is extended beyond the past 30 yr (as previously noted). Similarly, our results are also in agreement with those of an analysis of the Eastern Australian region in 1870-2010, showing a distinct downward trend in tropical cyclone activity in northeast Queensland[37] (τ = -0.4, P $<$0.001).

4.4 Summary

The Australian region seems to be experiencing the most pronounced phase of tropical cyclone inactivity for the past 550-1,500 yr. The dramatic reductions in activity since the industrial revolution suggest that climate change cannot be ruled out as a causative factor. This reduction is also in line with present projections for the late twenty-first century from global climate models, yet our results suggest that this is occurring much sooner than expected. However, we cannot say whether this downward trend in activity will be sustained.

We anticipate that CAI will be a starting point for more sophisticated analysis of other palaeotempest records from around the globe as potential inputs for regional or global climate models and long-range statistical or dynamical forecast models. Deriving a scale of tropical cyclone activity from established high-resolution climate palaeorecords such as stalagmites makes it possible to examine tropical cyclone activity on multiple temporal scales in conjunction with other climate indices, such as temperature, atmospheric CO_2 concentrations, El Niño/Southern Oscillation, the Madden-Julian Oscillation and the Dipole Mode Index. Therefore, CAI provides one seamless index allowing for the incorporation of much longer tropical cyclone records into climate or forecasting models. CAI could be calculated from other stalagmite records and potentially other palaeotempest records from other basins when verified against the local instrumental tropical cyclone record using the method presented here. This provides the means to examine not only how tropical cyclone activity has varied as a result of industrialization but also potentially

to forecast future trends in tropical cyclone activity under changing climate conditions, given that it is now possible to discern natural variability from anthropogenically induced change.

4.5 Author Contributions

Jordahna Haig collected one stalagmite, processed the two stalagmites and analysed the data, developed and tested CAI and wrote the manuscript. Jonathan Nott collected the two stalagmites, provided funding for the project through the ARC grant and participated in critical discussions on the development of CAI. Gert-Jan Reichart provided access to facilities and advice on the data processing. All authors discussed the results and commented on the manuscript.

Chapter 5

Solar forcing over the last 1500 years and Australian Tropical Cyclone activity

Jordahna Haig [1] Jonathan Nott [1] Gert-Jan Reichart [2,3]

[1] *Centre for Tropical Environmental and Sustainability Science, School of Earth and Environmental Science, James Cook University, Cairns, 4870 QLD, Australia.*

[2] *Department of Geochemistry, Utrecht University, Utrecht 3508 TA, The Netherlands.*

[3] *Geology Department, Royal Netherlands Institute for Sea Research, Den Hoorn (Texel) 1797 SZ, The Netherlands*

Prepared for submission to: *Bulletin of the American Meteorological Society (BAMS)*

The global costs associated with tropical cyclone damage are expected to rise to $56 billion per year by the end of this century[99]. Accurate seasonal and decadal predictions of tropical cyclone activity are essential for the development and application of mitigation strategies for the 2.7 billion residents living within cyclone prone regions. In recent years, the traditional indices (Southern Oscillation Index and the Niño3.4 sea surface temperature index) have not been performing well as seasonal predictors within the Australian region[55,99,139] as current statistical models can only decipher variability which is present within the instrumental record[139]. The limited length of these records (i.e.<50 years) has meant that our current knowledge of larger scale drivers at inter-decadal, centennial and millennial scales is non-existent. The development of a new technique CAI[100] calibrating these instrumental records with longer-term, high-resolution geochemical records of tropical cyclone activity spanning the last 1500 years has enabled the examination of tropical cyclone climatology at higher temporal resolution than was previously possible. Here we show that in addition to other well known indices such as the Northern Oscillation Index, Madden-Julian Oscillation and the Trade Wind Index; solar-forcing largely drives decadal, inter-decadal and centennial cycles within the tropical cyclone record.

5.1 Introduction

Kuleshov et al[139] highlight the shortfall of long-range tropical cyclone forecasts in recent seasons from statistical models largely based on the traditional regional, inter-annual to decadal predictors such as Sea Surface Temperature and the Southern Oscillation Index. Whilst sophisticated statistical analysis of the instrumental tropical cyclone record is essential for deciphering associations between climate indices over the short term (regional decadal to inter-decadal time scales) the short length of these records (i.e.$<$50 years) has meant that our current knowledge of larger scale drivers (those at inter-decadal to centennial or millennial scales) is somewhat limited. Analysis of palaeotempest records from multiple locations globally has shown that the frequency and magnitude of tropical cyclones has indeed varied on centennial to millennial scales[52,187]. The majority of these records are from the Atlantic Ocean[52,170], northwest Pacific[231] and Gulf of Mexico[163,164,143] with few records from the Southern Hemisphere namely the Southwest Pacific[187] and Southeast Indian Ocean[187]. It has been suggested that the centennial scale variability within these records is due to variations in ENSO, yet as Nott and Forsyth[187] state, uncertainties in the accuracy of the long-term ENSO records available make these comparisons difficult. Assessing links between the long-term tropical cyclone record and short-term climate indices such as the SSN (Sun Spot Number) and ENSO related indices such as Pacific Decadal Oscillation (PDO), Nino3.4 and Southern Oscilation Index (SOI) are in turn hampered by the lower-temporal resolution of some types of palaeo cyclone records. Here we employ the use of a new high-temporal resolution (seasonal) palaeo-record of tropical cyclone activity from two sites in eastern and western Australia, to assess the connection between both short term and long term climate indices and the multi-temporal scale variability present within the record.

Recently published records of tropical cyclone activity index (CAI) from eastern Australia (CH-1) and Western Australia (CR-1) spanning the last 1500 years show repeated decadal and multi-centennial cycles of tropical cyclone activity[100]. Wavelet analysis at both sites indicates that oscillations in CAI occur within the 4-32yr, 16-64yr and 128-

250yr frequency band[100] (Chapter 4, Fig. 4.4). The following paper compares lower-frequency regional climate oscillations previously linked with tropical cyclone variability in the Australian region such as the Southern Oscillation Index and Trade Wind Index. Lower frequency oscillations within the CAI record occur within the 8-32yr, 16-64yr and 128-250yr frequency bands[100] (Fig. 4.4). As recent works have suggested that Sun Spot Numbers are just as important as El Niño Southern Oscillation as seasonal predictors in tropical cyclone activity[114] we compared these lower-frequency oscillations with known solar driven indices namely the Schwabe 11yr solar cycle, complete 22yr Hale Cycle and longer-term Gleißberg (70-100yrs) and de Vries (Suess) (210yr) cycles.

5.2 Methods

Haig et al[100] developed a new technique to allow direct comparison between the instrumental record and the longer-term proxy record of tropical cyclones. The resulting Tropical Cyclone Index (CAI) allows for a direct comparison between the past and present, and enables the examination of tropical cyclone climatology at higher temporal resolution than was previously possible i.e. at annual, decadal or millennial scales simultaneously, without the need to interpolate or extrapolate to account for missing data. CAI was developed by calibrating instrumental records of tropical cyclone activity in the eastern and western Australian regions from the Australian Bureau of Meteorology Best Track Database[27] against annually resolved geochemical tropical cyclone signatures within stalagmites. Stalagmites are formed as part of the meteoric water cycle and therefore record changes in the composition of precipitation overtime. As tropical cyclones produce precipitation that is isotopically depleted in the heavier oxygen isotope (^{18}O)[90,153], variations in the ratio of ^{18}O to ^{16}O within stalagmites from tropical cyclone prone regions can reveal trends in tropical cyclone activity overtime[78,188]. The CAI model is defined as the average accumulated energy expended over the tropical cyclone season within range of the site, accounting for the number of days since genesis and the intensity and size of the storm relative to its distance from the site at each point along its track. Refer to Haig et al[100] for the derivation, calibration and testing of CAI.

The climate indices used in this analysis were obtained from a number of international government agencies; the Asia-Pacific Data Research Centre, Australian Bureau of Meteorology, NASA Goddard Space Flight Center, National Oceanic and Atmospheric Association, Wilcox Solar Observatory and the University of Wisconsin. These include i) the Northern Oscillation Index (NOI), which is a measure of the difference in sea level pressure anomalies between the northeast Pacific and Darwin. It is similar to the Southern Oscillation Index (SOI) but differs in that it contains a meridional component between the tropics and extratropics[201]. (ii) The Atlantic Meridional Mode, a coupled ocean-atmosphere variability in the Atlantic characterized by anomalous SST, winds, and convection which is subject to external forcing from the equatorial Pacific (ENSO)[93] and analogous to the Pacific Meriodional Mode[39]. (iii) The ENSO precipitation index (ESPI), describes the largest mean precipitation anomalies across the Pacific Basin associated with inter-annual variations of the ascending and descending branches of the Walker circulation and like the NOI and AMM also contains a meridional component (calculation provided in[44]). (iv) The Madden-Julian Oscillation (MJO), and eastward propagating wave of instability within the tropics. (v) The Trade Wind Index (TWI), a measure of the strength of the easterly trade winds driven by the temperature gradient between the lower and higher latitudes.

We employed the use of the continuous wavelet transform and cross wavelet analysis to assess the relationships between CAI record from Chillagoe and Cape Range against Sun Spot Number (August-October averaged) (SSN) and longer-term solar proxies from comogenic isotope data i.e. southern hemisphere tree ring δ^{14}C data[116] and NGRIP Greenland ^{10}Be concentration data[20]. Cross wavelet analysis has been previously employed in the analysis of various geological time series to detect relationships between two nonstationary time series by simultaneously decomposing these signals as a function of both time and frequency. The theoretical basis has been outlined in detail by previous works[98,198,211]. The CAI records at both sites were first tested for stationarity using the Kwiatkowski, Phillips, Schmidt, and Shin test indicating that both times series are

non-stationary (P = 0.01, n = 777-1500). Following the methods outlined by Grinsted et al[98], the distribution of each series was tested and transformed into a series of percentiles before calculating the continuous wavelet transform. Significance testing of the cross wavelet transform was performed using Monte Carlo methods outlined by[98,211] against a red noise background estimated using the first-order autoregressive AR(1) process.

Tests for monotonic relationships were performed between CAI and the climate indices using classical statistical methods namely the nonparametric Spearman's Rank-Order and Kendall's Rank correlation. The value of the test statistic and significance levels are given within the text. Each series was standardized prior to statistical analysis using their z-scores.

5.3 Results

5.3.1 High frequency cycles in CAI

Table 5.1 shows the resulting correlations between the eastern and western Australian CAI over the instrumental period (i.e. last 50 yrs) and the following regional climate variables: Gulf of Carpentaria centred MJO, West Pacific Trade Wind Index, Indian Monsoon, Northern Oscillation Index (NOI), ENSO precipitation index (ESPI), Atlantic Meridional Mode and SSN. Each index listed in Table 5.1 was tested against both Eastern and Western Australian CAI. The majority of significant correlations occur between the climate indices and Western Australian CAI; only two indices exhibit a relationship with Eastern Australian CAI, namely the AMM and MJO. Of all the indices, only the MJO shows a significant (negative) relationship with CAI at both sites. The TWI and NOI exhibit the strongest correlations with Western Australian CAI (ρ= -0.5, 0.5). Interestingly, the NOI (ρ = 0.5; p <0.01; n = 58) is more strongly associated with CAI in this region than the SOI (ρ = <0.22; p <0.1; n = 58) over the same time period. Strong positive associations also exist between CAI and the Northern Oscillation Index (NOI) in the three month lead up to the tropical cyclone season (August to October) (ρ = 0.5; P <0.001).

Table 5.1: Statistical comparison of high frequency cycles in CAI and regional climate indices over the instrumental period.

Index	Spearman's Rho (ρ)	P-value	N
MJO (Gulf centred †)	-0.4, -0.4*	<0.05	33, 27*
Pacific Warm Pool (Aug-Oct)	-0.4	<0.01	60
West Pacific Trade Wind Index ‡	-0.5	<0.01	32
NOI †	0.5	<0.01	58
Indian Monsoon Index (Jun-Aug)[2]	0.43	<0.01	62
ENSO precipitation index (ESPI)[177]	-0.4	<0.05	29
Atlantic Meridional Mode[39]	-0.4*	<0.05*	57*

*refers to CH-1, † dry season averaged (May-Oct), ‡ wet season averaged (Nov-Apr), N = sample size.

5.3.2 Low frequency cycles in CAI

Following the methods of Hodges and Elsner[113], we regressed the upper 95th percentile of SSN with the Eastern and Western CAI (pre 1970) (ρ = -0.8, -0.7; p <0.05; n = 9). The length of this record (n=9) is too short to derive definitive conclusions regarding the strength of the relationship between CAI and SSN, we therefore employ the use of cross wavelet analysis to compare the two complete series (n=262) within time-frequency space and focus only on statistically significant regions (those bounded by black contours). Figure 5.1 presents the results of the cross wavelet analysis of the Western and Eastern Australian CAI against the August-October Averaged Sun Spot Numbers (SSN) (Fig 5.1 a and b respectively), southern hemisphere tree ring ^{14}C data[116] (Fig 5.1 c and d), and NGRIP Greenland ice core ^{10}Be data[20] (Fig 5.1 e and f). The graduated colour represents power (with red regions indicating the strongest relationships). Arrows indicate the phase behaviour of the two series with right pointing indicating that the relationship is in-phase, left indicating anti-phase. Grinsted et al[98] cautions against converting phase-angles into time lags as this can be ambiguous i.e. down pointing arrows may suggest that CAI is leading the climate index by 90°or lagging by 270°(the resulting time lag is wavelength dependent). We have therefore not made angle/time conversions here.

Fig 5.1 a shows that significant common power (at the 5% level) is evident throughout the ∼6-14 year band between Western Australian CAI and SSN. Eastern Australian CAI (Fig 5.1 b) exhibits fewer of these regions, evident between AD1760-1790, 1820-1830, 1840-1860 and again from 1910-1990. The CAI-tree ring ^{14}C cross wavelet spectra (Fig 5.1 c) indicates three significant regions of common power in Western Australia within the ∼24-96 yr band between AD700 and 1250 (although at lower power), a longer period of strong correlation within the 96-192 yr band from AD850-1400, with the strongest and most robust (given the constant anti-phase behaviour) from AD1100-1700 within the 192-256 year band. Eastern Australian CAI (Fig 5.1 d) and tree ring ^{14}C exhibits the same anti-phase behaviour within the >128 year band from ∼AD1300 to ∼1800, although this time period may be longer as this region extends beyond the cone of influence. Other regions are highlighted in Fig 5.1 d throughout the length of the series within the 32-128 year band excepting a period of quiescence between AD1450-1790 within the 64-128 yr band. The CAI- ^{10}Be cross wavelet spectra are remarkably similar between western Australia (Fig 5.1 e) and eastern Australia (Fig 5.1 f). At both sites, the strongest power is indicated at periods >128 yrs (between AD1600 and 1800) and a small region between AD1700 and 1800 within the 40 - 64 yr frequency band. Both sites exhibit the same phase behaviour within these regions. The Eastern Australian site (Fig 5.1 f) shows more periods of activity at periods <24 yrs throughout the length of the time series (AD1400 - 2005) than Western Australia which remains relatively quiet at periods <12 yr throughout the 1600s, 1700s and early 1800s.

5.4 Discussion

5.4.1 High frequency cycles in CAI

Analyses between CAI and known climate indices within the instrumental period (spanning the last few decades) indicate associations between predictor variables of both zonal and meridional nature in tropical cyclone variability (see Fig. 5.2). Both sites are influenced by the preceding dry season Gulf of Carpentaria centred MJO. Increased tropical

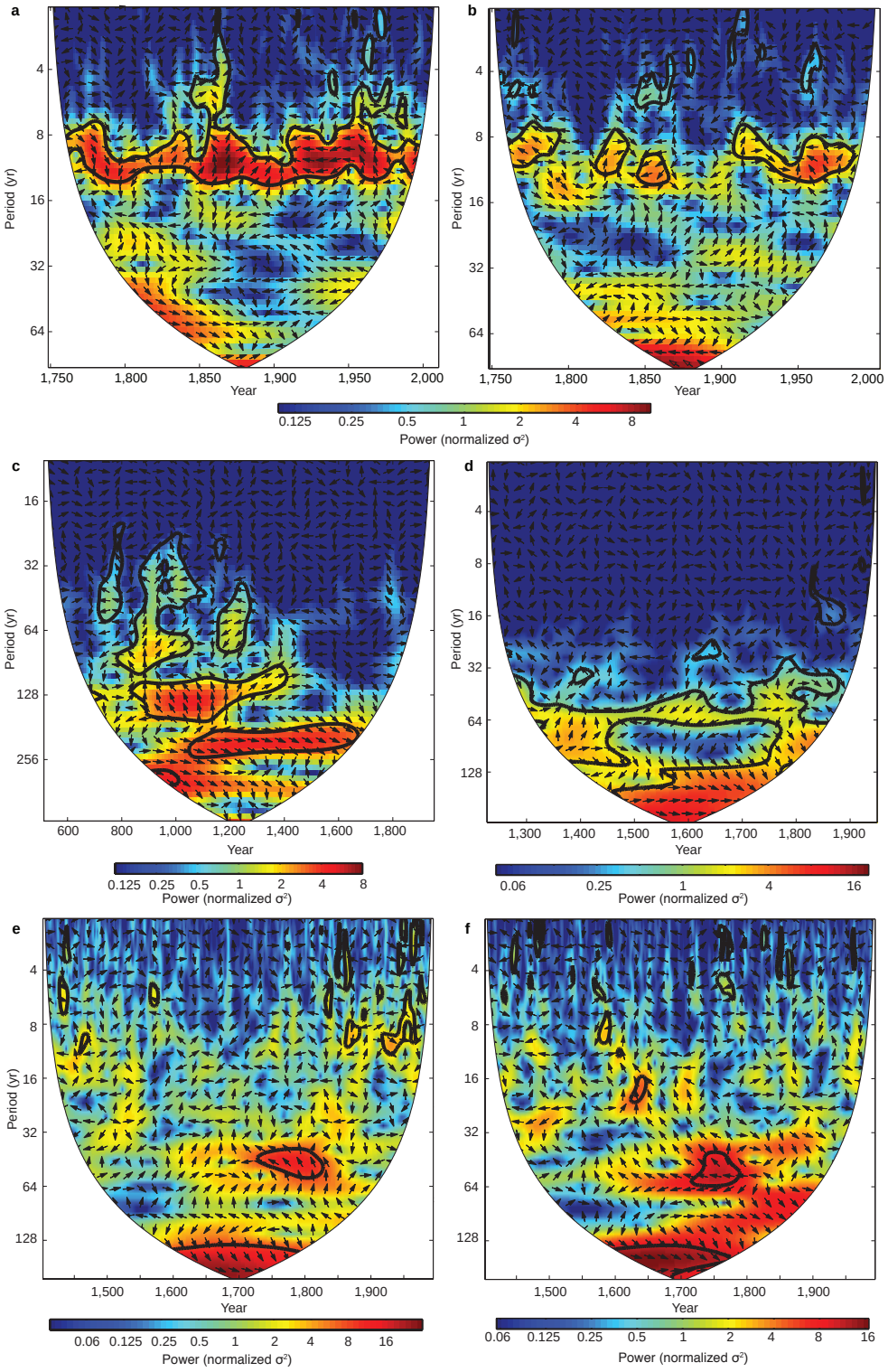

Figure 5.1: Cross Wavelet Transform (Morlet wavelet) of Cape Range CAI (a,c,e) and Chillagoe CAI (b,d,f) vs Sun Spot Number (August-October averaged)[203] (a,b); Southern Hemisphere Tree Ring $\delta^{14}C$[116] (c,d) and NGRIP Greenland ^{10}Be concentration data[20] (e,f). Power spectrum from blue to red (red contours indicating greater power), black contours indicate regions above the 95% confidence level (assuming an AR-1 process) and the region subject to edge effects (white shading). Arrows indicate the phase behaviour of the two series with right pointing indicating that the relationship is in-phase, left indicating anti-phase. The 5 yearly $\delta^{14}C$ data in 5.1d was interpolated using a cubic spline so as to produce the same time step in the corresponding annual Chillagoe CAI data. Given the length of the Western Australian CAI data, no interpolation was used in fig 5.1c. Software provided by Aslak Grinsted (http://noc.ac.uk/using-science/crosswavelet-wavelet-coherence).

cyclone activity is linked to a stronger MJO and thus enhanced convection in this region. A weakening of the average wet season 850 mb West Pacific Trade Wind Index during the wet season is associated with an increase in tropical cyclone activity on the West Coast of Australia, likely as a result of strengthening northwesterly winds from the Indian Ocean and southern Asia associated with the monsoon. Subsequently, Western Australian CAI is positively associated with the previous Jun-Aug Indian Monsoon Index such that a stronger Indian Monsoon is generally followed by a more active tropical cyclone season in the West of Australia. Interestingly, CAI in Western Australia is more closely related to the NOI than the SOI over the same period, probably largely due to the fact that NOI is a measure of the North Pacific High and the South Pacific High which influences climate variations in the Southeast Asia and the tropical Indo-Pacific regions[201]. In addition, SOI reflects little about the meridional circulation of the Hadley Cells, whilst the NOI is an index of meridional and zonal atmospheric patterns though the tropics and extra-tropics[201]. Positive NOI are generally associated with La Niña events thus, the strongly positive associations between NOI in the three month lead up to the tropical cyclone season (August to October) and the Western Australian CAI imply an ENSO connection. This is also highlighted in the ENSO precipitation index (ESPI)[177] which is negatively correlated with CAI with high ESPI values associated with El Niño conditions and a reduction in tropical cyclone activity on the West Australian Coast. Teleconnections are highlighted between the Western Australian CAI and the ENSO Precipitation Index in addition to the NOI and TWI; and significant albeit weak correlations between the Eastern Australian CAI and the Atlantic Meridional Mode, suggest the influence of larger spatial scale drivers of both zonal and meridional nature in longer term tropical cyclone variability.

5.4.2 Low frequency cycles in CAI

Hodges, Jagger and Elsner[61,114,112] found that between the western and eastern Atlantic the number of intense tropical cyclones decreases (increases) during periods of higher (lower) Sun Spot Activity. In regions where sea surface temperatures are higher (and therefore already conducive to tropical cyclo-genesis) this negative relationship is at-

tributed to a decrease in the potential energy available for tropical cyclo-genesis (in accordance with the heat engine theory of tropical cyclones) due to a reduction in the temperature gradient between the warm surface waters and the warmer (relative) air aloft via heating of the upper atmosphere[61,113,114,112,197], the reverse occurs when cooler ocean waters are the limiting factor (such as in the eastern Atlantic). Similarly, Hung[224] cites that increased absorption of radiation by ozone within the lower stratosphere and upper troposphere leads to a decrease in the potential energy available for and frequency of tropical cyclogenisis in the northwest Pacific. Hutton et al[120] found that sun spot extremes rather than the complete sunspot cycle along with other solar indicators such as Cosmic Ray Intensity exhibited the greatest correlations with tropical cyclone activity. Therefore, according to the heat engine theory described above and given the relatively warm ocean waters surrounding both the East and West coasts of Australia, tropical cyclone activity should decrease when SSN is higher (in the extremes). Our findings, while based on a limited record (9 events), indicate that an increased number of sun spots (within the upper 95th percentile) does appear to coincide with a reduction in tropical cyclone activity in both locations. Our cross wavelet analysis also highlights a strong connection between sunspot and tropical cyclone activity, particularly within the Western Australian record however, Fig. 5.1 shows that the significant commonalities between CAI and SSN are not phase locked (arrows indicate phase) but appear to alternate between anti-phase (left facing) and in-phase (right) relationships over relatively short time periods of 20-40 years. This is in contrast to the findings of Hutton et al[120] who state that the variance in Atlantic tropic cyclone activity remained the same regardless of the sun spot cycle phase. The common power accompanied by a reversal in phase relationships between significant periods within the cross wavelet analysis indicates that the connection between the two series cannot be explained by a simple cause and effect relationship[98]. Additional significance testing indicates a good relationship between CAI in both regions and 20nhz low pass filtered solar Polar Field measurements[193] over the last 35 years (ρ = 0.5, -0.7; P $<$0.01; n = 35, 28), a measure of sunspot polarity following the Hale Cycle ($\sim$25 years) and subsequent polar reversals. This result is interesting, given the phase reversal be-

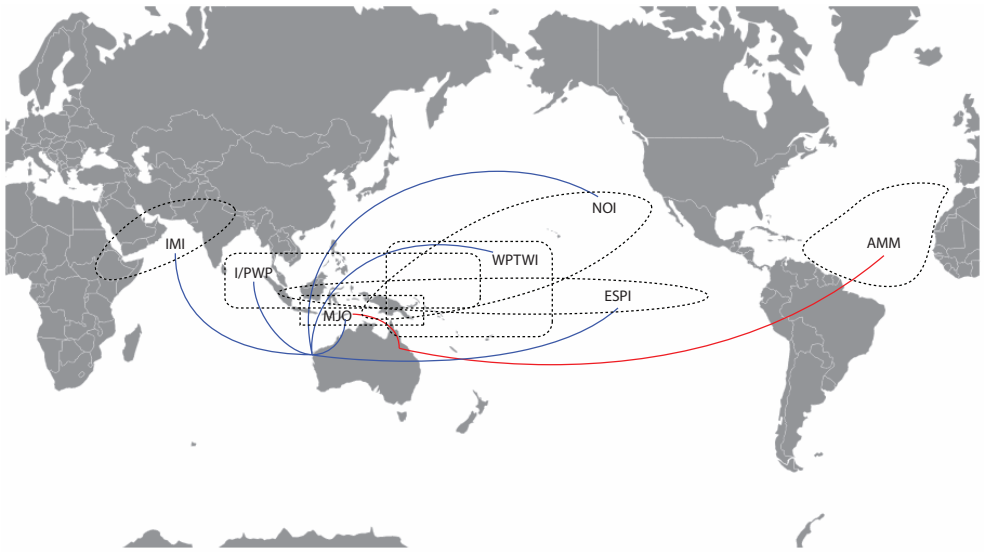

Figure 5.2: Geographical representation of the relationships between instrumental climate indices and the western Australian and eastern Australian CAI.

haviour shown in Fig 5.1 (a,b), particularly as sun spot polarity reverses each solar cycle at sun spot maximum. However, the current Polar Field record is too short (covers only one reversal) to be able to decipher any definitive relationships between Polarity and the subsequent (perhaps indirect) effects on tropical cyclone activity.

Should solar forcing be a likely driver in the natural variability of tropical cyclone activity the relationship must not only be evident within the instrumental records but also persist throughout the paleo record. Such comparisons have until now not been possible. The cosmogenic isotopes ^{10}Be and ^{14}C are produced in the Earth's atmosphere via the spallation of ^{16}O and/or ^{14}N by galactic cosmic rays[18]. ^{10}Be recorded in ice cores and tree ring ^{14}C are used as solar activity proxies as galactic cosmic rays are modulated by changes in the sun's magnetic field, which is in turn correlated to solar irradiance[206–209,216]. Correlations between CAI and both solar activity proxies potentially follow the 88 yr Gleißberg and 205 yr de Vries Cycles. Unlike the sun spot results, the two sites appear to exhibit the same phase behaviour within the statistically significant regions within the same periods. For example, the region of highest power in Fig 5.1c,d lies within the 128-256 year band (which we assume to be the $\sim$210 year de Vries cycle). In this instance CAI in both Cape Range and Chillagoe are in-phase with ^{14}C. The higher resolution ^{10}Be records (Fig 5.1 e,f) reveal that statistically significant regions within the 40-55yr band (perhaps responding to the sun's meridional flow[107]) and 128-yr band ($\sim$100yr Gleißberg cycle) occur at the same time within the two sites during AD1750-1800 (coinciding with the Maunder Minimum) and AD1600-1800 (coinciding with the Dalton Minimum) respectively. While both sites appear to exhibit the same phase behaviour, CAI at each site remains in anti-phase with each of the solar proxies for periodicities less than 128yrs and in-phase at all periodicities greater than 128yrs. This suggests that an increase in solar activity in all instances (excluding periodicities $>$128yrs) results in a reduction in tropical cyclone activity.

5.5 Conclusion

The shortfall in recent decades of traditional predictor variables SST and SOI in accurately predicting seasonal tropical cyclone activity[139] coupled with a lack of understanding of tropical cyclone activity drivers beyond the scope of the short-term instrumental tropical cyclone record has highlighted the need for a broader investigation of this variability over decadal, inter-decadal and centennial scales. Until now, statistical comparisons were made difficult due to the relatively short instrumental record (<50 years) coupled with the lack of a quantifiable, annually resolved palaeo-activity index. The advent of the CAI has enabled the examination of tropical cyclone climatology at higher temporal resolution than was previously possible. The link between tropical cyclone activity in Western and Eastern Australia and solar cycles at decadal, and centennial scales is certainly compelling and deserves further investigation. As the sun-hurricane connection has now been made within the East and West Atlantic, the South West Pacific and South East Indian Ocean, perhaps a multi basin approach to tropical cyclone climatology is warranted in the search for more reliable seasonal predictors and a better understanding of the climatic drivers.

5.6 Author Contributions

Jordahna Haig collected one stalagmite, processed the two stalagmites developed the research question, analysed the data and wrote the manuscript. Jonathan Nott collected the two stalagmites, provided funding for the project through the ARC grant and participated in critical discussions on the development of the manuscript. Gert-Jan Reichart provided access to facilities and advice on the data processing. All authors discussed the results and commented on the manuscript.

Chapter 6

Rapid vegetative response to reduced tropical cyclone activity and regional climate indices since 1960 recorded in stalagmites in eastern and western tropical Australia

Jordahna Haig[1], Jonathan Nott[1], Damien O'Grady[1], Allison Hoskin-Kain[1,2], Renske Löffler[3] and Gert-Jan Reichart[3,4]

[1] *Centre for Tropical Environmental and Sustainability Science, School of Earth and Environmental Science, James Cook University, Cairns, 4870 QLD, Australia.*

[2] *Biosecurity Queensland, Department of Agriculture, Fisheries and Forestry, Bellbowrie, 4070 QLD, Australia.*

[3] *Department of Geochemistry, Utrecht University, Utrecht 3508 TA, The Netherlands.*

[4] *Geology Department, Royal Netherlands Institute for Sea Research, Den Hoorn (Texel) 1797 SZ, The Netherlands*

Submitted to: *Journal of Climate*

Here we provide the first high-resolution record of a vegetation response to changing global temperature anomalies and tropical cyclone activity in both C3 and C4 dominated vegetation communities in eastern and western Australia, spanning the last century. We identify a strong geochemical link between the ratio of the stable isotopes of Carbon and Oxygen in stalagmites from two different tropical environments and global climate indices including the Global Land-Ocean Temperature Index[178], Atmospheric CO_2[69] , Mean Annual Global Solar Exposure[28]; and regional indices including the Indo-Pacific Warm Pool[70], Inter-Decadal Pacific Oscillation[196], Pacific Decadal Oscillation[182], and the Madden Julian Oscillation[181]. The most significant perturbation in the stalagmite records coincides with the documented rapid global climatic shift occurring in the late 1960s[8]. In all three locations a strong linear relationship is found between global indices and the calcite $^{13}C/^{12}C$: $^{18}O/^{16}O$ (δ:δ ratio) (ρ = -0.5 to 0.7 (Spearman's Rho), P>0.05, n = 61 to 105). This relationship is inverted between the climatic extremes (C3 vs C4 dominated environments). Our results indicate that the two environments (tropical woodland vs semiarid savannah) react dramatically in response to rising global temperatures and changes in natural disturbance regimes resulting from the reduction in tropical cyclone activity in both regions.

6.1 Introduction

Tropical cyclones have significant effects on the structure and diversity of vegetation communities particularly coastal forests[213]. These effect include changes to canopy openness, tree fall, defoliation, invasion of exotic species during recovery and changes in forest microclimates in response to changes in light, temperature and humidity regimes[214]. In addition to factors such as the radius of maximum winds, maximum sustained wind speed and proximity to the storm track, large scale ecological damage patterns are influenced by variations in topographic exposure; and differences in geology, climate, and disturbance history[29]. Given the reduction in tropical cyclone activity in recent decades in eastern and western Australia[100] we examine what effects if any, this has had on the two vegetation communities at each site.

We have demonstrated previously that changes in tropical cyclone activity are recorded in the δ^{18}O ratio of stalagmite calcite as precipitation composition (rather than cave temperature and rainfall amount or frequency, or both) influences the resulting δ^{18}O at these sites[100]. Conversely, the carbonate bedrock; atmospheric and soil CO_2 (driven by changes in vegetation type and cover) influence the δ^{13}C of the calcite (expressed as $\delta^{13}C = [(\delta^{13}C/\delta^{12}C)_{sample}/(\delta^{13}C/\delta^{12}C)_{VPDB} - 1)]x1000\ ‰$). Thus, stalagmites as palaeoclimate archives provide the means with which to examine changes in these parameters simultaneously. Given the absence of longitudinal vegetation surveys at the site over the last 50-100 years, we propose the application of a duel isotope approach to analysing vegetation change in response to changes in disturbance regimes from tropical cyclones and changing climate regimes in the form of a δ:δ ratio (similar to that recently employed in tree ring analysis)[17,200] in combination with analysis of changes in the Normalized Difference Vegetation Index (NDVI) at both sites using remote sensing techniques.

6.2 Site Locations and Methods

Two tropical sites were chosen which significantly differ both environmentally and geographically: Chillagoe, Queensland (stalagmite CH-2); Cape Range and Western Australia (stalagmite CR-1) (Fig 3.1). The Chillagoe landscape is characterised by vegetation which utilise the C3 pathway namely dry tropical woodland with patches of deciduous vine thicket (liana species). While the western coastal plain of Cape Range is dominated by Spinifex (C4) with Melaleuca and Hibbertia (C3) species also present[129].

CH-2 and CR-1 are regular, symmetrical candle stalagmites exhibiting a very slow (spanning thousands of years) reduction in width over time. The stalagmites exhibit annual couplets of alternating light and dark calcite layers of lenticular shape. The diameters of the stalagmites are large i.e. 5-11cm (CH-2) and 6-8cm (CR-1). The stalagmites were sectioned along their growth axes using a water-cooled diamond saw and a 1-2cm thick section prepared from one half. The remaining half was then archived. The centred faces of the working sections were polished using fine sandpaper and steel wool in order to accurately resolve individual growth layers. The samples were then cleaned with UHQ water in an ultrasonic bath.

The most recent 105 dark calcite layers (corresponding to wet season deposition) were sub-sampled using a video-controlled Micromill. Trenches ($\sim$10mm long, $\sim$60 μm wide) were milled from the centre of the stalagmite in in most cases extending 5mm each side of the growth axis. These trenches were kept well within half the radius of the sample in order to avoid collecting material towards the flanks which could be subject to kinetic disequilibium edge effects. Oxygen and carbon isotope analyses were performed using a Kiel III carbonate device coupled to a Finnigan MAT 253 IRMS. The calcite samples were reacted with 3 drops of H_3PO_4 at 70 °C. Replicate analysis of the standard NBS-19 resulted in a standard deviation of 0.04‰ for δ^{13}C and 0.06‰ for δ^{18}O. All measurements are reported relative to Vienna PeeDee Belemnite (VPDB).

The climate indices used in this analysis were obtained from the american National Aeronautics and Space Administration and National Oceanic and Atmospheric Administration; and the Australian Bureau of Meteorology. The land Ocean Temperature Index provided by the Goddard Institute for Space Studies (GISS) is an index of global surface temperature change calculated using a gridded dataset over both land and ocean weather station sites, de-trended using 1951-1980 as the base period[102]. Pacific Decadeal Oscillation is an El Niño like pattern of Pacific climate variability defined as the leading principal component of North Pacific monthly sea surface temperature anomalies in the northeast and tropical Pacific Ocean[234]. The Madden-Julian Oscillation (MJO), is an eastward propagating wave of instability within the tropics. Average Annual Global Solar Exposure, is a measure of the amount of solar radiation that reaches the earth's surface. Lastly, the Indo-Pacific Warm Pool (PWP), which plays a significant role in driving the zonal Walker and meridional Hadley circulations in the region. The PWP is a measure of the strength of the warm pool surrounding the Indonesian Archipelago, a major source of latent heat for the global atmosphere[128].

The δ^{18}O and δ^{13}C relationship, (referred to in the following text as δ:δ) was calculated using equation 6.1. Tests for monotonic relationships between δ:δ and the climate indices defined above were performed using classical statistical methods. The value of the test statistic and significance levels are given within the text. Each series was standardised prior to statistical analysis using their z-scores.

$$\delta : \delta = \frac{[(\delta^{13}C/\delta^{12}C)_{sample}/(\delta^{13}C/\delta^{12}C)_{VPDB} - 1)] \times 1000}{[(^{18}O/^{16}O)_{sample}/(^{18}O/^{16}O)_{VPDB} - 1)] \times 1000} = \frac{\delta^{13}C}{\delta^{18}O} \tag{6.1}$$

6.3 Results

Figure 6.1 plots the stable isotope results over time indicating expected C3 vs C4 ranges derived from the δ^{13}C results as defined by McDermott et al[171]; with the expected range for secondary carbonates deposited in equilibrium with C3 respired CO_2 between -14‰

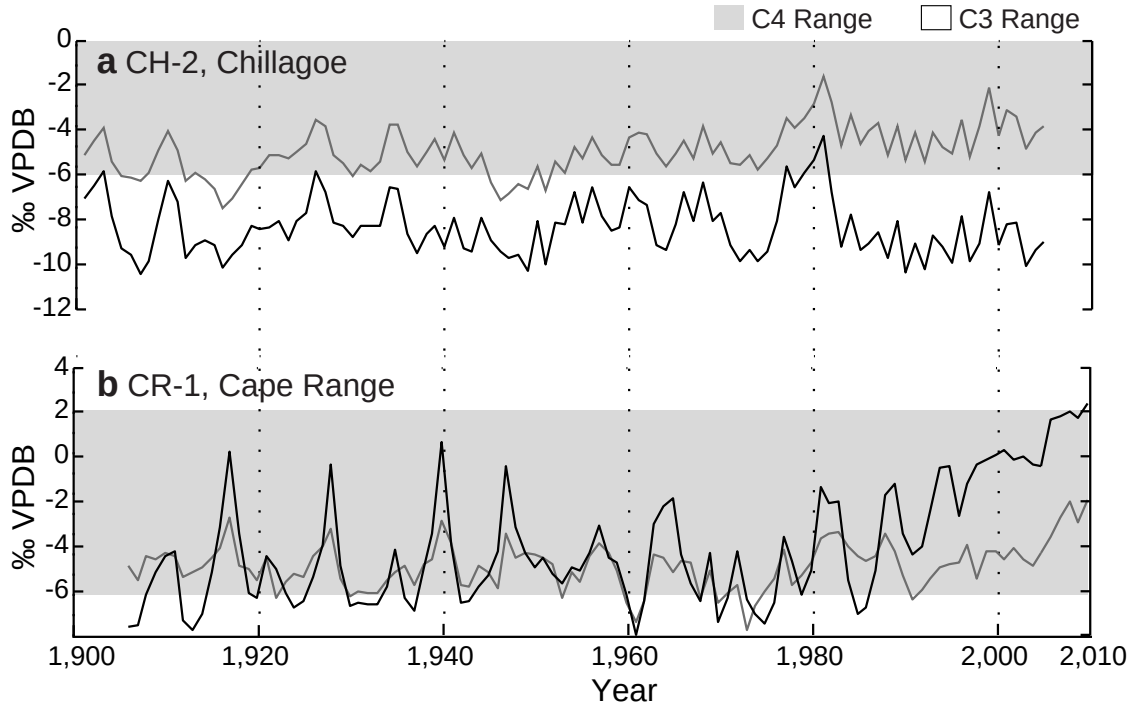

Figure 6.1: δ^{13}C and δ^{18}O profiles of stalagmites a CH-2 and b CR-1. The expected C3 vs. C4 ranges[171] derived from the δ^{13}C results. Grey shaded areas indicate the C4 vegetation range. Black line indicates δ^{13}C and grey line indicates δ^{18}O.

to -6‰ and between -6‰ to 2‰ VPDB for C4. For majority of the period 1910-2010, annual δ^{13}C from CR-1 falls within the C4 vegetation range while the δ^{13}C results from CH-2 indicate that the vegetation above the cave has been predominantly C3 since 1905. The δ^{13}C of CR-1 exhibits the greatest annual variation of all the time series (σ^2 = 6.88) whilst annual variability in δ^{18}O between CR-1 and CH-2 is comparable (σ^2 = 1.11 and 1.17 respectively). CR-1 exhibits the greatest range in δ^{13}C (a difference of 10.34‰ between maxima and minima over the length of the time series). The average difference between δ^{18}O and δ^{13}C values is greatest in CH-2 while the difference between δ^{18}O and δ^{13}C values in CR-1 is small prior to 1980, after 1970 δ^{18}O and δ^{13}C begin to diverge. This coincides with an abrupt and progressive enrichment in ^{13}C and ^{18}O towards the present day (Kendall's Taub (τ) = 0.73 and 0.44, P<0.01, n = 41).

6.3.1 Testing for kinetic isotope disequilibrium effects

A Hendy Test for equilibrium deposition[110] was conducted on CH-2 and CR-1 at 18cm and 16.2cm from the apex respectively. 3-6 subsamples were milled for each test at 1-8mm intervals along the growth horizon from the centre of the layer to the flanks. The Hendy test reveals a variation of 0.58‰ and 0.61‰ in δ^{18}O and 0.29‰ and 0.77‰ in δ^{13}C for CH-2 and CR-1 respectively (fig. 3.4). All stalagmites pass Hendy's first test for equilibrium as the variation in δ^{18}O is less than 0.8‰ and neither exhibits significant progressive enrichment in either δ^{18}O or δ^{13}C. Whilst the variation in δ^{13}C across a layer is greater than that of δ^{18}O, no sample exhibits a range >0.8‰indicating that neither rapid degassing nor evaporation (thus kinetic disequilibrium effects) are present during the precipitation of the calcite and that the calcite has been deposited in isotopic equilibrium with the cave drip water. Yet each stalagmite presented in this study exhibits moderate to strong positive covariation between the stable isotopes δ^{18}O and δ^{13}C (ρ = 0.4 to 0.7; P<0.01; n = 105). The relationship between δ^{13}C and δ^{18}O at the three sites over the last 100 years is given in Fig 6.2. Each site demonstrates that δ^{13}C has a positive relationship with δ^{18}O, however the addition of a third dimension 'time' indicates that the degree of offset is not constant, a result that is not evident simply by examining both isotopes separately. CH-2

shows a progressive decadal depletion in δ:δ towards the present day. Interestingly, CR-1 shows the opposite effect with a progressive decadal increase in δ:δ towards the present day, whilst in both cases the slope of this relationship appears to remain constant.

6.3.2 Testing for climatic causes of δ:δ patterns

In the absence of anthropogenic site disturbance, it is assumed that the observed multi-decadal changes in the offset of the regression line have an underlying environmental cause. Table 6.1 gives ρ of the standardised δ:δ from each location with respect to standardised global and regional climate indices mentioned above and Fig 6.3 presents a comparison of the Eastern and Western Australian sites in relation to the global climate indices. All sites have a strong overall correlation with the Land Ocean Temperature Index and Atmospheric CO_2; and the regional Indo-Pacific Warm Pool. Site-specific regional influences of the Inter-Decadal Pacific Oscillation, Pacific Decadal Oscillation and the Madden-Julian Oscillation are also evident albeit weaker and in one instance, the Mean Annual Global Solar Exposure Index correlates at only one site (Cape Range). All indices are positively correlated with CH-2 and vice versa in CR-1. None of the sites exhibit a significant relationship with either seasonal or annual rainfall totals or the number of rain days at the site (ρ>0.2, P $\geq$0.1, n = 47 to 103). Yet a reduction in average annual rainfall of 100mm since the early 1900s is evident in the Cape Range dataset (see Fig. 6.4).

Table 6.1: Relationships between δ:δ in CH-2 and CR-1 and Global/Regional Climate Indices. All series have been standardised prior to statistical analysis.

Sample	Index	Sample Size (n)	(ρ)	P
CH-2	Pacific Decadal Oscillation	100	0.36	<0.001
	Inter-Decadal Pacific Oscillation	100	0.54	<0.001
WA-1	Madden Julian Oscillation (140°E Centred)	32	-0.36	0.050
	Mean Annual Global Solar Exposure (MJ/m^{-2})	18	-0.66	<0.010

6.4 Discussion

Mickler et al's[173] analysis of 165 published stalagmite records globally found 59% of these exhibited covariation between δ^{18}O and δ^{13}C. Sixty-three percent of the tropical

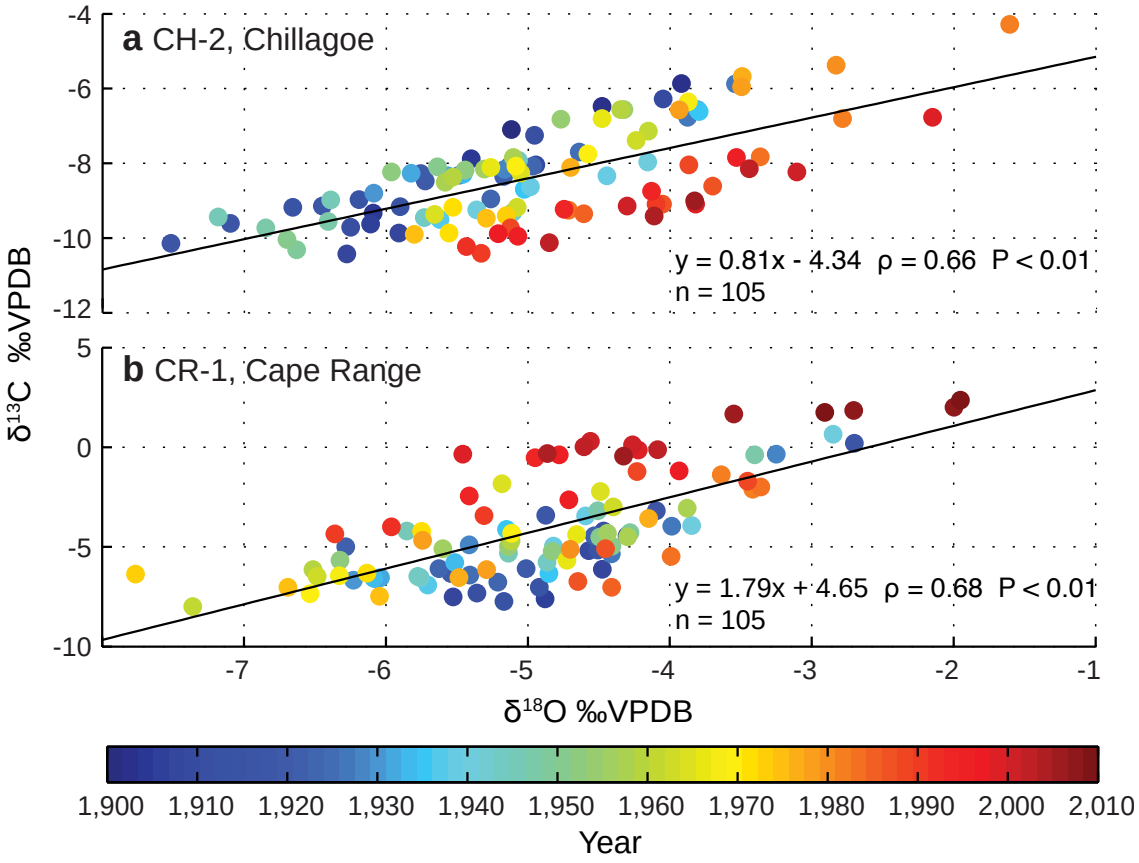

Figure 6.2: δ^{13}C vs δ^{18}O of stalagmites a) CH-2 and b) CR-1. Colour shading indicates time.

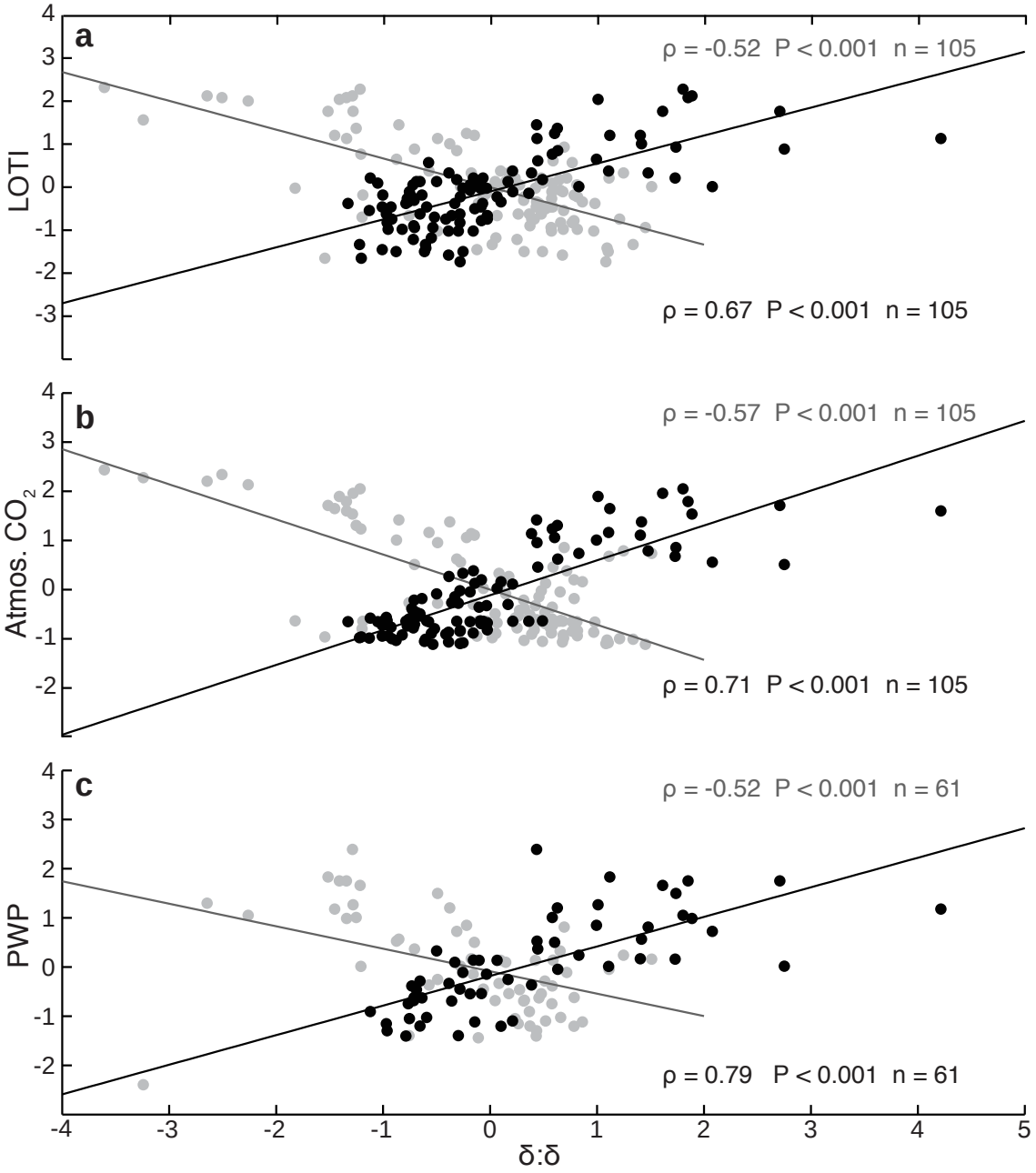

Figure 6.3: δ:δ (CH-2 and CR-1) versus the a) Land Ocean Temperature Index, b) Atmospheric CO_2 and c) Indo-Pacific Warm Pool. Grey colour refers to CR-1 and black to CH-2. All series have been standardised prior to statistical analysis.

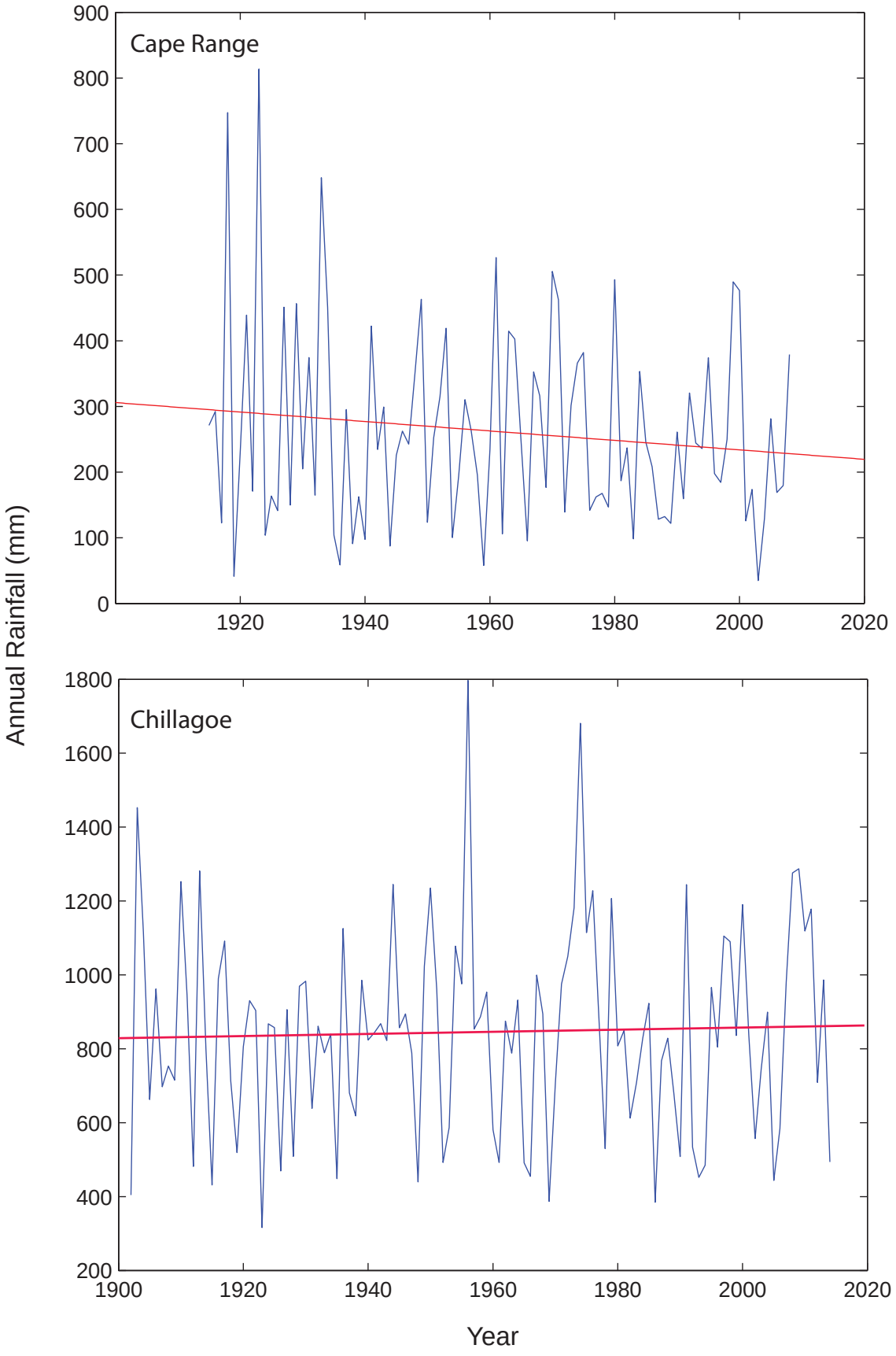

Figure 6.4: Annual rainfall totals for Cape Range (Exmouth Gulf station number 5004) from 1915 to 2008 (a) and Chillagoe (Walkamin Research station number 31108) from 1965 to 2005 (b)

stalagmites examined (that is those collected within 23°of the equator) exhibited statistically significant covariation, all of which were positively correlated. Whilst traditionally thought of as evidence for kinetic disequilibrium effects, a growing body of work suggests that there may also be a climatic control on the covariation of δ^{18}O and δ^{13}C[80,140] as increasing precipitation 'amount effects' in monsoonal regions (which typically lead to more negative carbonate δ^{18}O values) may also lead to more negative δ^{13}C values through an increase in soil moisture, greater contribution of biogenic plant respired CO_2[36] and/or soil respiration rates[140]. Both stalagmites presented in this study exhibits moderate to strong positive covariation between the stable isotopes δ^{18}O and δ^{13}C yet continuous sampling along the growth horizon indicates limited variation in δ^{18}O and δ^{13}C ($<$0.8‰) from the centre of the growth bands towards the flanks and neither exhibits a progressive enrichment in δ^{18}O or δ^{13}C, suggesting the absence of kinetic disequilibrium effects via rapid degassing and/or evaporation[110]. A strong mirroring effect between Eastern and Western Australia is evident in 3 of the 4 global indices common to both sites suggesting that the C3 and C4 communities in question are responding in an opposing fashion to changes in these climate parameters. In the case of LOTI and Atmospheric CO_2, the slopes of the lines of best fit are very similar, that is, -0.67 (CR-1) and 0.65 (CH-2); and -0.71 (CH-2) and 0.71 (CR-1) respectively. While the Indo-Pacific Warm Pool is most closely related to the Chillagoe dataset. A statistically significant shift in δ:δ is evident from around 1960 (τ = 0.57 and -0.67 for CH-2 and CR-1 respectively; P$>$0.01).

Modern soil δ^{13}C alone, can vary by as much as 9.7‰within savannas[166]. Soil δ^{13}C can also vary by as much as 3‰with depth before stabilising at depths $>$50cm[48,9] through kinetic fractionation during humification and/or the Terrestrial Suess effect (contributing a difference of 1.5‰over the last 100 years). Given that the soil depth at both sites is shallow (much less than 50cm) it is likely that the source of the δ^{13}C is predominantly from annual variations in soil organic matter content in combination with atmospheric δ^{13}C. The large 5-10‰difference in δ^{13}C over the last 50 years at both sites suggests a change in the percentage vegetation cover at the sites in response to changes in the climate param-

eters mentioned above. We propose that the progressive enrichment in δ^{18}O yet depletion in δ^{13}C within the C3 community (CH-2, Chillagoe) indicates a greater contribution of isotopically light biogenic carbon to the soil zone and enhanced root respiration at the site, eluding to its ability to regenerate given the reduction in wind disturbance noted at this location[100] resulting in an increase in vegetation cover at the site. δ^{13}C progressively decreases towards the modern day suggesting an increase in soil respiration rates in the absence of a significant downward trend in precipitation amount and may therefore be a result of CO_2 fertilisation which has recently been reported in other areas of Australia[53] and/or greater vegetation production above the cave. In contrast, the C4 community (CR-1, Cape Range) exhibits enrichment in δ^{13}C and δ^{18}O. As atmospheric CO_2 is more enriched in ^{13}C than soil CO_2, increasing additions of atmospheric CO_2 to the soil zone may increase the resulting stalagmite carbonate values[205] as a result of a reduction in mean annual precipitation[118] and soil respiration rates; likely due to a reduction in vegetation coverage. We believe this is at least in part due to a reduction in tropical cyclone activity at the site given that tropical cyclone rainfall account for 20% of the total annual rainfall, and the noted $\sim$100mm decrease in precipitation at the site over the last 100 years in Cape Range.

To test our assumptions regarding the interpretation of the δ:δ function in reference to vegetation cover we assess the % change in vegetation cover at both sites using remote sensing techniques. The results of the Normalised Difference Vegetation Index (NDVI) analysis is given in Fig. 6.5. Near Infrared (NIR) and red bands for successive Landsat images were converted to radiance values and the NDVI calculated following equation 6.2 and differences calculated using equation 6.3, and converted to percentages. As Landsat images for the two sites prior to 2000 in Cape Range and 1984 in Chillagoe are not available we cannot make conclusions regarding vegetation change prior to this period. However, the results of the NDVI between 1984-2013 in Chillagoe and 2000-2009 in Cape Range indicate predominantly an increase in vegetation cover in Chillagoe (Fig. 6.5 a) of 2-11% and a reduction in vegetation cover of 4-9% in Cape Range. This is in

agreement with our interpretation of the δ:δ results, however as remote sensing data is not available over the whole period in question we are not able to effectively quantify δ:δ change in relation to % change in vegetation cover but believe this may be possible with the publication of longer-term Landsat imagery.

$$NDVI = (NIR - Red)/(NIR + Red) \tag{6.2}$$

$$DIFF = NDVI(old) - NDVI(new) \tag{6.3}$$

6.5 Summary

We conclude that the observed decrease in vegetation cover in the Cape Range site indicated by the analysis of the δ:δ function and NDVI analysis is likely due to a reduction in annual rainfall at the site, due indirectly to a reduction in tropical cyclone activity over the last 50 years. The dominance of C4 vegetation at the site, whilst resistant to tropical cyclone disturbance, is likely dependent on the additional 20% of rainfall brought by tropical cyclone activity annually. In contrast, NDVI analysis of the predominately C3 community in Chillagoe indicates an increase in vegetation cover. Perhaps due to the reduction in natural wind disturbance in the region resulting from a reduction in tropical cyclone activity at the site. This is further highlighted by the close relationship to climate indices which are demonstrated as having a relationship with tropical cyclone activity in the region as found in Chapter 5 namely the MJO and Pacific Warm Pool. Additional connections to global climate indices such as the LOTI and Atmospheric CO_2 indicate that the two environments (tropical woodland vs semiarid savannah) are reacting in opposing fashion to rising global temperatures in conjunction with changes in natural disturbance regimes resulting from the reduction in tropical cyclone activity in both regions.

6.6 Author Contributions

Jordahna Haig processed the three stalagmites, analysed the data, developed the research question and wrote the manuscript. Jonathan Nott collected the three stalagmites, provided funding for the project through the

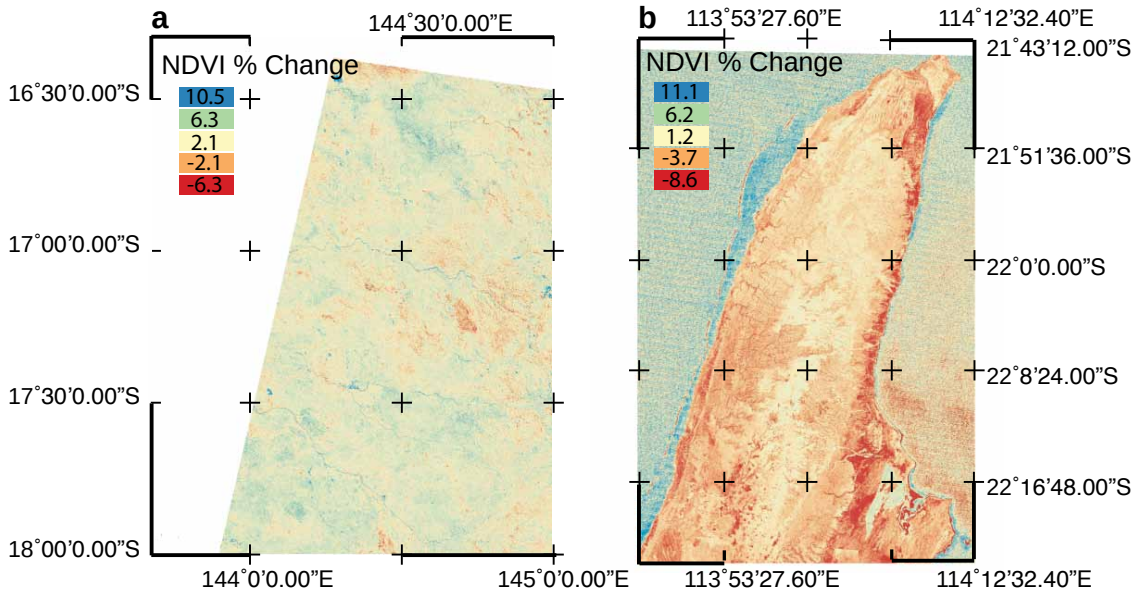

Figure 6.5: Change in the Normalized Difference Vegetation Index (NDVI) (as a percentage) between a, 2000 and 2009 (Cape Range) and b, 1984 and 2013 (Chillagoe). Yellow - blue regions indicate an increase in vegetation health while orange and red regions indicate a decrease. Green region surrounding the cape range coastline is ocean. Winter images (dry-season passes) were used when calculating the NDVI so as to minimise the effects of wet-season rainfall events on the calculations (Landsat images courtesy of the U.S. Geological Survey).

ARC grant and participated in critical discussions on the development of the manuscript. Gert-Jan Reichart provided access to facilities and advice on the data processing. Damien O'Grady provided GIS assistance. Allison Hoskin-Kain provided field assistance in the collection of one stalagmite. Renske Löffler provided laboratory assistance for one stalagmite. All authors discussed the results and commented on the manuscript.

Chapter 7
Summary and Future Directions

The first aim of this thesis was to effectively bridge the gap between the high-temporal resolution instrumental tropical cyclone record and geological proxy record to generate one seamless, quantifiable record spanning the last 1.5 millennia. This involved the development of a new tropical cyclone index by linking isotope dynamics with the meteorological characteristics of tropical cyclones, testing the effectiveness of this theory and calibrating the high-resolution, long-term isotope record against the instrumental tropical cyclone record. The second aim was to examine the tropical cyclone climatology in these two regions at annual, decadal and centennial scales in an attempt to decipher natural variability from anthropogenically induced change. The third aim was to take steps towards applying the palaeorecord, by comparing the long term CAI against other climate indices in an attempt to deduce the drivers of change within the geological record and thus shortlist potential inputs for long-range tropical cyclone forecast models. Stalagmites are palaeoclimate archives providing not only information of changes in the composition and amount of precipitation but other climate variables such as vegetation type and coverage. The fourth aim was to assess the potential impacts of the reduction in CAI at both sites on the surrounding environment. The following chapter summarises the results of the thesis and discusses the practical implications of those results, provides a discussion of the limitations and possible avenues for future work.

The first aim was achieved though the development of CAI, a new technique, which calibrates the high-resolution, long-term negative δ^{18}O excursions in stalagmites against the instrumental tropical cyclone record within each region. CAI allows for a direct comparison between the past and present, and enables an examination of tropical cyclone climatology at higher temporal resolution and on annual, decadal or millennial scales si-

multaneously, without the need to interpolate or extrapolate to account for missing data. This index is based on tropical cyclone activity indices developed by the National Oceanic and Atmospheric Administration and others, which describe the severity of a season in terms of the number of storms, their intensity (V_{max}), their size (R_{max}) and their longevity. The principles of CAI were tested against measured tropical cyclone rainfall, and the δ^{18}O of the stalagmite calcite detrended using a model for the monsoonal δ^{18}O component and established monsoon record from a non-tropical cyclone prone region. CAI is the average accumulated energy expended over the tropical cyclone season within range of the site, accounting for the number of days since genesis and the intensity and size of the storm relative to its distance from the site at each point along its track. The second aim was achieved using trend and wavelet analysis to determine if cyclicity was present in the records. Trend analysis was used to compare the modern period (i.e. $<$100 years) against the complete 1500 year record at each site to decipher anthropogenic effects from natural variability. The third aim of the thesis was achieved using classical statistical techniques and cross wavelet analysis to compare the long-term CAI record with other regional and global climate indices and solar activity proxies to identify any links between these parameters in time-frequency space. This identified a list of potential drivers of tropical cyclone activity, whose influence appears to be scale dependent (i.e. decadal - centenial) and dynamic (i.e. not necessarily consistent throughout time). An investigation of the impacts on the surrounding vegetation at the sites (the fourth aim) was achieved by the application of a duel isotope approach thus, investigating changes in δ^{13}C concurrently with δ^{18}O ($\delta : \delta$) over the most recent 100 years in conjunction with regional and global climate indices.

7.1 Summary of main findings of the thesis

Although it is clear from the analysis of instrumental records that the west coast of Australia is more prone to tropical cyclones than the east coast[106, 165], the long term datasets present here indicate that this is not a recent phenomenon. Tropical cyclone activity on the mid West coast of Australia is on average three times higher than on the northeast coast.

Analysis of CAI indicates that tropical cyclone activity has been highly variable over the past 1,500 yr and wavelet analysis indicates the presence of decadal, inter-decadal and centennial and inter-centennial scale oscillations at both sites. These results indicate that tropical cyclone activity in the Australian region has been significantly less in recent years when compared to the last 550-1,500 yr. In fact, tropical cyclone activity on the west coast of Australia is at an all time low. This reduction in activity is in-line with the most recent IPCC findings noting that the latest global climate model runs project a decrease in the frequency of tropical cyclones towards the end of the twenty-first century in the southwest Pacific[65,195], southern Indian[195,238] and Australian[1] regions. Our results, although based on a limited record, suggest that this may be occurring much earlier than expected. This is in contrast to the increasing frequency and destructiveness of Northern Hemisphere tropical cyclones since 1970 in the Atlantic Ocean[62,64,65] and the western North Pacific Ocean[64,65]. The dramatic reductions in activity since the industrial revolution does not prove an anthropogenic influence on tropical cyclone activity but does suggest that climate change cannot be ruled out as a causative factor. It is not possible to say whether this downward trend in activity will be sustained.

Development of the CAI has enabled the examination of tropical cyclone climatology at higher temporal resolution than was previously possible. Thus the findings outlined in Chapter 4 lead to the investigation of how these cycles in CAI may be driven by other climate phenomena such as the NOI, highlighting the influence of meridional atmospheric patterns in addition to zonal (e.g. SOI), and cross basin teleconnections between CAI and AMM, ESPI, NOI, TWI and the AMM which have not been previously identified (with the exception of TWI). This is an important step forward as the traditional indices (Southern Oscillation Index and the Niño3.4 sea surface temperature index) have not been performing well as predictors of seasonal tropical cyclone activity within the Australian region in recent years[55,99,139] this coupled with a lack of understanding of tropical cyclone activity drivers beyond the scope of the short-term instrumental tropical cyclone record has highlighted the need for a broader investigation of this variability over

decadal, inter-decadal and centennial scales as current statistical models cannot decipher variability which is not present within the instrumental record[139]. The use of the continuous wavelet transform and cross wavelet analysis to assess the relationships between CAI record from Chillagoe and Cape Range against Sun Spot Number (August-October averaged) and longer-term solar proxies from cosmogenic isotope data i.e. southern hemisphere tree ring δ^{14}C data[116] and NGRIP Greenland ^{10}Be concentration data[20], reveals a link between tropical cyclone activity in Western and Eastern Australia and solar cycles at decadal, and centennial scales. As the sun-tropical cyclone connection has now been made within the East and West Atlantic, and now the South West Pacific and South East Indian Ocean, perhaps a multi basin approach to tropical cyclone climatology is warranted in the search for more reliable seasonal predictors and a better understanding of the climatic drivers. Further exploration of the solar forcing connection has highlighted other, more detailed avenues for investigation: namely the solar polar field connection, cosmic ray flux relationships and perhaps even a connection to the sun's meridional flow (although not discussed in depth in text).

This thesis rounds off our investigation of tropical cyclone activity at the two sites by examining the impacts of the reduction in CAI noted in both sites on the surrounding vegetation at the site over the last 100 years (Chapter 6). We conclude that the observed decrease in vegetation cover in the Cape Range site indicated by the analysis of the δ:δ function and NDVI analysis is likely due to a reduction in annual rainfall at the site, due indirectly to a reduction in tropical cyclone activity over the last 50 years. The dominance of C4 vegetation at the site, whilst resistant to tropical cyclone disturbance, is likely dependent on the additional 20% of rainfall brought by tropical cyclone activity annually. In contrast, NDVI analysis of the predominately C3 community in Chillagoe indicates an increase in vegetation cover. Perhaps due to the reduction in natural disturbance in the region resulting from a reduction in tropical cyclone activity at the site. This is further highlighted by the close relationship to climate indices which are demonstrated as having a relationship with tropical cyclone activity in the region as found in Chapter 5 namely

the MJO and Pacific Warm Pool. Additional connections to global climate indices such as the LOTI and Atmospheric CO_2 indicate that the two environments (tropical woodland vs semiarid savannah) are reacting in opposing fashion to rising global temperatures in conjunction with changes in natural disturbance regimes resulting from the reduction in tropical cyclone activity in both regions.

7.2 Practical Implications of this research

Assessing changes in tropical cyclone activity within the context of anthropogenically influenced climate change has been limited by the short temporal resolution of the instrumental tropical cyclone record[131,189] (less than 50 years). Furthermore, controversy exists regarding the robustness of the observational record, especially before 1990[105,126,142]. The development of CAI provides the means to examine not only how tropical cyclone activity has varied as a result of industrialization but also potentially to forecast future trends in tropical cyclone activity under changing climate conditions, given that it is now possible to discern natural variability from anthropogenically induced change. CAI could be a starting point for more sophisticated analysis of other palaeotempest records from around the globe as potential inputs for regional or global climate models and long-range statistical or dynamical forecast models. Deriving a scale of tropical cyclone activity from established high-resolution climate palaeorecords such as stalagmites makes it possible to examine tropical cyclone activity on multiple temporal scales in conjunction with other climate indices, which are thought to influence tropical cyclone activity such as El Niño/Southern Oscillation and as highlighted here, solar activity, and may provide the means with which to uncover other as yet unknown drivers of tropical cyclone activity. CAI could be calculated from other stalagmite records and potentially other palaeotempest records from other basins when verified against the local instrumental tropical cyclone record using a variation of the method presented in this thesis.

7.3 Main Limitations of this work

Whilst due care was taken to ensure an accurate representation and analysis of the data, it is important to outline the main limitations of the thesis and the specific limitations of the results presented in chapter 6, chapter 4 and chapter 5. All stalagmites were actively growing when collected and exhibit clearly visible laminations of alternating dark to light calcite corresponding to wet and dry season calcite precipitation. These sites were specifically selected given the distinct wet and dry season rainfall patterns required to produce such clearly laminated stalagmites and their location within tropical cyclone prone areas. The chronology of the samples was obtained using traditional layer counting methods as the samples were clearly laminated, their layer thicknesses corresponded well to precipitation amounts at the site and there were no visible hiatuses. Unfortunately, the chronology could not be corroborated using conventional methods such as dating via uranium-series dating techniques or radiocarbon methods. An inherent problem arising from the site requirements stated above (distinct wet and dry seasons) is the resulting precipitation of 'dirty' calcite during the wet season which usually renders the samples unsuitable for traditional dating methods due to the presence of excess detrital thorium within the samples. Dating via uranium-series techniques was however attempted but found to be inconclusive. Identification of the 'Bomb Peak' circa 1950 via radiocarbon dating was considered as an alternative, however we concluded that this was impractical given that this would be too early in the series to validate the chronology given the length of the series (1500 years). Attempts were also made to analyse the copper and lead content of CH-1 via laser ablation ICP-MS to compare against the opening and closing of the Chillagoe Smelter, yet these results were inconclusive. Additional, less conventional methods for dating 'dirty' calcite are discussed in section 7.5 below.

Replication within sites using multiple stalagmites from the same cave would have been desirable. Replication was attempted within the Chillagoe Cave by subsampling a further 1500 layers from another stalagmite in proximity to CH-1 yet laboratory issues resulted in these results being discarded due to reliability issues. Further funding and permit re-

strictions prevented the collection of multiple stalagmites from the other two sites. Given the need to obtain high-temporal resolution samples at a seasonal scale from multiple locations spanning the last 1500 years, replication within a single cave whilst desirable, was also not cost effective and impractical given both time and financial constraints.

7.3.1 Limitations specific to the CAI model

There is room for improvement in the current CAI model particularly in the removal of monsoonal signal from stalagmite δ^{18}O. As we currently lack a tropical cyclone *exclusive* monsoon proxy to de-trend the stalagmite δ^{18}O data, $\delta^{18}O_M$ beyond the instrumental record was de-trended from the δ^{18}O data using a spline-interpolated, normalized data set generated from an established Australian-Indonesian monsoonal proxy record[97]. This record has a resolution of 10 yr and extends from 7 yr BP to 12,000 yr BP, the region experiences a relatively low tropical cyclone frequency (on average, 0.24 tropical cyclones per year pass within 400 km of the site[27]), and the record is comparable with other established monsoonal records from the region[97]. The model used to derive $\delta^{18}O_M$ does not take into account factors such as the source region, transport and condensation history of the air masses. Precipitation at Chillagoe is derived from sources in the Coral Sea and the Gulf of Carpentaria. These may have originally been part of a larger air mass, which has travelled north from cooler waters or south from warmer waters. In contrast, precipitation at Cape Range is largely derived from oceanic air masses from the Indian Ocean. However, at this stage there are no other longitudinal, in-depth analyses of δ^{18}O in precipitation from the East or West coast of Australia excepting the model used here from Liu et al[161].

With respect to the meteorological characteristics of the tropical cyclones within the Bureau of Meteorlogy's Best Track Database, 225 of the 2,114 observation points within the combined data sets do not contain wind speed measurements. Given the limited number of environmental pressure measurements available, V_{max} was estimated using the Atkinson/Holliday wind-pressure relationship[3] and missing R_{max} estimates from 1,702

observations were calculated using Willoughby and Rahn[229]. In addition, a revised wind-pressure relationship noted by Knaff and Zehr[130] is optimal however due to the limited number of records with environmental pressure measurements this conversion/estimation was not used. Given the lack of long term, high-temporal resolution tropical cyclone rainfall isotope records in Australia, testing of the CAI model was made against Hurricane Olivia, (a 1994 eastern North Pacific hurricane). While these tests do indicate that K_t is an effective measure of ^{18}O depletion within a tropical cyclone system, ideally testing K_t against ^{18}O from Australian tropical cyclones would be more appropriate. In addition, $K_{n,t}$ does not, take into account the angle of approach of the tropical cyclone (for example, the parameter d does not take into account the orientation of the system relative to the study site and does not distinguish between approach or retreat of the system). This could be improved once a database of Australian Tropical cyclone rainfall $\delta^{18}O$ has been established.

7.3.2 Current Limitations of the Datasets

While this is currently the longest (1500 years) seasonal-resolution tropical cyclone dataset available globally, its relatively short length (in geological terms) limits the investigation of millennial and multimillennial scale oscillations. Due to the edge effects inherent in wavelet analysis (see chapter 4), investigations of periodicities $>$256 years is currently not possible with this record. To examine potential millennial scale climate oscillations the length of the series would need to be extended over several thousand years. In addition, the limited length of some of the climate indices such as SSN and Solar Polarity prevent our ability to quantify these relationships and perhaps limit their inclusion in subsequent seasonal forecast models until a longer record is established.

7.4 Contribution to the field

Other paleo records of tropical cyclone activity include overwash deposits; wave or flood deposits (tempestites) in marine or lagoonal sediment cores; and parallel coral shingle,

shell and/or sand beach ridge sequences. These records can be accurately dated using radiometric methods (therefore providing a chronology of events) and their intensity determined a number of ways using sand layer thickness, sediment grain size, ridge height (in the case of beach ridges) and via comparison of recent events of known intensity. The disadvantage of these records is that they do not record events below a certain threshold as the swash must be high enough to overtop the frontal dunes, this will be dependent on the size of the storm surge, the local topography, and angle of approach of the storm. In Australia, paleorecords of tropical cyclone activity have been recovered from Princess Charlotte Bay; Fitzroy, Normanby, Curacoa, Wallaby and Lady Elliot islands[189]; Wonga[77] and Cowley Beaches[190]; and Shark[185] and Rockingham Bays[76]. Coral shingle and coarse-grained beach ridges (deposited above the highest astronomical tide) are advantageous in that they provide evidence of individual events from which the intensity of the event can be determined empirically (from crest heights) and timing of the event determined using radiocarbon and OSL methods. Analyses of these Australian records indicate that larger more intense events occur with recurrence intervals of two to three centuries (as opposed to once every several millennia as previously thought)[187,189]. Our results have built upon the existing body of knowledge by 'filling the gaps' between and within these centuries with a seasonal activity index (CAI). The advantage of our CAI approach is that it provides high temporal information about the tropical cyclone season as a whole (rather than individual events above a certain threshold), and covers a large section of the coastline. Most palaeorecords of tropical cyclone activity are not normally presented in a way that can be immediately used by climatologists risk assessors or planning agencies for input into GCMs, seasonal forecast models or in risk analysis except when presented as recurrence intervals (an estimate of the likelihood of an event of certain magnitude). The records presented here are quantifiable, allowing for statistical comparisons between tropical cyclone activity and indices which measure climate variability (e.g CAI vs solar activity), and is calibrated against instrumental records of tropical cyclones.

7.5 Future Work

We would like to explore the possibility of using unconventional methods of corroborating the chronology of these samples. We would like to explore the possibility of extracting organic material (derived from the soil zone) from the carbonate layers using either organic geochemical methods (wet chemistry) and/or trapping of the thermally labile macromolecular organic matter using Hydrogen pyrolysis and attempting to date this material. The extraction/trapping and subsequent dating of the liberated material would require the development of a new protocol itself. This should be tested using stalagmites which have been previously dated successfully using conventional uranium-series techniques. These extracts could be dated using radiocarbon methods providing we can recover $>$0.08mg of organic carbon for the ^{14}C AMS dates.

Future works will endeavour to develop alternative non-tropical cyclone precipitation palaeoproxies with the aid of trace element analysis, which can then be used to detrend the monsoon signal from the tropical cyclone signal in-situ. The CAI model (including the derivation of $K_{n,t}$) should be updated once longitudinal studies of ^{18}O in Australian Tropical cyclone precipitation become available. In addition to testing the same methodology in other tropical cyclone prone sites throughout the tropics, an attempt at applying this methodology to other palaeotempest records such as overwash deposits and potentially tree ring records could also be made. The candidate would like to investigate the sun-cyclone connection further, particularly teleconnections between the various characteristics of the 'Solar Dynamo' implied in this thesis including sun spot polarity[174] and it's effects on Cosmic Ray Flux[210], the suns meridional flow recently presented by Hathaway and Rightmire[107] and how these parameters effect the timing, location and severity of tropical cyclogensis on Earth.

References

[1] ABBS, D. The impact of climate change on the climatology of tropical cyclones in the Australian region. Tech. rep., CSIRO, 2010.

[2] APDRC. Webster and Yang Monsoon Index, 2014.

[3] ATKINSON, G. D., AND HOLLIDAY, C. R. Tropical Cyclone Minimum Sea Level Pressure/Maximum Sustained Wind Relationship for the Western North Pacific. *Monthly Weather Review 105*, 4 (1977), 421–427.

[4] ATWATER, B. F. Evidence for Great Holocene Earthquakes Along the Outer Coast of Washington State. *Science 236*, 4804 (1987), 942–944.

[5] ATWATER, B. F., AND MOORE, A. L. A Tsunami About 1000 Years Ago in Puget Sound, Washington. *Science 258*, 5088 (1992), 1614–1617.

[6] AYALON, A., BAR-MATTHEWS, M., AND KAUFMAN, A. Petrography, Strontium, Barium and Uranium Concentrations, and Strontium and Uranium Isotope Ratios in Speleothems as Palaeoclimatic Proxies: Soreq Cave, Israel. *The Holocene 9*, 6 (1999), 715–722.

[7] BAINES, G. B. K., AND MCLEAN, R. F. Sequential studies of hurricane deposit evolution at Funafuti atoll. *Marine Geology 21*, 1 (1976), M1–M8.

[8] BAINES, P. G., AND FOLLAND, C. K. Evidence for a Rapid Global Climate Shift across the Late 1960s. *Journal of Climate 20*, 12 (2007), 2721–2744.

[9] BAISDEN, W., AMUNDSON, R., BRENNER, D., COOK, A., KENDALL, C., AND HARDEN, J. A multiisotope C and N modeling analysis of soil organic matter turnover and transport as a function of soil depth in a California annual grassland soil chronosequence. *Global Biogeochemical Cycles 16*, 4 (2002), 1135.

[10] BAKER, A., ASRAT, A., FAIRCHILD, I. J., LENG, M. J., WYNN, P. M., BRYANT, C., GENTY, D., AND UMER, M. Analysis of the climate signal contained within δ^{18}O and growth rate parameters in two Ethiopian stalagmites. *Geochimica Et Cosmochimica Acta 71*, 12 (2007), 2975–2988.

[11] BAKER, A., ITO, E., SMART, P. L., AND MCEWAN, R. F. Elevated and variable values of ^{13}C in speleothems in a British cave system. *Chemical Geology 136* (1997), 263–270.

[12] BAKER, A., PROCTOR, C., AND BARNES, W. Variations in Stalagmite Luminescence Laminae Structure at Poole's Cavern, England, AD 1910-1996: Calibration of a Palaeoprecipitation Proxy. *The Holocene 9*, 6 (1999), 683–688(6).

[13] BAKER, A., SMART, P. L., EDWARDS, R. L., AND RICHARDS, D. A. Annual Growth Banding in a Cave Stalagmite. *Nature 364*, 6437 (1993), 518.

[14] BAKER, R. G. V., HAWORTH, R. J., AND FLOOD, P. G. Warmer or cooler late Holocene marine palaeoenvironments?: interpreting southeast Australian and Brazilian sea-level changes using fixed biological indicators and their δ^{18}O composition. *Palaeogeography, Palaeoclimatology, Palaeoecology 168*, 3-4 (2001), 249–272.

[15] BALDINI, J. U. L., MCDERMOTT, F., BAKER, A., BALDINI, L. M., MATTEY, D. P., AND RAILSBACK, L. B. Biomass effects on stalagmite growth and isotope ratios: A 20th century analogue from Wiltshire, England. *Earth and Planetary Science Letters 240*, 2 (2005), 486–494.

[16] BARD, E., DELAYGUE, G., ROSTEK, F., ANTONIOLI, F., SILENZI, S., AND SCHRAG, D. P. Hydrological conditions over the western Mediterranean basin during the deposition of the cold Sapropel 6 (ca. 175 kyr BP). *Earth and Planetary Science Letters 202*, 2 (2002), 481 – 494.

[17] BARNARD, H. R., BROOKS, J. R., AND BOND, B. J. Applying the dual-isotope conceptual model to interpret physiological trends under uncontrolled conditions. *Tree Physiol 32*, 10 (2012), 1183–98.

[18] BEER, J. Long-term indirect indices of solar variability. *Space Science Reviews 94*, 1-2 (2000), 53–66.

[19] BELL, G. D., HALPERT, M. S., SCHNELL, R. C., HIGGINS, R. W., LAWRIMORE, J., KOUSKY, V. E., TINKER, R., THIAW, W., CHELLIAH, M., AND ARTUSA, A. Climate Assessment for 1999. *Bulletin of the American Meteorological Society 81*, 6 (2000), 1328–1328.

[20] BERGGREN, A. M., BEER, J., POSSNERT, G., ALDAHAN, A., KUBIK, P., CHRISTL, M., JOHNSEN, S. J., ABREU, J., AND VINTHER, B. M. A 600-year annual ^{10}Be record from the NGRIP ice core, Greenland. *Geophysical Research Letters 36*, 11 (2009), L11801.

[21] BERNER, R. A. A model for atmospheric CO_2 over Phanerozoic time. *American Journal of Science 291*, 4 (1991), 339–376.

[22] BIGELEISEN, J. Chemistry of Isotopes: Isotope chemistry has opened new areas of chemical physics, geochemistry, and molecular biology. *Science 147*, 3657 (1965), 463–471.

[23] BIGG, G. *The Oceans and Climate: 2nd Edition*, 2nd ed. Cambridge University Press, Cambridge, 2003.

[24] BOGLI, A. *Karst Hydrology and Physical Speleology*. Springer-Verlag, Berlin ; New York, 1980.

[25] BOM. Monthly Rainfall, Chillagoe Weather Station No. 030140 (1902-2011), 2011.

[26] BOM. Monthly Rainfall, Exmouth Gulf Weather Station No. 5004 (1915-2011), 2011.

[27] BOM. Australian Tropical Cyclone Database, 12-03-12 2012.

[28] BOM. Daily Global Solar Exposure, 12-03-12 2012.

[29] BOOSE, E. R., FOSTER, D. R., AND FLUET, M. Hurricane impacts to tropical and temperate forest landscapes. *Ecological Monographs 64*, 4 (11 1994), 369.

[30] BRAGANZA, K., POWER, S., TREWIN, B., ARBLASTER, J., TIMBAL, B., HOPE, P., FREDERIKSEN, C., MCBRIDE, J., JONES, D., AND PLUMMER, N. Update on the state of the climate, long-term trends and associated causes. *Climate Science Update: A Report to the 2011 Garnaut Review* (2011), 3.

[31] BRANDT, D. S., AND ELIAS, R. J. Temporal variations in tempestite thickness may be a geologic record of atmospheric CO_2. *Geology 17*, 10 (1989), 951–952.

[32] BRIGGS, W. M. On the Changes in the Number and Intensity of North Atlantic Tropical Cyclones. *Journal of Climate 21*, 6 (2008), 1387–1402.

[33] BROCCOLI, A. J., AND MANABE, S. Can existing climate models be used to study anthropogenic changes in tropical cyclone climate. *Geophysical Research Letters 17*, 11 (1990), 1917–1920.

[34] BROOK, G., SHEEN, S.-W., RAFTER, M., RAILSBACK, L., AND LUNDBERG, J. A High-Resolution Proxy Record of Rainfall and ENSO since AD 1550 from Layering in Stalagmites from Anjohibe Cave, Madagascar. *The Holocene 9*, 6 (1999), 695–705(11).

[35] BRYAN, W. A monograph of Marcus Island. *Occasional Papers of the Bernice Pauahi Bishop Museum 2*, 1 (1903), 77–139.

[36] BURNS, S. J., FLEITMANN, D., MUDELSEE, M., NEFF, U., MATTER, A., AND MANGINI, A. A 780-year annually resolved record of Indian Ocean monsoon precipitation from a speleothem from south Oman. *Journal of Geophysical Research: Atmospheres 107*, D20 (2002), ACL 9–1–ACL 9–9.

[37] CALLAGHAN, J., AND POWER, S. Variability and decline in the number of severe tropical cyclones making land-fall over eastern Australia since the late nineteenth century. *Climate Dynamics 37*, 3-4 (2011), 647–662.

[38] CHAPPELL, J., CHIVAS, A., RHODES, E., AND WALLENSKY, E. Holocene palaeo-environmental changes, central to north Great Barrier Reef inner zone. *BMR Journal of Australian Geology and Geophysics 8* (1983), 223–235.

[39] CHIANG, J. C. H., AND VIMONT, D. J. Analogous Pacific and Atlantic Meridional Modes of Tropical Atmosphere-Ocean Variability. *Journal of Climate 17*, 21 (2004), 4143–4158.

[40] CHU, P.-S., AND ZHAO, X. Bayesian Change-Point Analysis of Tropical Cyclone Activity: The Central North Pacific Case. *Journal of Climate 17*, 24 (2004), 4893–4901.

[41] CHU, P.-S., AND ZHAO, X. A Bayesian Regression Approach for Predicting Seasonal Tropical Cyclone Activity over the Central North Pacific. *Journal of Climate 20*, 15 (2007), 4002–4013.

[42] CROMPTON, R. P., AND MCANENEY, K. J. Normalised Australian insured losses from meteorological hazards: 1967-2006. *Environmental Science and Policy* (In Press).

[43] CULLINGFORD, C. H. D., AND FORD, T. D. *The Science of Speleology*. Academic Press, London ; New York, 1976.

[44] CURTIS, S., AND ADLER, R. ENSO Indices Based on Patterns of Satellite-Derived Precipitation. *Journal of Climate 13*, 15 (2000), 2786–2793.

[45] DANSGAARD, W. Stable Isotopes in Precipitation. *Tellus 16* (1964), 436–468.

[46] DARIENZO, M. E., AND PETERSON, C. D. Episodic tectonic subsidence of Late Holocene salt marshes, northern Oregon central Cascadia margin. *Tectonics 9*, 1 (1990), 1–22.

[47] DENNISTON, R., GONZALEZ, L., BAKER, R., REAGAN, M., ASMEROM, Y., EDWARDS, R., AND ALEXANDER, E. Speleothem Evidence for Holocene Fluctuations of the Prairie-Forest Ecotone, North-Central USA. *The Holocene 9*, 6 (1999), 671–676(6).

[48] DIOCHON, A., AND KELLMAN, L. Natural abundance measurements of 13C indicate increased deep soil carbon mineralization after forest disturbance. *Geophysical Research Letters 35*, 14 (2008), n/a–n/a.

[49] DONNELLY, J. P., BUTLER, J., ROLL, S., WENGREN, M., AND WEBB, T. A backbarrier overwash record of intense storms from Brigantine, New Jersey. *Marine Geology 210*, 1-4 (2004), 107–121.

[50] DONNELLY, J. P., ROLL, S., WENGREN, M., BUTLER, J., LEDERER, R., AND WEBB, T. Sedimentary evidence of intense hurricane strikes from New Jersey. *Geology 29*, 7 (2001), 615.

[51] DONNELLY, J. P., SMITH BRYANT, S., BUTLER, J., DOWLING, J., FAN, L., HAUSMANN, N., NEWBY, P., SHUMAN, B., STERN, J., WESTOVER, K., AND WEBB III, T. 700 yr sedimentary record of intense hurricane landfalls in southern New England. *Geological Society of America Bulletin 113*, 6 (2001), 714–727.

[52] DONNELLY, J. P., AND WOODRUFF, J. D. Intense hurricane activity over the past 5,000 years controlled by El Nino and the West African monsoon. *Nature 447*, 7143 (2007), 465–8.

[53] DONOHUE, R. J., RODERICK, M. L., MCVICAR, T. R., AND FARQUHAR, G. D. Impact of CO_2 fertilization on maximum foliage cover across the globe's warm, arid environments. *Geophysical Research Letters 40*, 12 (2013), 3031–3035.

[54] DORALE, J. A., EDWARDS, R. L., ITO, E., GONZ, AACUTE, AND LEZ, L. A. Climate and Vegetation History of the Midcontinent from 75 to 25 ka: A Speleothem Record from Crevice Cave, Missouri, USA. *Science 282*, 5395 (1998), 1871–1874.

[55] DOWDY, A. J. Long-term changes in Australian tropical cyclone numbers. *Atmospheric Science Letters* (2014), n/a–n/a.

[56] DREYBRODT, W. Kinetics of the dissolution of calcite and its applications to karstification. *Chemical Geology 31* (1980), 245–269.

[57] DREYBRODT, W. A possible mechanism for growth of calcite speleothems without participation of biogenic carbon dioxide. *Earth and Planetary Science Letters 58*, 2 (1982), 293–299.

[58] DUKE, W. L. Hummocky cross-stratification, tropical hurricanes, and intense winter storms. *Sedimentology 32*, 2 (1985), 167–194.

[59] ELSNER, J., AND LIU, K.-B. Examining the ENSO-Typhoon hypothesis. *Climate Research 25*, 1 (2003), 43–54.

[60] ELSNER, J. B., AND JAGGER, T. H. Prediction Models for Annual U.S. Hurricane Counts. *Journal of Climate 19*, 12 (2006), 2935–2952.

[61] ELSNER, J. B., AND JAGGER, T. H. United States and Caribbean tropical cyclone activity related to the solar cycle. *Geophysical Research Letters 35*, 18 (2008), L18705.

[62] ELSNER, J. B., KOSSIN, J. P., AND JAGGER, T. H. The increasing intensity of the strongest tropical cyclones. *Nature 455*, 7209 (2008), 92–95.

[63] EMANUEL, K. A simple model of multiple climate regimes. *Journal of Geophysical Research 107*, D9 (2002), 4077.

[64] EMANUEL, K. Increasing destructiveness of tropical cyclones over the past 30 years. *Nature 436*, 7051 (2005), 686–688.

[65] EMANUEL, K., SUNDARARAJAN, R., AND WILLIAMS, J. Hurricanes and Global Warming: Results from Downscaling IPCC AR4 Simulations. *Bulletin of the American Meteorological Society 89*, 3 (2008), 347–367.

[66] EMANUEL, K. A. An Air-Sea Interaction Theory for Tropical Cyclones. Part I: Steady-State Maintenance. *Journal of the Atmospheric Sciences 43*, 6 (1986), 585–605.

[67] EMANUEL, K. A. The Maximum Intensity of Hurricanes. *Journal of the Atmospheric Sciences 45*, 7 (1988), 1143–1155.

[68] EMANUEL, K. A. Sensitivity of Tropical Cyclones to Surface Exchange Coefficients and a Revised Steady-State Model incorporating Eye Dynamics. *Journal of the Atmospheric Sciences 52*, 22 (1995), 3969–3976.

[69] ESRL. Mauna Loa CO_2 annual mean data, 2011.

[70] ESRL. Pacific Warm Pool 1st EOF of SST (60e-170E, 15S-15N), 2011.

[71] FAIRCHILD, I., FRISIA, S., BORSATO, A., AND TOOTH, A. *Speleothems*. Blackwells, Oxford, 2006, ch. 7, pp. 200–245.

[72] FAIRCHILD, I. J., SMITH, C. L., BAKER, A., FULLER, L., SPTL, C., MATTEY, D., MCDERMOTT, F., AND E.I.M.F. Modification and preservation of environmental signals in speleothems. *Earth-Science Reviews 75*, 1-4 (2006), 105–153.

[73] FAURE, G. *Principles and Applications of Geochemistry: a Comprehensive Textbook for Geology Students*, 2nd ed. ed. Prentice Hall, Upper Saddle River, N.J., 1998.

[74] FISCHER, M. *Quaternary environmental change in the Australian region: through the theory, observation and inference of patterns in the speleothem record*. Division of Geography, School of Geosciences, Faculty of Science, University of Sydney, 2001.

[75] FISCHER, M., GALE, S., HEIJNIS, H., AND DRYSDALE, R. *Low latitude speleothems and palaeoclimatic reconstruction (Northwest Queensland, Australia)*, vol. Special Publication 2. Karst Waters Institute, 1996, pp. 26–29.

[76] FORSYTH, A. J., NOTT, J., AND BATEMAN, M. D. Beach ridge plain evidence of a variable late-Holocene tropical cyclone climate, North Queensland, Australia. *Palaeogeography, Palaeoclimatology, Palaeoecology 297*, 3–4 (2010), 707 – 716.

[77] FORSYTH, A. J., NOTT, J., BATEMAN, M. D., AND BEAMAN, R. J. Juxtaposed beach ridges and foredunes within a ridge plain — Wonga Beach, northeast Australia. *Marine Geology 307–310*, 0 (2012), 111 – 116.

[78] FRAPPIER, A., AND SAHAGIAN, D. Individual Tropical Storm Events in Speleothem Records; a New Tool for Paleotempestology?, 20001128 2000.

[79] FRAPPIER, A. B. A stepwise screening system to select storm-sensitive stalagmites: Taking a targeted approach to speleothem sampling methodology. *Quaternary International 187*, 1 (2008), 25–39.

[80] FRAPPIER, A. B. Masking of interannual climate proxy signals by residual tropical cyclone rainwater: Evidence and challenges for low-latitude speleothem paleoclimatology. *Geochemistry, Geophysics, Geosystems 14*, 9 (2013), 3632–3647.

[81] FRAPPIER, A. B., SAHAGIAN, D., CARPENTER, S. J., GONZALEZ, L. A., AND FRAPPIER, B. R. High-Resolution Paleotempestology: Proxy Models for Reconstructing Interannual-Decadal Variations in Pre-Historic Tropical Cyclone Frequency and Intensity, 2005.

[82] FRAPPIER, A. B., SAHAGIAN, D., CARPENTER, S. J., GONZALEZ, L. A., AND FRAPPIER, B. R. Stalagmite stable isotope record of recent tropical cyclone events. *Geology 35*, 2 (2007), 111–114.

[83] FRAPPIER, A. E. High-Resolution Stable Isotope Dynamics Recorded by Speleothem Calcite; New Opportunities for Paleotempestology, Paleometeorology, and Paleoecology. Master's, Department of Earth Sciences, 2002.

[84] FRAPPIER, A. M. Y., KNUTSON, T., LIU, K.-B., AND EMANUEL, K. Perspective: coordinating paleoclimate research on tropical cyclones with hurricane-climate theory and modelling. *Tellus 59* (2007), 529–537.

[85] FRITZ, P., AND POPLAWSKI, S. ^{18}O and ^{13}C in the shells of freshwater molluscs and their environments. *Earth and Planetary Science Letters 24*, 1 (1974), 91–98.

[86] GASCOYNE, M. Trace Element Geochemistry of Speleothems, 1977.

[87] GEDZELMAN, S., AND LAWRENCE, J. The Isotopic Composition of Precipitation from two Extratropical Cyclones. *Monthly Weather Review 118* (1990), 495–509.

[88] GEDZELMAN, S., LAWRENCE, J., GAMACHE, J., AND BLACK, M. Probing Hurricanes with Stable Isotopes of Rain and Water Vapor. *Monthly Weather Review 131*, 6 (2003), 1112.

[89] GEDZELMAN, S. D., LAWRENCE, J., AND WHITE, J. The Isotopic Composition of Precipitation and Water Vapor in New York, 198302 1983.

[90] GEDZELMAN, S. D., AND LAWRENCE, J. R. The Isotopic Composition of Cyclonic Precipitation. *Journal of Applied Meteorology 21*, 10 (1982), 1385–1404.

[91] GEDZELMAN, S. D., AND LAWRENCE, J. R. Tropical Ice Core Isotopes: Do they Reflect Changes in Storm Activity? *Geophysical Research Letters 30*, 2 (2003), 1072–1074.

[92] GEDZELMAN, S. D., LAWRENCE, J. R., WHITE, J. W. C., AND SMILEY, D. The Isotopic Composition of Precipitation at Mohonk Lake, New York; the Amount Effect. *Journal of Geophysical Research: Part D, Atmospheres 92*, 1 (1987), 1033–1040.

[93] GIANNINI, A., KUSHNIR, Y., AND CANE, M. A. Interannual Variability of Caribbean Rainfall, ENSO, and the Atlantic Ocean. *Journal of Climate 13*, 2 (2000), 297–311.

[94] GILLIESON, D. S. *Caves : Processes, Development, and Management*. The Natural environment. Blackwell Publishers, Cambridge, Mass., 1996.

[95] GONZALEZ, L., CARPENTER, S., AND LOHMANN, K. Inorganic calcite morphology: roles of fluid chemistry and fluid flow. *Journal of Sedimentary Petrology 62* (1992), 382–99.

[96] GRANGER, K., JONES, T., LEIBA, M., AND SCOTT, G. Community Risk in Cairns: A multi-hazard risk assessment. Tech. rep., Community Risk in Cairns: A multi-hazard risk assessment, 1999.

[97] GRIFFITHS, M. L., DRYSDALE, R. N., GAGAN, M. K., ZHAO, J. X., AYLIFFE, L. K., HELLSTROM, J. C., HANTORO, W. S., FRISIA, S., FENG, Y. X., CARTWRIGHT, I., PIERRE, E. S., FISCHER, M. J., AND SUWARGADI, B. W. Increasing Australian-Indonesian monsoon rainfall linked to early Holocene sea-level rise. *Nature Geosci 2*, 9 (2009), 636–639.

[98] GRINSTED, A., MOORE, J. C., AND JEVREJEVA, S. Application of the cross wavelet transform and wavelet coherence to geophysical time series. *Nonlin. Processes Geophys. 11*, 5/6 (2004), 561–566.

[99] GRINSTED, A., MOORE, J. C., AND JEVREJEVA, S. Projected Atlantic hurricane surge threat from rising temperatures. *Proceedings of the National Academy of Sciences 110*, 14 (2013), 5369–5373.

[100] HAIG, J., NOTT, J., AND REICHART, G.-J. Australian tropical cyclone activity lower than at any time over the past 550-1,500 years. *Nature 505*, 7485 (2014), 667–671.

[101] HAMILTON-SMITH, E., AND FINLAYSON, B. *Beneath the Surface : a Natural History of Australian Caves*. University of New South Wales Press, Sydney, 2003.

[102] HANSEN, J., RUEDY, R., SATO, M., AND LO, K. Global Surface Temperature Change. *Reviews of Geophysics 48*, 4 (2010), RG4004.

[103] HARDY, T. A., MASON, L. B., AND ASTORQUIA, A. Queensland climate change and community vulnerability to tropical cyclones - ocean hazards assessment - stage 3: the frequency of surge plus tide during tropical cyclones for selected open coast locations along the Queensland east coast. Tech. rep., James Cook University Marine Modelling Unit, 2004.

[104] HARMON, R., SCHWARCZ, H., GASCOYNE, M., HESS, J., AND FORD, D. *Palaeoclimate Information From Speleothems: the Present as Guide to The Past*. Kluwer Academic/Plenum Publishers, New York, 2004, pp. 199–225.

[105] HARPER, B., STROUD, S., MCCORMACK, M., AND WEST, S. A. A review of historical tropical cyclone intensity in north-western Australia and implications for climate change trend analysis. *Australian Meteorological Magazine 57*, 2 (2008), 121–141.

[106] HASSIM, M. E. E., AND WALSH, K. J. E. Tropical cyclone trends in the Australian region. *Geochemistry, Geophysics, Geosystems 9*, 7 (2008), Q07V07.

[107] HATHAWAY, D. H., AND RIGHTMIRE, L. Variations in the Sun's Meridional Flow over a Solar Cycle. *Science 327*, 5971 (2010), 1350–1352.

[108] HAYNE, M., AND CHAPPELL, J. Cyclone frequency during the last 5000 years at Curacoa Island, north Queensland, Australia. *Palaeogeography,Palaeoclimatology,Palaeoecology 168*, 3-4 (2001), 207–219.

[109] HENDERSON-SELLERS, A., ZHANG, H., BERZ, G., EMANUEL, K., GRAY, W., LANDSEA, C., HOLLAND, G., LIGHTHILL, J., SHIEH, S. L., WEBSTER, P., AND MCGUFFIE, K. Tropical Cyclones and Global Climate Change: A Post-IPCC Assessment. *Bulletin of the American Meteorological Society 79*, 1 (1998), 19–38.

[110] HENDY, C. H. The isotopic geochemistry of speleothems-I. The calculation of the effects of different modes of formation on the isotopic composition of speleothems and their applicability as palaeoclimatic indicators. *Geochimica et Cosmochimica Acta 35*, 8 (1971), 801–824.

[111] HIGGINS, P., AND MACFADDEN, B. J. 'Amount Effect' recorded in oxygen isotopes of Late Glacial horse (Equus) and bison (Bison) teeth from the Sonoran and Chihuahuan deserts, southwestern United States. *Palaeogeography, Palaeoclimatology, Palaeoecology 206*, 3-4 (2004), 337–353.

[112] HODGES, R., JAGGER, T., AND ELSNER, J. The sun-hurricane connection: Diagnosing the solar impacts on hurricane frequency over the North Atlantic basin using a space-time model. *Natural Hazards 73*, 2 (2014), 1063–1084.

[113] HODGES, R. E., AND ELSNER, J. B. Evidence linking solar variability with US hurricanes. *International Journal of Climatology 31*, 13 (2011), 1897–1907.

[114] HODGES, R. E., AND ELSNER, J. B. The Spatial Pattern of the Sun-Hurricane Connection across the North Atlantic. *ISRN Meteorology 2012* (2012), 9.

[115] HOEFS, J. *Stable Isotope Geochemistry*, 5th ed. Springer, London, 2004.

[116] HOGG, A. G., HUA, Q., BLACKWELL, P. G., NIU, M., BUCK, C. E., GUILDERSON, T. P., HEATON, T. J., PALMER, J. G., REIMER, P. J., REIMER, R. W., TURNEY, C. S. M., AND ZIMMERMAN, S. R. H. SHCal13 Southern Hemisphere Calibration, 0-50,000 Years cal BP. *Radiocarbon 55*, 4 (2013), 1889–1903.

[117] HOLLAND, G. J. The Maximum Potential Intensity of Tropical Cyclones. *Journal of the Atmospheric Sciences 54*, 21 (1997), 2519–2541.

[118] HOLPER, P. N. Climate change, science information paper [electronic resource]: Australian rainfall : past, present and future, 2011.

[119] HOYOS, C. D., AGUDELO, P. A., WEBSTER, P. J., AND CURRY, J. A. Deconvolution of the factors contributing to the increase in global hurricane intensity. *Science 312*, 5770 (2006), 94–7.

[120] HUTTON, B. T., SCHEITLIN, K. N., AND DIXON, P. G. Solar cycle extremes as a seasonal predictor of Atlantic-Basin tropical cyclones. *Southeastern Geographer 53*, 1 (2013), 50–60.

[121] IONOV, D., AND HARMER, R. E. Trace element distribution in calcite-dolomite carbonatites from Spitskop: inferences for differentiation of carbonatite magmas and the origin of carbonates in mantle xenoliths. *Earth and Planetary Science Letters 198* (2002), 495–510.

[122] ITO, M., ISHIGAKI, A., NISHIKAWA, T., AND SAITO, T. Temporal variation in the wavelength of hummocky cross-stratification: Implications for storm intensity through Mesozoic and Cenozoic. *Geology 29*, 1 (2001), 87–89.

[123] JAGGER, T. H., AND ELSNER, J. B. Climatology Models for Extreme Hurricane Winds near the United States. *Journal of Climate 19*, 13 (2006), 3220–3236.

[124] JAMES, J. *The Crystal Gallery*. University of New South Wales Press, Sydney, 2003, ch. 2, pp. 53–88.

[125] JENNINGS, J. N. *Karst Geomorphology*. B. Blackwell, New York, 1985.

[126] KAMAHORI, H., YAMAZAKI, N., MANNOJI, N., AND TAKAHASHI, K. Variability in Intense Tropical Cyclone Days in the Western North Pacific. *SOLA 2* (2006), 104–107.

[127] KANTHA, L. Time to replace the Saffir-Simpson hurricane scale? *Eos, Transactions American Geophysical Union 87*, 1 (2006), 3–6.

[128] KEENAN, T., MAY, P., HOLLAND, G., RUTLEDGE, S., CARBONE, R., WILSON, J., MONCRIEFF, M., CROOK, A., TAKAHASHI, T., TAPPER, N., PLATT, M., HACKER, J., SEKELSKY, S., SAITO, K., AND GAGE, K. The Maritime Continent Thunderstorm Experiment (MCTEX): Overview and Some Results. *Bulletin of the American Meteorological Society 81*, 10 (2015/01/15 2000), 2433–2455.

[129] KENDRIC, P., AND MAU, R. Carnarvon 1 (CAR1 - Cape Range subregion). Tech. rep., Department of Conservation and Land Management, Perth, 2002.

[130] KNAFF, J. A., AND ZEHR, R. M. Reexamination of Tropical Cyclone Wind-Pressure Relationships. *Weather and Forecasting 22*, 1 (2007), 71–88.

[131] KNUTSON, T. R., MCBRIDE, J. L., CHAN, J., EMANUEL, K., HOLLAND, G., LANDSEA, C., HELD, I., KOSSIN, J. P., SRIVASTAVA, A. K., AND SUGI, M. Tropical cyclones and climate change. *Nature Geosci 3*, 3 (2010), 157–163.

[132] KNUTSON, T. R., SIRUTIS, J. J., GARNER, S. T., VECCHI, G. A., AND HELD, I. M. Simulated reduction in Atlantic hurricane frequency under twenty-first-century warming conditions. *Nature Geoscience 1*, 6 (2008), 359–364.

[133] KNUTSON, T. R., AND TULEYA, R. E. Impact of CO_2-induced warming on simulated hurricane intensity and precipitation: Sensitivity to the choice of climate model and convective parameterization. *Journal of Climate 17*, 18 (2004), 3477–3495.

[134] KOLODNY, Y., BAR-MATTHEWS, M., AYALON, A., AND MCKEEGAN, K. A high spatial resolution δ^{18}O profile of a speleothem using an ion-microprobe. *Chemical Geology 197*, 1-4 (2003), 21–28.

[135] KOLODNY, Y., CALVO, R., AND ROSENFELD, D. "Too low" δ^{18}O of paleo-meteoric, low latitude, water; do paleo-tropical cyclones explain it? *Palaeogeography, Palaeoclimatology, Palaeoecology 280*, 3–4 (2009), 387 – 395.

[136] KONG, X. G., WANG, Y. J., WU, J. Y., CHENG, H., EDWARDS, R. L., AND WANG, X. F. Complicated responses of stalagmite δ^{13}C to climate change during the last glaciation from Hulu Cave, Nanjing, China. *Science in China Series D-Earth Sciences 48*, 12 (2005), 2174–2181.

[137] KORNEXL, B. E., WERNER, R. A., AND GEHRE, M. Standardization for oxygen isotope ratio measurement - still an unsolved problem. *Rapid communications in mass spectrometry : RCM 13*, 13 (1999), 1248–1251.

[138] KOSSIN, J. P., KNAPP, K. R., VIMONT, D. J., MURNANE, R. J., AND HARPER, B. A. A globally consistent reanalysis of hurricane variability and trends. *Geophysical Research Letters 34* (2007), L04815.

[139] KULESHOV, Y., WANG, Y., APAJEE, J., FAWCETT, R., AND JONES, D. Prospects for Improving the Operational Seasonal Prediction of Tropical Cyclone Activity in the Southern Hemisphere. *Atmospheric and Climate Sciences 2*, 3 (2012), 298–306.

[140] LACHNIET, M. S. Climatic and environmental controls on speleothem oxygen-isotope values. *Quaternary Science Reviews 28*, 5-6 (2009), 412–432.

[141] LANDSEA, C., ANDERSON, C., CHARLES, N., CLARK, G., DUNION, J., FERNÁNDEZ-PARTAGÁS, J., HUNGERFORD, P., NEUMANN, C., AND ZIMMER, M. *The Atlantic Hurricane Database Re-analysis Project: Documentation for 1851-1910 Alterations and Addition to the HURDAT Database*. Columbia University Press, New York, 2004, pp. 177 – 221.

[142] LANDSEA, C. W., HARPER, B. A., HOARAU, K., AND KNAFF, J. A. Climate change. Can we detect trends in extreme tropical cyclones? *Science 313*, 5786 (2006), 452–454.

[143] LANE, P., DONNELLY, J. P., WOODRUFF, J. D., AND HAWKES, A. D. A decadally-resolved paleohurricane record archived in the late Holocene sediments of a Florida sinkhole. *Marine Geology 287*, 1-4 (2011), 14–30.

[144] LAURITZEN, S., FORD, D., AND SCHWARCZ, H. Humic Substances in Spelothem Matrix - Palaeoclimatic Significance, Aug. 1-8 1986.

[145] LAURITZEN, S.-E., AND LUNDBERG, J. Calibration of the Speleothem Delta Function: an Absolute Temperature Record for the Holocene in Northern Norway. *The Holocene 9*, 6 (1999), 659–669(11).

[146] LAURITZEN, S.-E., AND LUNDBERG, J. Speleothems and climate: a special issue of The Holocene. *The Holocene 9*, 6 (1999), 643–647(5).

[147] LAWRENCE, J. Isotopic Spikes from Tropical Cyclones in Surface Waters: Opportunities in Hydrology and Paleoclimatology. *Chemical Geology 144* (1998), 153–160.

[148] LAWRENCE, J., GEDZELMAN, S., WHITE, J., SMILEY, D., AND LAZOV, P. Storm Trajectories in the Eastern United States and the D/H Isotopic Composition of Precipitation. *Nature 296* (1982), 638–640.

[149] LAWRENCE, J., AND WHITE, J. Growing Season Precipitation from the D/H Ratios of Eastern White Pine. *Nature 311* (1984), 558–560.

[150] LAWRENCE, J., AND WHITE, J. *The elusive climate signal in the isotopic composition of precipitation*. The Geochemical Society (Lancaster Press, Trinity University, San Antonio, TX), 1991, pp. 169–186.

[151] LAWRENCE, J. R. Winds, Water Budgets, and Stable Isotopes in Tropical Cyclones Using TRMM and QUICKSCAT. Tech. rep., Environmental Institute of Houston, 2000.

[152] LAWRENCE, J. R., AND GEDZELMAN, S. D. Detection of Tropical Cyclone Activity in the Geologic Past, 19951107 1995.

[153] LAWRENCE, J. R., AND GEDZELMAN, S. D. Low Stable Isotope Ratios of Tropical Cyclone Rains. *Geophysical Research Letters 23*, 5 (1996), 527–530.

[154] LAWRENCE, J. R., GEDZELMAN, S. D., DEXHEIMER, D., CHO, H.-K., CARRIE, G. D., GASPARINI, R., ANDERSON, C. R., P., B. K., AND BIGGERSTAFF, M. I. The Stable Isotopic Composition of Water Vapor in the Tropics. *Journal of Geophysical Research 109*, D6 (2004), D06115, Paper No. 10.1029/2003JD004046.

[155] LAWRENCE, J. R., GEDZELMAN, S. D., GAMACHE, J., AND BLACK, M. Stable Isotope Ratios: Hurricane Olivia. *Journal of Atmospheric Chemistry 41* (2002), 67–82.

[156] LAWRENCE, J. R., GEDZELMAN, S. D., ZHANG, X., AND ARNOLD, R. Stable Isotope Ratios of Rain and Vapor in 1995 Hurricanes. *Journal of Geophysical Research 103*, D10 (1998), 11381–11400.

[157] LEE, T., AND MCPHADEN, M. J. Decadal phase change in large-scale sea level and winds in the Indo-Pacific region at the end of the 20th century. *Geophysical Research Letters 35* (2008).

[158] LENG, M. J., AND MARSHALL, J. D. Palaeoclimate interpretation of stable isotope data from lake sediment archives. *Quaternary Science Reviews 23*, 7Äì8 (2004), 811–831.

[159] LI, M. Z., AND AMOS, C. L. Sheet flow and large wave ripples under combined waves and currents: field observations, model predictions and effects on boundary layer dynamics. *Continental Shelf Research 19* (1999), 637–663.

[160] LIGHTHILL, J., HOLLAND, G., GRAY, W., LANDSEA, C., CRAIG, G., EVANS, J., KURIHARA, Y., AND GUARD, C. Global climate change and tropical cyclones. *Bulletin of the American Meteorological Society v75*, n11 (1994), p2147(11).

[161] LIU, J., FU, G., SONG, X., CHARLES, S. P., ZHANG, Y., HAN, D., AND WANG, S. Stable isotopic compositions in Australian precipitation. *J. Geophys. Res. 115*, D23 (2010), D23307.

[162] LIU, K.-B. *Paleoclimate Reconstruction - Paleotempestology*. Elsevier, Oxford, 2007, pp. 1974–1985.

[163] LIU, K.-B., AND FEARN, M. L. Lake-sediment record of late Holocene hurricane activities from coastal Alabama. *Geology 21*, 9 (1993), 793–796.

[164] LIU, K.-B., AND FEARN, M. L. Reconstruction of Prehistoric Landfall Frequencies of Catastrophic Hurricanes in Northwestern Florida from Lake Sediment Records. *Quaternary Research 54*, 2 (2000), 238–245.

[165] LIU, K. S., AND CHAN, J. C. L. Interannual variation of Southern Hemisphere tropical cyclone activity and seasonal forecast of tropical cyclone number in the Australian region. *International Journal of Climatology 32*, 2 (2012), 190–202.

[166] MAGNUSSON, W. E., SANAIOTTI, T. M., LIMA, A. P., MARTINELLI, L. A., VICTORIA, R. L., DE ARAÚJO, M. C., AND ALBERNAZ, A. L. A comparison of 13C ratios of surface soils in savannas and forests in Amazonia. *Journal of Biogeography 29*, 7 (2002), 857–863.

[167] MALMQUIST, D. Oxygen isotopes in cave stalagmites as a proxy record of past tropical cyclone activity, 393-394 1997.

[168] MANN, M. E. Smoothing of climate time series revisited. *Geophysical Research Letters 35*, 16 (2008), L16708.

[169] MANN, M. E., AND EMANUEL, K. A. Atlantic hurricane trends linked to climate change. *Eos, Transactions American Geophysical Union 87*, 24 (2006), 233–241.

[170] MANN, M. E., WOODRUFF, J. D., DONNELLY, J. P., AND ZHANG, Z. Atlantic hurricanes and climate over the past 1,500 years. *Nature 460*, 7257 (2009), 880–883.

[171] MCDERMOTT, F., SCHWARCZ, H., AND ROWE, P. J. *Isotopes in speleothems*, vol. 10. Springer, 2006, pp. 185–218.

[172] MICHAELS, P. J., KNAPPENBERGER, P. C., AND LANDSEA, C. Comments on 'Impacts of CO_2-Induced Warming on Simulated Hurricane Intensity and Precipitation: Sensitivity to the Choice of Climate Model and Convective Scheme'. *Journal of Climate 18*, 23 (2005), 5179–5182.

[173] MICKLER, P. J., STERN, L. A., AND BANNER, J. L. Large kinetic isotope effects in modern speleothems. *Geological Society of America Bulletin 118*, 1-2 (2006), 65–81.

[174] MIYAHARA, H., YOKOYAMA, Y., AND MASUDA, K. Possible link between multi-decadal climate cycles and periodic reversals of solar magnetic field polarity. *Earth and Planetary Science Letters 272*, 1-2 (2008), 290–295.

[175] MÜHLINGHAUS, C., SCHOLZ, D., AND MANGINI, A. Modelling fractionation of stable isotopes in stalagmites. *Geochimica Et Cosmochimica Acta 73*, 24 (2009), 7275–7289.

[176] NANAYAMA, F., SATAKE, K., FURUKAWA, R., SHIMOKAWA, K., ATWATER, B. F., SHIGENO, K., AND YAMAKI, S. Unusually large earthquakes inferred from tsunami deposits along the Kuril Trench. *Nature 424*, 6949 (2003), 660–663.

[177] NASA. Time Series of the ENSO Precipitation Index (ESPI), 19/10/2014 2011.

[178] NASA. Global Land-Ocean Temperature Index (LOTI), 2012.

[179] NICHOLLS, N., LANDSEA, C., AND GILL, J. Recent trends in Australian region tropical cyclone activity. *Meteorology and Atmospheric Physics 65*, 3 (1998), 197–205.

[180] NIGGEMANN, S., MANGINI, A., RICHTER, D. K., AND WURTH, G. A paleoclimate record of the last 17,600 years in stalagmites from the B7 cave, Sauerland, Germany. *Quaternary Science Reviews 22*, 5-7 (2003), 555–567.

[181] NOAA. Pentad MJO indices, 2009.

[182] NOAA. Pacific Decadal Osscilation (PDO) Index, 2012.

[183] NOAA. HURDAT Best Track Data, 2013.

[184] NOTT, J. Palaeotempestology: the study of prehistoric tropical cyclones-a review and implications for hazard assessment. *Environment International 30*, 3 (2004), 433–447.

[185] NOTT, J. A 6000 year tropical cyclone record from Western Australia. *Quaternary Science Reviews 30*, 5–6 (2011), 713 – 722.

[186] NOTT, J., CHAGUE-GOFF, C., GOFF, J., SLOSS, C., AND RIGGS, N. Anatomy of sand beach ridges: Evidence from severe Tropical Cyclone Yasi and its predecessors, northeast Queensland, Australia. *Journal of Geophysical Research: Earth Surface 118*, 3 (2013), 1710–1719.

[187] NOTT, J., AND FORSYTH, A. Punctuated global tropical cyclone activity over the past 5,000 years. *Geophysical Research Letters 39*, 14 (2012), L14703.

[188] NOTT, J., HAIG, J., NEIL, H., AND GILLIESON, D. Greater frequency variability of landfalling tropical cyclones at centennial compared to seasonal and decadal scales. *Earth and Planetary Science Letters 255*, 3-4 (2007), 367–372.

[189] NOTT, J., AND HAYNE, M. High frequency of 'super-cyclones' along the Great Barrier Reef over the past 5,000 years. *Nature 413*, 6855 (2001), 508–512.

[190] NOTT, J., SMITHERS, S., WALSH, K., AND RHODES, E. Sand beach ridges record 6000 year history of extreme tropical cyclone activity in northeastern Australia. *Quaternary Science Reviews 28*, 15–16 (2009), 1511 – 1520.

[191] NOTT, J. F. Intensity of prehistoric tropical cyclones. *Journal of Geophysical Research: Part D, Atmospheres 108*, D7 (2003).

[192] NOTT, J. F., AND JAGGER, T. H. Deriving robust return periods for tropical cyclone inundations from sediments. *Geophysical Research Letters 40*, 2 (2013), 370–373.

[193] OBSERVATORY, W. S. Wilcox Solar Observatory Polar Field Observations, 2014.

[194] O'NEIL, J., CLAYTON, R., AND MAYEDA, T. Oxygen isotope fractionation in divalent metal carbonates. *Journal of Chemical Physics 51* (1969), 5547–5559.

[195] OOUCHI, K., YOSHIMURA, J., YOSHIMURA, H., MIZUTA, R., KUSUNOKI, S., AND NODA, A. Tropical Cyclone Climatology in a Global-Warming Climate as Simulated in a 20 km-Mesh Global Atmospheric Model: Frequency and Wind Intensity Analyses. *Journal of the Meteorological Society of Japan 84*, 2 (2006), 259–276.

[196] PARKER, D., FOLLAND, C., SCAIFE, A., KNIGHT, J., COLMAN, A., BAINES, P., AND DONG, B. Decadal to multidecadal variability and the climate change background. *Journal of Geophysical Research: Atmospheres 112*, D18 (2007), D18115.

[197] PÈREZ-PERAZA, J., KAVLAKOV, S., VELASCO, V., GALLEGOS-CRUZ, A., AZPRA-ROMERO, E., DELGADO-DELGADO, O., AND VILLICAÒA-CRUZ, F. Solar, geomagnetic and cosmic ray intensity changes, preceding the cyclone appearances around Mexico. *Advances in Space Research 42*, 9 (2008), 1601–1613.

[198] PROKOPH, A., AND EL BILALI, H. Cross-Wavelet Analysis: a Tool for Detection of Relationships between Paleoclimate Proxy Records. *Mathematical Geosciences 40*, 5 (2008), 575–586.

[199] RASBURY, M., AND AHARON, P. ENSO-controlled rainfall variability records archived in tropical stalagmites from the mid-ocean island of Niue, South Pacific. *Geochemistry, Geophysics, Geosystems 7*, 7 (2006), Q07010.

[200] RODEN, J. S., AND FARQUHAR, G. D. A controlled test of the dual-isotope approach for the interpretation of stable carbon and oxygen isotope ratio variation in tree rings. *Tree Physiol 32*, 4 (2012), 490–503.

[201] SCHWING, F. B., MURPHREE, T., AND GREEN, P. M. The Northern Oscillation Index (NOI): a new climate index for the northeast Pacific. *Progress in Oceanography 53*, 2-4 (2002), 115–139.

[202] SHOPOV, Y. Y., FORD, D. C., AND SCHWARCZ, H. P. Luminescent Microbanding in Speleothems: High-Resolution Chronology and Paleoclimate. *Geology 22*, 5 (1994), 407.

[203] (SIDC), S. I. D. A. C. The Sunspot Cycle, 2014.

[204] SOUTHARD, J. B., LAMBIE, J. M., FEDERICO, D. C., PILE, H. T., AND WEIDMAN, C. R. Experiments on bed configurations in fine sands under bidirectional purely oscillatory flow, and the origin of hummocky cross-stratification. *SEPM Journal of Sedimentary Research 60*, 1 (1990), 1–17.

[205] STEVENSON, B. A., KELLY, E. F., MCDONALD, E. V., AND BUSACCA, A. J. The stable carbon isotope composition of soil organic carbon and pedogenic carbonates along a bioclimatic gradient in the Palouse region, Washington State, USA. *Geoderma 124*, 1-2 (2005), 37–47.

[206] STUIVER, M., AND BRAZIUNAS, T. F. Atmospheric ^{14}C and century-scale solar oscillations. *Nature 338*, 6214 (1989), 405–408.

[207] STUIVER, M., AND BRAZIUNAS, T. F. Sun, ocean, climate and atmospheric $^{14}CO_2$: an evaluation of causal and spectral relationships. *The Holocene 3*, 4 (1993), 289–305.

[208] STUIVER, M., AND QUAY, P. D. Changes in Atmospheric Carbon-14 Attributed to a Variable Sun. *Science 207*, 4426 (1980), 11–19.

[209] STUIVER, M., AND QUAY, P. D. A 1600 year long record of solar change derived from atmospheric ^{14}C levels. *Solar Physics 74*, 2 (1981), 479–481.

[210] THOMAS, S. R., OWENS, M. J., AND LOCKWOOD, M. The 22-Year Hale Cycle in Cosmic Ray Flux - Evidence for Direct Heliospheric Modulation. *Solar Physics 289*, 1 (2014), 407–421.

[211] TORRENCE, C., AND COMPO, G. A Practical Guide to Wavelet Analysis. *Bulletin of the American Meteorological Society 79*, 1 (1998), 61–78.

[212] TREBLE, P., SHELLEY, J. M. G., AND CHAPPELL, J. Comparison of high resolution sub-annual records of trace elements in a modern (1911-1992) speleothem with instrumental climate data from southwest Australia. *Earth and Planetary Science Letters 216* (2003), 141–153.

[213] TURTON, S.M.; STORK, N. *Impacts of tropical cyclones on forests of the Wet Tropics of Australia*. Living in a Dynamic Tropical Forest Landscape. Blackwell Publishing, Oxford, UK., 2008.

[214] TURTON, S. M., AND DALE, A. An assessment of the environmental impacts of Cyclone Larry on the forest landscapes of northeast Queensland, with reference to responses to natural resource management issues in the aftermath. Tech. rep., Bureau of Meteorology, 2007.

[215] VAN BEYNEN, P., BOURBONNIERE, R., FORD, D., AND SCHWARCZ, H. Causes of colour and fluorescence in speleothems. *Chemical Geology 175*, 3-4 (2001), 319–341.

[216] VAN DER PLICHT, J. *Radiocarbon Dating: Variations in Atmospheric ^{14}C*. Elsevier, Oxford, 2007, pp. 2923–2931.

[217] VELDEN, C., HARPER, B., WELLS, F., BEVEN, J. L., ZEHR, R., OLANDER, T., MAYFIELD, M., GUARD, C., LANDER, M., EDSON, R., AVILA, L., BURTON, A., TURK, M., KIKUCHI, A., CHRISTIAN, A., CAROFF, P., AND MCCRONE, P. The Dvorak Tropical Cyclone Intensity Estimation Technique: A Satellite-Based Method that Has Endured for over 30 Years. *Bulletin of the American Meteorological Society 87*, 9 (2006), 1195–1210.

[218] WALSH, K. Tropical cyclones and climate change: unresolved issues. *Climate Research 27*, 1 (2004), 77–83.

[219] WALSH, K., AND PITTOCK, A. B. Potential changes in tropical storms, hurricanes, and extreme rainfall events as a result of climate change. *Climatic Change 39*, 2-3 (1998), 199–213.

[220] WALSH, K. J. E. Simulating the effect of climate change on tropical cyclones: current issues, December 2005 2005.

[221] WALSH, K. J. E., AND RYAN, B. F. Tropical cyclone intensity increase near Australia as a result of climate change. *Journal of Climate 13*, 16 (2000), 3029.

[222] WASSON, R. *Appendix L: Research on coral rubble ridges NW Vernon Island: Severe cyclone history in the vicinity of Darwin*. Community Group for the Review of NT Cyclone Risks Inc., Darwin, 2006, ch. L, pp. –.

[223] WEBSTER, P. J., HOLLAND, G. J., CURRY, J. A., AND CHANG, H. R. Changes in tropical cyclone number, duration, and intensity in a warming environment. *Science 309*, 5742 (2005), 1844–1846.

[224] WEN HUNG, C. A 300-Year Typhoon Record in Taiwan and the Relationship with Solar Activity. *Terr. Atmos. Ocean. Sci. 24*, 4 (2013), 737–743.

[225] WHITE, W. *Cave Minerals and Speleothems*. Academic Press, London, 1976, ch. 8, p. 267.

[226] WHITE, W. *Paleoclimate Records from Speleothems in Limestone Caves*. Kluwer Academic/Plenum Publishers, New York, 2004, pp. 135–175.

[227] WIBERG, P. L., AND HARRIS, C. K. Ripple geometry in wave-dominated environments. *J. Geophys. Res. 99*, C1 (1994), 775–789.

[228] WILLIAMS, P., MARSHALL, A., FORD, D., AND JENKINSON, A. Palaeoclimatic Interpretation of Stable Isotope Data from Holocene Speleothems of the Waitomo District, North Island, New Zealand. *The Holocene 9*, 6 (1999), 649–657(9).

[229] WILLOUGHBY, H. E., AND RAHN, M. E. Parametric Representation of the Primary Hurricane Vortex. Part I: Observations and Evaluation of the Holland (1980) Model. *Monthly Weather Review 132*, 12 (2004), 3033–3048.

[230] WITTER, R. C., ZHANG, Y. J., AND PRIEST, G. R. Testing Numerical Tsunami Simulations Against the Inland Extents of Prehistoric Cascadia Tsunami Deposits at Cannon Beach, Oregon. *AGU Fall Meeting Abstracts* (Dec. 2007), A162.

[231] WOODRUFF, J. D., DONNELLY, J. P., AND OKUSU, A. Exploring typhoon variability over the mid-to-late Holocene: evidence of extreme coastal flooding from Kamikoshiki, Japan. *Quaternary Science Reviews 28*, 17-18 (2009), 1774–1785.

[232] YAPP, C. J., AND EPSTEIN, S. J. Seasonal contributions to the climatic variations recorded in tree ring deuterium/hydrogen data. *Journal of Geophysical Research: Part D, Atmospheres 90*, 2 (1985), 3747–3752.

[233] YU, J. Y., CHOU, C., AND CHIU, P. G. A revised accumulated cyclone energy index. *Geophysical Research Letters 36* (2009), L14710.

[234] YUKIMOTO, S., ENDOH, M., KITAMURA, Y., KITOH, A., MOTOI, T., AND NODA, A. ENSO-like interdecadal variability in the Pacific Ocean as simulated in a coupled general circulation model. *Journal of Geophysical Research: Oceans 105*, C6 (2000), 13945–13963.

[235] ZALASIEWICZ, J., BARRY, T., COE, A., CANTRILL, D., GALE, A., GIBBARD, P., GREGORY, J., OATES, M., RAWSON, P., AND SMITH, A. Global warming: a perspective from earth history A position paper of the Stratigraphy Commission of the Geological Society of London, 2004.

[236] ZHANG, H., LI, S., FENG, Q., AND ZHANG, S. Environmental change and human activities during the 20th century reconstructed from the sediment of Xingyun Lake, Yunnan Province, China. *Quaternary International 212*, 1 (2010), 14–20.

[237] ZHAO, K., WANG, Y., EDWARDS, R. L., CHENG, H., AND LIU, D. High-resolution stalagmite δ^{18}O records of Asian monsoon changes in central and southern China spanning the MIS 3/2 transition. *Earth and Planetary Science Letters 298*, 1-2 (2010), 191–198.

[238] ZHAO, M., HELD, I. M., LIN, S. J., AND VECCHI, G. A. Simulations of Global Hurricane Climatology, Interannual Variability, and Response to Global Warming Using a 50-km Resolution GCM. *Journal of Climate 22*, 24 (2009), 6653–6678.

[239] ZHAO, X., AND CHU, P.-S. Bayesian Multiple Changepoint Analysis of Hurricane Activity in the Eastern North Pacific: A Markov Chain Monte Carlo Approach. *Journal of Climate 19*, 4 (2006), 564–578.